University of Kentucky
UKnowledge

Theses and Dissertations--Plant and Soil Sciences

Plant and Soil Sciences

2012

Method Development for Detecting and Characterizing Manufactured Silver Nanoparticles in Soil Pore Water Using Asymmetrical Flow Field-Flow Fractionation

Annie R. Whitley
University of Kentucky, Annie.whitley@uky.edu

Right click to open a feedback form in a new tab to let us know how this document benefits you.

Recommended Citation

Whitley, Annie R., "Method Development for Detecting and Characterizing Manufactured Silver Nanoparticles in Soil Pore Water Using Asymmetrical Flow Field-Flow Fractionation" (2012). *Theses and Dissertations--Plant and Soil Sciences*. 9.
https://uknowledge.uky.edu/pss_etds/9

This Master's Thesis is brought to you for free and open access by the Plant and Soil Sciences at UKnowledge. It has been accepted for inclusion in Theses and Dissertations--Plant and Soil Sciences by an authorized administrator of UKnowledge. For more information, please contact UKnowledge@lsv.uky.edu.

STUDENT AGREEMENT:

I represent that my thesis or dissertation and abstract are my original work. Proper attribution has been given to all outside sources. I understand that I am solely responsible for obtaining any needed copyright permissions. I have obtained and attached hereto needed written permission statements(s) from the owner(s) of each third-party copyrighted matter to be included in my work, allowing electronic distribution (if such use is not permitted by the fair use doctrine).

I hereby grant to The University of Kentucky and its agents the non-exclusive license to archive and make accessible my work in whole or in part in all forms of media, now or hereafter known. I agree that the document mentioned above may be made available immediately for worldwide access unless a preapproved embargo applies.

I retain all other ownership rights to the copyright of my work. I also retain the right to use in future works (such as articles or books) all or part of my work. I understand that I am free to register the copyright to my work.

REVIEW, APPROVAL AND ACCEPTANCE

The document mentioned above has been reviewed and accepted by the student's advisor, on behalf of the advisory committee, and by the Director of Graduate Studies (DGS), on behalf of the program; we verify that this is the final, approved version of the student's dissertation including all changes required by the advisory committee. The undersigned agree to abide by the statements above.

Annie R. Whitley, Student

Dr. Jason Unrine, Major Professor

Dr. Mark Coyne, Director of Graduate Studies

METHOD DEVELOPMENT FOR DETECTING AND CHARACTERIZING MANUFACTURED SILVER NANOPARTICLES IN SOIL PORE WATER USING ASYMMETRICAL FLOW FIELD-FLOW FRACTIONATION

THESIS

A thesis submitted in partial fulfillment of the
requirements for the degree of Master of Science in the
College of Agriculture
at the University of Kentucky

By
Annie Rose Whitley
Lexington, Kentucky
Co-Directors: Dr. Jason Unrine, Research Assistant Professor of Plant and Soil Science
and Dr. Paul Bertsch, Professor of Environmental Chemistry and Toxicology
Lexington, Kentucky
2012
Copyright © Annie Rose Whitley 2012

ABSTRACT OF THESIS

METHOD DEVELOPMENT FOR DETECTING AND CHARACTERIZING MANUFACTURED SILVER NANOPARTICLES IN SOIL PORE WATER USING ASYMMETRICAL FLOW FIELD-FLOW FRACTIONATION

Recent advances in nanotechnology have led to the production of materials with nanoscale dimensions (<100 nm) and properties distinctly different from their bulk (>100 nm) counterparts. With increased use, it is inevitable that nanomaterials will accumulate in the environment and there is concern that the novel properties of nanomaterials could result in detrimental environmental and human health effects. In particular, there has been concern recently regarding the use of silver (Ag) based nanomaterials as antimicrobial agents in consumer and medical products. Current regulations dealing with the discharge of metals into the environment are based on total concentrations with no consideration for the form (e.g., ionic, nanoparticle, colloid) which can largely determine toxicity. Methods for the identification and characterization of nanoparticulates within complex matrices are lacking and the development of robust methods for this purpose are considered a high priority research area. This research focuses on the development and application of a novel method for characterizing Ag manufactured nanoparticles (MNPs) within terrestrial environments, in particular in soil pore water, with applications relevant to other metal MNPs as well. The method was then applied to understand the dynamics and behavior of Ag MNPs in soil and soil amended with sewage sludge biosolids.

KEYWORDS: silver nanoparticle, manufactured nanoparticle, soil, asymmetrical flow field-flow fractionation, pore water

Annie Rose Whitley

September 7, 2012

METHOD DEVELOPMENT FOR DETECTING AND CHARACTERIZING MANUFACTURED SILVER NANOPARTICLES IN SOIL PORE WATER USING ASYMMETRICAL FLOW FIELD FLOW FRACTIONATION

By

Annie Rose Whitley

Jason Unrine

Co-Director of Thesis

Paul Bertsch

Co-Director of Thesis

Mark Coyne

Director of Graduate Studies

September 7, 2012

ACKNOWLEDGMENTS

This work would not have been possible without the guidance, support, and encouragement from several key people. I would first of all like to thank my advisor, Dr. Jason Unrine. He played a key role in the development of my project. More than that, he was always available for discussion and to address any questions and concerns. I am grateful to him for taking me on as a student, for his consistent optimism and having faith in me and my future. Thank you Jason. I would also like to thank my committee members, Dr.Paul Bertsch and Dr.Chris Matocha for their guidance and direction. Thank you for the discussions which typically addressed components of my project I had not yet considered. Ultimately, this helped me broaden my mindset and better understanding my research. Additionally, everyone in my research group offered moral support and I feel extremely lucky to have had the opportunity to interact with such friendly and knowledgeable scientists! Specifically, I want to thank Jon Judy for regularly being available to address questions, bounce ideas off of, and to have great discussions. Finally, I would like to thank my family. They have been incredibly supportive in everything that I do and that has meant the world to me. I would not be where I am today without them. Thank you. Finally, I would like to acknowledge the United States Environmental Protection Agency and National Science Foundation for funding this work through cooperative agreements CR-83515701 (Office of Research and Development) and EF-0830093 (Center for Environmental Implications of Nanotechnology) and through the EPA Science to Achieve Results (STAR) program (RD-83485701).

TABLE OF CONTENTS

Acknowledgments …… iii
List of Tables …… v
List of Figures …… vi

Chapter 1
Introduction and Literature Review……1
1.1 Introduction…… 1
1.2 Literature Review…… 2
1.3 Objectives and Research Outline……18

Chapter 2
Optimization of carrier solution composition for analyzing silver nanoparticles and soil colloids using asymmetrical flow field-flow fractionation…… 20
2.1 Introduction…… 21
2.2 Experimental…… 23
2.3 Results and Discussion…… 29

Chapter 3
Behavior of silver nanoparticles in soil pore water: effects of particle surface coating, aging, and sewage sludge amendment…… 42
3.1 Introduction…… 43
3.2 Experimental…… 45
3.3 Results …… 49
3.4 Discussion…… 59
3.5 Acknowledgements…… 63

Chapter 4
Summary and Conclusions……64

Appendices
Appendix A……67
References……88
Vita …… 98

LIST OF TABLES

Table 2-1, Summary of operating conditions used for asymmetrical flow field-flow fractionation.. …...……..……25

Table 2-2, Mean hydrodynamic radius (**r_h** ± standard deviation) and corresponding zeta potential (ZP) are shown for soil colloids, polyvinylpyrrolidone (PVP) coated Ag MNPs, and citrate (CIT) coated Ag MNPs suspended in18 M Ω DI water and AF4 carrier solutions to observe effects of carrier solution. ……...…..…31

Table 2-3, Recovery and retention time of each sample peak are shown as a result of changing AF4 carrier solution composition and holding all other AF4 parameters constant including a sample injection mass of 50 µg for soil colloids and 0.625 µg for PVP and CIT-Ag MNPs….…33

LIST OF FIGURES

Figure 1-1, Schematic showing asymmetrical flow field-flow fractionation of colloids through the channel in normal mode……...……...…….. 17

Figure 2-1, Calibration of the AF4 channel with size standards for a crossflow of (a) 0.3- 0.03 ml min^{-1} over 30 min and (b) decreasing from 1.5-0.3 ml min^{-1} up to a retention time of 15 min followed by (c) a gradient of 0.3-0.03 ml min^{-1} from 15- 45 min….…… 29

Figure 2-2, Transmission electron microscopy images display the size of the CIT-Ag MNPs (a-c) and PVP-Ag MNPs (d-f).……. 30

Figure 2-3, Combined AF4 fractograms show the size distribution of 0.625 µg PVP-Ag NPs eluted with different carrier solutions including 500 µl L^{-1} FL-70 (* including 200 mg L^{-1} azide), 500 mg L^{-1} sodium dodecyl sulfate (SDS)*, or 223 mg L^{-1} sodium pyrophosphate (NaPP)...….. 35

Figure 2-4, Combined AF4 fractograms show the size distribution of 50 µg soil colloids when particles are eluted with different carrier solutions including 500 µl L^{-1} FL-70 (red), 500 mg L^{-1} sodium dodecyl sulfate (SDS) and mg L^{-1} azide (green), 223 mg L^{-1} sodium pyrophosphate (NaPP; orange) or a combination of 500 mg L^{-1} SDS , 223 mg L^{-1} NaPP and mg L^{-1} azide (blue)…….……...…….. 36

Figure 2-5, Fractogram repeatability is shown for duplicate AF4 sample injections of 0.625 µg (A) polyvinylpyrrolidone (PVP) coated Ag MNPs or (B) citrate (CIT) coated Ag MNPs and for (C) 50 µg soil colloids…….……...38

Figure 2-6, Overlaid asymmetrical flow field-flow fractograms using ICP-MS detection of Ag (m/z = 107) for extracted sewage sludge biosolids (sludge) or Yeager Sandy Loam (YSL) soil colloids combined with (**A**) polyvinylpyrrolidone coated (PVP) Ag MNPs or (**B**) citrate coated (CIT) Ag MNPs. ……40

Figure 3-1, Total Ag expressed as a percentage of the soil concentration (w/w%) contained within filtered (1.0 µm) pore water samples from soils treated with silver nitrate ($AgNO_3$), polyvinylpyrrolidone coated Ag nanoparticles (PVP-Ag MNP), or citrate coated Ag nanoparticles (CIT-Ag MNP) amended with 0, 1, or 3% sludge (w/w; dry mass) and aged for 1 week, 2 or 6 months. …….…….……....51

Figure 3-2, Dissolved Ag in filtered (1.0 µm) pore water samples from soil treated with silver nitrate ($AgNO_3$), polyvinylpyrrolidone coated Ag nanoparticles (PVP-Ag MNP), or citrate coated Ag nanoparticles (CIT-Ag MNP) amended with 0, 1, or 3% sludge (w/w; dry mass) and aged for 1 week, 2 or 6 months following ultracentrifugation (ultrasupernatant) or ultrafiltration (ultrafiltrate)…..…….…….……..…….53

Figure 3-3, Asymmetrical flow field-flow fractograms using ICP-MS detection of Ag (m/z= 107) for pore waters extracted from polyvinylpyrrolidone coated Ag nanoparticles (PVP-Ag MNP; **A-C**), citrate coated Ag nanoparticles (CIT-Ag MNP; **D-F**) or silver nitrate ($AgNO_3$; **G-I**) treated soils amended with 0% (**A, D, G**), 1% (**B, E, H**), or 3% (**C, F, I**) sludge (w/w; dry mass) and aged for 1 week, 2 or 6 months. ……...……. 55

Figure 3-4, Representative asymmetrical flow field-flow fractogram using ICP-MS detection of Al (m/z = 27), Si (m/z = 28) and Ag (m/z = 107) for pore water extracted from soil amended with 3% sludge containing PVP-Ag MNP (w/w; dry mass).……. 57

Figure 3-5, Transmission electron microscopy (TEM) images confirming the presence of Ag nanoparticles in pore waters extracted after 1 week from non-amended CIT-Ag MNP treated soil (a-c), 3% sludge (w/w; dry mass) CIT-Ag MNP treated soil (d-f) and 3% sludge amended PVP-Ag MNP treated soil (g-i)…….....…… 59

Chapter 1: Introduction and Literature Review

1.1 Introduction

The number of consumer products containing nanomaterials continues to increase despite insufficient knowledge of the environmental risk [1]. In order to avoid the historical detrimental environmental effects inadvertently caused by the introduction of "new" materials, such as dichlorodiphenyltrichloroethane (DDT) and polychlorinated biphenyls (PCBs), researchers are taking preemptive measures to consider the impact of nanomaterials on environmental and human health [2,3]. One of the most widely used classes of nanomaterials are manufactured Ag nanoparticles (Ag MNPs). Studies have shown that Ag in its ionic form is toxic to many aquatic and terrestrial organisms [4,5]. Recently, there has been considerable research on the fate, behavior, and transformations of Ag MNPs after product end-use. Due to the known toxicity of Ag^+ and the widespread use of Ag MNPs, studies on Ag MNPs have been assigned a high priority for investigation [6]. Research suggests that a vast majority of Ag MNPs will enter terrestrial ecosystems through the application of biosolids [7]. The complexity of the soil matrix and limits to analytical techniques create difficulties when investigating Ag MNPs and determining Ag bioavailability in soil [8].

The available studies largely focus on aquatic environments and organisms [9]; although the number of terrestrial studies continues to increase. This chapter will provide a review of literature concerning Ag MNP fate, transformations, and toxicity relevant to the terrestrial environment, followed by a review of available methods for isolation and detection of MNPs. Finally, the objectives of this thesis will be outlined as they apply to the challenges associated with detecting and characterizing Ag MNPs in soil.

1.2 Literature review

Silver nanoparticle production and environmental fate

Manufactured nanoparticles (MNPs) are being produced at an increasing rate and entering the environment without much knowledge of potential negative environment effects.[1,7] Silver MNPs have been widely commercialized due to their antimicrobial properties, and are being used in products including cosmetics, fabrics, medical devices, and plastics. [10,11,12,13] During normal use, consumer products including paint, textiles, and toys have already been observed to release up to 99% of the Ag MNPs contained within a product after simulated weathering such as exposure to rain events, consecutive washes and prolonged exposure to natural waters. [13,14,15] Silver MNPs are expected to be released to the environment via various exposure pathways [9]. One important pathway is through waste water treatment plants (WWTP); sewage sludge is proposed to be a main reservoir of Ag MNPs. [11,16,17] Since a large proportion of sewage sludge is recycled as biosolids and amended to agricultural fields, soils may potentially accumulate Ag MNPs. [16,18] Models have predicted Ag MNP concentrations in biosolids amended soils to range from 0.02-7.4 μg kg^{-1} [18,19] and Ag MNP inputs are expected to rise as the use of Ag MNP containing consumer products continues to expand.[1]

The general defining quality of MNPs is at least one dimension is in the range of 1- 100 nm.[20] Under circumstances in which MNPs are dispersed in a fluid, MNPs are also classified as colloids (1 nm- 1 μm).[21] Several studies have attempted to apply colloid theory to understanding MNP behavior, but dissimilarities including the small size, potential non-uniform shape and charged surface modifications of MNPs have made this difficult.[21,22,23] Derjaguin, Landau, Verwey and Overbeek (DLVO) theory assumes van der Waals attractive forces and electrostatic repulsion for a particle predictably change with size. However, complications arise because decreasing particle size increases the proportion of atoms found at the particle surface.[21] This

also increases the local specific surface area, favoring aggregation of smaller particles as a driving force to decrease particle surface energy.[24] Likewise, decreasing particle size increases the ratio of the electrical double layer thickness to the particle radius for nanoparticles, increasing uncertainty in predicting particle behavior including aggregation.[21] DVLO theory also fails to account for nanoparticle surface charges imparted by manufactured surface coatings, environmental surface transformations, or nanoparticle chemical composition.[8] In order to predict aggregation potential, DLVO theory relies on a Hamaker constant which describes van der Waals attractions based on particle type. However, choice of Hamaker constant is somewhat ambiguous and is difficult to directly measure.[25] If unaccounted for, particle surface modifications, such as ion adsorption, can greatly alter surface chemistry and limit DLVO theory predictions.[26] Extended DLVO (XDLVO) theory was developed to account for polar particle interactions and Brownian movement.[27] However, further difficulties arise in using DLVO and XDLVO theory when particle surface charge is non-uniform and can lead to incorrect predictions in particle aggregation behavior.[10]

Colloid filtration theory could also be applied to MNP behavior in soil, as it has previously been used to investigate the mobility of natural colloids through soil.[28] Filtration theory takes into account particle collisions based on size and particle sticking efficiency which could effectively cause immobilization.[29] This model is helpful for estimating particle transport through soil, but can be limited due to realistic soil conditions which include heterogeneously sized soil particles.[29] With inevitable environmental release, MNPs are expected to undergo many transformations, including desorption of surface coating[30] which increase difficulties in applying existing colloid theories to their behavior. Likewise, the complexity of soil, including the wide range of natural particle sizes and surface chemistry also hinders colloid theory predictions.

Transformation of Ag MNPs

Environmental transformations and fate of Ag MNPs are poorly studied thus far; however, they may be dependent on factors including size, MNP capping agent, aggregation and dissolution potential, soil and water chemistry, natural organic matter (NOM), and aging processes.[21,31,32,33,34] Understanding transformations and surface modifications of Ag MNPs under environmental conditions is critical for predicting mobility and overall expected toxicity.

Intrinsic properties of Ag MNPs may be a key determinant in Ag MNP environmental behavior. In a simple aquatic suspension study, the rate of Ag MNP dissolution was shown to be dependent on both concentration and initial particle size but was not affected by aggregation state.[33] Additionally, several studies have observed smaller Ag MNPs to have a higher rate of dissolution than larger particles, a phenomenon suggested to be due to increased specific surface area.[33,35] Using a modified Kelvin equation, Ma et al., were able to predict Ag MNP solubility based on particle radius.[36] Solubility was found to be correlated with size, with little effect due to Ag MNP synthesis method or surface coating. These studies suggest that intrinsic properties, such as size, shape, and core composition may play a key role in predicting the fate of Ag MNPs in the environment.

Transformations of Ag MNP coating

Manufactured nanoparticles are typically coated with capping agents which increase particle dispersion and decrease aggregation through mechanisms like electrostatic or steric stabilization.[37,38,39] Sodium citrate (CIT) and polyvinylpyrrolidone (PVP) are the two most commonly used stabilizing agents for Ag MNPs.[40] Through electrostatic stabilization CIT increases repulsion between particles due to high negative charge imparted via CIT surface sorption. This mechanism is effective at keeping MNPs dispersed under ideal conditions, but external factors such as increased ionic strength can shield the charges and cause

Aggregation.[31,41] Conversely, PVP is comprised of water soluble nonionic long chain polymers which coat the Ag MNP surface, providing a steric stabilization mechanism, which is less affected by variations in ionic strength or cation valence. Studies have observed PVP-Ag MNPs to be more resistant to aggregation than other coated Ag MNPs when exposed to high ionic strength electrolyte solutions.[23, 42] The stability of PVP-Ag MNPs suggests enhanced environmental mobility in comparison to other capping agents.[31,43] Additionally, Ag MNPs sterically stabilized with polysorbate (a non-ionic surfactant known by the trade name Tween) provided enhanced stability, limiting particle dissolution in comparison to electrostatically stabilized Ag MNPs.[44] Observed differences in the ability of MNP surface coatings to stabilize particles could also be due to differences in particle synthesis or duration of storage. Aging has been shown to alter MNP aqueous dispersions, usually resulting in dissolution or aggregation.[36,45] Under conditions of changing pH, ionic strength, and aging capping agents will largely influence Ag MNP aggregation potential.

Less is known about how Ag MNP stabilization mechanisms (capping agents) will influence behavior under more realistic environmental settings. Environmental constituents like natural organic matter (NOM) will likely alter the stability of Ag MNPs through interactions with the surface coatings. Interestingly, one study suggests organic acids could have varied roles in MNP dissolution. Copper based MNPs were shown to undergo extensive dissolution in the presence of citric acid, whereas oxalic acid acted as an inhibitor due to weak and strong interactions resulting from outer and inner sphere complexes.[46] In another study, NOM released from aquatic plants prevented the aggregation PVP-Ag MNPs within the water column, while conversely stimulating dissolution of gum arabic coated Ag MNPs.[47] Like CIT, gum arabic provides electrostatic stabilization and therefore could provide insight as to the behavior of CIT-Ag MNPs, but due to the high molecular weight of gum arabic, steric stabilization mechanisms may be at play as well. In environments having substantial levels of O_2, oxidative dissolution has

been observed to enhance solubility of Ag MNPs; however, increased pH, low temperatures or the presence of NOM all slow this process.[48] Likewise, previous work with naturally occurring soil nanoparticles found that NOM in soil pore water provides nanoparticle stabilization.[49] In addition to capping agent chemistry, Ag MNP persistence and behavior will also largely depend on the environmental matrix and its components.

Few studies have investigated the role of capping agents on the behavior of Ag MNPs in complex matrices like soil. Following a 28 day earthworm toxicity assay, extended X-ray absorption fine structure analysis (EXAFS) revealed that 11-20% of PVP and oleic acid coated Ag MNPs were oxidized to Ag_2O, suggestive of Ag MNP oxidative dissolution.[50] Studies examining the behavior of Ag MNPs in aquatic studies may further aid in determining Ag MNP behavior in soil pore water. For instance, coating desorption or exchange have been shown to lead to particle aggregation,[30,51] suggesting coating desorption in soil would likewise lead to aggregation. Little information is available on weathering of PVP coatings in soils, but desorption of high molecular weight polymers is likely to be a kinetically slow process since numerous points of attachment allow for strong van der Waals interactions.[21,52] Regardless, covalently bound polymer MNP coatings have been shown to undergo biodegradation.[30] In a medium (soil) in which biota are prevalent, it is likely that soil organisms will play a role in determining Ag MNP availability and fate. For instance, since CIT plays a central role in the tricarboxylic acid cycle (TCA), it is likely that microbes could assist in coating removal.[30] Additionally, the Ag MNP capping agent may play a role in particle stability from aggregation.[31,34] One study using sequential extraction to assess bioavailability of Ag in soil observed CIT-Ag MNPs to be less bioavailable than uncoated Ag MNPs.[34] However, the same study concluded that soil properties had more of an effect on Ag speciation in soil than initial Ag form (Ag ions vs. uncoated Ag-MNPs vs. CIT-Ag MNPs). Other work has shown the addition of humic substances to increase Ag MNP mobility through soil, while a decrease in average soil

aggregate size tended to increase Ag MNP retention, likely due to filtration mechanisms.[53] Although there is little information on Ag MNP transformations following prolonged environmental exposure, surface coatings are likely to be modified and lead to changes in overall Ag bioavailability.

Transformations of the Ag core during wastewater treatment

During wastewater treatment, Ag MNPs will be exposed to extremely anaerobic environments and are expected to undergo major transformations. Recent studies have reported that Ag MNPs transform into insoluble Ag_2S within sewage sludge.[17,54] Due to the low solubility of Ag_2S ($K_{sp}= 10^{-50}$)[55], Ag MNP sulfidation strongly decreases dissolution rates and increases particle aggregation which could effectively limit mobility.[56] In addition to complete sulfidation of Ag MNPs, the formation of Ag-Ag_2S core-shell nanoparticles[57] or a Ag_2S bridge linking metallic Ag MNPs are also possible as a result of Ag MNP surface dissolution and reprecipitation of Ag_2S.[56] Regardless of the specific mechanism, Ag MNPs are likely to be sulfidized due to large quantities of sulfur present in both wastewater[58] and wastewater treatment plants.[59] Both dissolved charged polychloro complexes ($AgCl_x$) and solid AgCl precipitates will also readily form,[60] comparably decreasing toxicity. At this point, more information is needed on the stability of transformed Ag MNPs (e.g., sulfidized) in sewage sludge in order to assess potential soil toxicity.

Transformations in soil

Upon subsequent addition of sewage sludge to soil, Ag MNPs may be further modified by soil minerals, biota, or organic matter as has been shown for naturally occurring nanoparticles.[61] In one study involving Ag MNP-amended sewage sludge added to soils, naturally occurring TiO_2 nanoparticles identified via transmission electron microscopy (TEM) and energy dispersive X-ray spectroscopy (EDX) revealed the presence of Ag.[62] Control

experiments suggested that the Ag originated from the Ag MNPs, although no distinction was made concerning the size or speciation of the Ag. Apart from this study, little work has been done concerning transformations of Ag MNPs following mixing of sewage sludge biosolids with soil. Since Ag MNPs in sewage sludge biosolids are largely sulfidized,[63] it will be important to determine how sulfidized Ag MNPs are transformed, if at all, in soil. In general, Ag_2S is strongly resistant to oxidation,[64] however, sulfidized Ag MNPs have been shown to undergo dissolution in aqueous environments.[59] The extent of Ag MNP sulfidation in addition to soil type and pore water chemistry will all affect Ag MNP speciation and bioavailability in soil.[34,53]

Silver nanoparticle bioavailability and toxicity

Metal bioavailability should be considered when assessing the potential toxicity of Ag MNPs in soil.[65,66] As discussed, a large proportion of Ag MNPs may be physiochemically altered in soil or irreversibly sorbed to soil constituents (immobile), minimizing bioavailability to terrestrial organisms. Immediate concern should be with Ag species that partition to the pore water since it is likely the most bioavailable fraction, as has been shown for metals.[65] However, organisms that ingest soil solids, like earthworms, will have increased exposure to Ag MNPs which adsorb to soil solids. Currently there is no standard method for assessing ecotoxicology of Ag MNPs in soils, but it is likely that the soil matrix induces Ag MNP transformations and therefore alters toxicity.[67]

Bioavailability of Ag MNPs will likely be altered due to changes in particle aggregation state. In one study, *Drosophila* , a low-level terrestrial model organism exhibited significantly greater toxicity to Ag particles > 100 nm in size compared to Ag < 100 nm.[68] Likewise, aggregated Ag MNPs had increased inhibitory effects on *E. coli* growth compared to dispersed particles.[69] In addition to particle size, one explanation for increased toxicity suggests smaller particles were more sulfidized than aggregates and therefore less toxic.[69] Conversely, smaller Ag

MNPs have been observed to have a much stronger antibacterial/antifungal effect compared to larger Ag MNPs.[70] This may be as a result of increased dissolution of smaller particles which have been shown to provide better antimicrobial activity compared to larger particles with less surface area.[71] Smaller Ag MNPs could also have increased bioavailability compared to larger particles and therefore be taken up more readily.[72]

At this point it is unclear whether observed toxicity is a result of Ag MNPs or the resulting Ag ion dissolution products. Several studies suggest that a large portion of observed Ag MNP toxicity is due to ions released through oxidation and dissolution.[73,74] Moreover, the form of Ag is important since past studies have observed limited toxicity of metallic Ag compared to soluble Ag species.[75] In a recent study, Ag MNPs caused limited toxicity to freshwater microbes and minor effects on sediment microbial respiration while addition of $AgNO_3$ to the same mesocosms resulted in substantially increased toxicity and decreased respiration.[76] Similarly, increased cell toxicity was evident for Ag MNP solutions observed to undergo more dissolution, resulting in more dissolved Ag.[73] Other studies have observed effects directly related to Ag MNPs.[35,77,78] In an aquatic study Ag MNPs acted as neurobehavioral disrupters in zebrafish in ways distinctly different than that caused by Ag^+.[78] Likewise, the common grass, *Lolium multiflorum* experienced significantly stronger growth inhibition when exposed to gum arabic coated Ag MNPs versus $AgNO_3$.[35] Variability among experimental conditions and nanoparticle synthesis heighten the need for more thorough toxicity testing, including assessment of dissolution at critical experimental time points.[8] Ultimately, understanding Ag MNP environmental behavior requires better characterization of aggregation and dissolution behavior.

Impact of transformations on toxicity

Organic matter and Ag MNP sulfidation have both been observed to alter Ag toxicity. In one study, *Ceriodaphnia dubia* exposed to Ag MNPs had reduced toxicity with increasing

concentrations of dissolved organic carbon (DOC) and decreased ionic strength,[79] likely due to decreased bioavailability caused by a DOC coating.[77,80] Conversely, Ag sulfidation results in a highly insoluble sulfide mineral [56] which can significantly reduce bioavailability and therefore toxicity due to sedimentation and reduced oxidation and dissolution.[5,69,81] There was no observed effect on corn or oat crop yields when biosolids containing Ag_2S concentrations as high as 106 mg Ag kg^{-1} were amended to soil.[81] Likewise, Reinsch et al. demonstrated that the degree of Ag MNP sulfidation strongly influenced toxicity, resulting in greater *E. coli* growth inhibition for less sulfidized Ag MNPs.[69] Although Ag MNPs in sewage sludge biosolids are expected to be largely sulfidized, no work has investigated Ag MNP transformations following biosolids addition to soil so alterations in Ag bioavailability are largely unknown.

The complexity of soil makes risk assessment difficult and as a result many tests use growth media or aqueous conditions to test organism response to Ag MNPs. A recent study using *Caenorhabditis elegans* observed epidermal effects directly related to exposure to 10 mg L^{-1} CIT-Ag MNPs in nematode growth medium.[82] Dissolved Ag^+ concentrations did not account for all of the observed toxicity to *C. elegans*. Typically, the use of media less complex than soil overestimates bioavailability.[81] A study comparing exposure media observed an EC_{50} of 13 mg CIT-Ag MNP L^{-1} for mung beans (*P. radiates*) grown in agar compared to negligible plant growth effects in soil containing up to 2000 mg kg^{-1} CIT-Ag MNP.[83] Although shorter roots and fewer rootlets were prevalent in plants grown in both types of media, it is apparent that the complexity of the soil including composition and high buffering capacity had a large effect on Ag MNP bioavailability. Another study observed earthworm apoptotic activity consistently 2-4 times higher when exposed to Ag MNPs in water versus soil.[84] While oxidative dissolution may be a key pathway for Ag MNPs under aquatic conditions, modification by minerals and organics may slow Ag MNP dissolution in soils and quickly immobilize any ions produced.[34] Conversely,

natural soil filtration mechanisms, like straining, could result in soil pores space more saturated with Ag species, including dissolution products, effectively increasing localized exposure.[85,86]

Increasingly, studies are using soil as an exposure medium, but there is still limited information concerning Ag MNP transformations, bioavailability, and toxicity in terrestrial ecosystems. In a limit-test toxicity study, earthworms were exposed to several metal MNPs and their corresponding salts at 1000 mg kg^{-1} soil.[87] While both Ag MNPs and $AgNO_3$ completely inhibited earthworm reproduction, only metal salts ($AgNO_3$, $CuCl_2$, and $NiCl_2$) caused lethality. Another study observed earthworm reproductive toxicity to be much greater when earthworms were exposed to $AgNO_3$ compared to PVP or oleic acid coated Ag MNPs.[50] Earthworm behavioral avoidance of Ag spiked soil occurred at similar concentrations regardless of Ag form although the effect was delayed for Ag MNPs but not $AgNO_3$.[88] Behavioral avoidance also occurred at environmentally relevant concentrations and at concentrations much lower than previously observed earthworm reproductive effects.[32] One study observed sublethal effects for earthworms exposed to Ag MNPs at a dose as low as 4 mg kg^{-1} soil.[84] Enhanced apoptotic activity was observed for many tissues including the cuticle which serves as an external antimicrobial barrier for the earthworm. Compromising essential earthworm tissues as a result of Ag MNP exposure will likely cause earthworms to be more susceptible to other stressors. Based on these studies it is clear that Ag MNP bioavailability and toxicity to soil organisms will change with Ag MNP modification and depend on the exposure medium.

Methods of detection of Ag MNPs

There are currently few reliable techniques capable of detecting, isolating and characterizing Ag MNPs in complex environmental matrices.[89] Nevertheless, methods used in colloid science can be used along with new techniques to handle studying the range of different MNPs. Dissimilarities in MNP composition and surface chemistry increase difficulties associated

with risk assessment. It is clear that analytical techniques and microscopy based methods must be specifically tailored to sample type and research objectives to obtain reliable information.[89] Since some forms of Ag may be toxic to many organisms,[90] it will be important to develop reliable detection methods in environments where Ag MNPs are more likely to be released in large quantities (e.g., soil). It is beyond the scope of this review to discuss all potential techniques which could be used for Ag MNP detection and characterization in soil; however, advantages and limitations of many commonly used techniques will be presented.

Microscopy techniques are extremely beneficial for characterizing MNPs. Transmission electron microscopy (TEM) and scanning electron microscopy (SEM) can resolve particles as small as 1 nm.[89] Electron dense materials (e.g., metal MNPs) are easily viewed using both techniques, but images can be viewed in three dimensions by SEM compared to only two dimensions for TEM.[67] For both techniques, sample pretreatment requires drying the sample on a grid or support media which can lead to artifacts including changes in particle aggregation.[67] Additionally, electron microscopy is costly, time-consuming, and ineffective for detecting and monitoring MNPs in environmental samples at relevant expected concentrations.[91] Atomic force microscopy (AFM) is another technique widely used to study polymers because of the high resolution and imaging potential under aqueous or ambient conditions.[92] This technique has the advantage of requiring little sample pretreatment and also results in a three-dimensional image projection. However, inaccuracies in particle height measurements could occur as a result of probe geometry, sample flattening by probe, artifacts, or effects of drying.[92] Nevertheless, microscopy techniques provide important information concerning particle morphology and when possible should be used in conjunction with other analytical techniques.

Several analytical techniques are often paired with electron microscopy.[93] Energy dispersive X-ray spectroscopy (EDS) and selected area electron diffraction (SAED) are two common techniques used in conjunction with electron microscopy. During EDS analysis an

electron beam excites sample atom inner shell electrons, leaving vacancies which are filled by outer shell electrons, generating X-rays with energies that are characteristic of different elements allowing for determination of elemental composition of individual particles.[93] The drawback of this technique is that it determines elemental composition, not speciation or oxidation state. When coupled with electron energy loss spectroscopy (EELS), it is possible to determine oxidation state and local electronic structure of atoms in a sample.[94] It is also possible to determine the crystal structure of particles using SAED.[67] Both EDS and SAED are routinely used with electron microscopy imaging and will be key for distinguishing between environmental and MNPs on the nanoscale.

Synchrotron based X-ray absorption spectroscopy (XAS) techniques allow for determination of local electronic structure of metal centers in a sample and have therefore become a staple in nanomaterials research.[56,63,95] The technique is based on a tunable incident X-ray source (typically obtained using a synchrotron light source) that is swept in energy across the absorption edge of the element of interest. The structure within the absorption spectrum contains information on oxidation state and coordination environment. [96] The two types of XAS include X-ray absorption near-edge spectroscopy (XANES) and extended X-ray absorption fine structure (EXAFS) which are used to observe different regions of the spectrum. Based on oscillations indicative of absorption behavior, EXAFS provides data on the absorbing atom as well as the identity and distance of neighboring atoms.[97] XANES is used to analyze oscillations closer to the absorption edge that result from multiple scattering, as well as the edge position itself. XANES can provide information on the oxidation state and coordination geometry of metal centers. Both techniques require minimal sample pretreatment; however access to synchrotron facilities is limited and the techniques require a high degree of expertise.[67] These techniques can also be combined with scanning X-ray fluorescence imaging in order to determine the spatial distribution and speciation of metals within a sample with resolution ranging from 10 μm to 30 nm.[89]

Light scattering techniques are routinely used to determine the size of particles suspended in a liquid. Dynamic light scattering (DLS) is one of the most commonly used techniques to assess the size of a colloidal dispersion. Average hydrodynamic diameter (d_h) is determined based on variations in the intensity of scattered light due to Brownian motion.[98] Scattered light is measured from a single angle of detection, typically 90˚. The same instrument is also typically equipped to measure electrophoretic mobility of particles in suspension using laser Doppler velocimetry or phase analysis light scattering.[67] Another light scattering technique is multi-angle laser light scattering (MALLS). MALLS detects light using several detectors positioned at different angles around the sample or a movable detector on a goniometer and can measure either the geometric radius of spherical particles or the root mean square radius (r_{rms}), which is a measurement of the mass weighted average distance around the center of mass of a particle.[98] Light scattering techniques are very effective at determining average size of spherical, monodisperse particles in solution, but they do not provide any distinction among particle type and are unreliable for environmental samples which are polydisperse and include non-spherical particles.[98] All light scattering techniques suffer from the same basic problem; since the intensity of scattered light is also related to the sixth power of the radius, they are also heavily biased towards larger particles and assumptions must be made about the optical properties to convert sizes to mass weighted averages from intensity weighted averages.

Several techniques have been specifically tailored to distinguish between differently sized particles of the same composition, including making the distinction between nanoparticles and ions. Single particle inductively coupled plasma mass spectrometry (SP-ICP-MS) differentiates between different sized particles of the same composition based on the magnitude of the pulse that reaches the detector following atomization of a single particle.[99] This technique can likewise distinguish between dissolved species and nanoparticles, but requires low particle concentrations to prevent particle coincidence which could result in two smaller MNPs measured as a single

large MNP. It also requires a low background of dissolved ions of the element of interest.[100] Although SP-ICP-MS offers high sensitivity and good size resolution of particles, it cannot yet resolve particles less than 20 nm and calculation of particle size requires that assumptions be made about the stoichiometry of the particles.[100] Two techniques that tend to be specifically aimed at differentiating between MNPs and dissolved species are ultracentrifugation and ultrafiltration.[91] Both are useful for quantifying dissolved species in a solution, however ionic species are often bound to the filter during ultrafiltration, specifically if bound to dissolved organic matter larger than the pore size.[89,101]

Several chromatographic techniques are becoming increasingly popular for separation of MNPs in suspension.[102] Size exclusion chromatography (SEC) separates particles during the elution of a sample through a bead-packed column.[102] Separation is based on the hydrodynamic volume of eluted polymers or particles.[103] However, decreased separation efficiency occurs as a result of analyte interaction with the stationary phase which leads to irreversible sample sorption to the stationary phase causing low recovery and misrepresented particle size distributions.[103] Comparatively, hydrodynamic chromatography (HDC) separates colloids in a packed column as a result of varying eluent velocities experienced by different sized particles as they approach the electrical double layer of the stationary phase.[104] This technique has shown promise for separating complex MNP-containing environmental matrixes,[105] but unfortunately has low resolution and is largely affected by solution ionic strength.[106] Under conditions of high ionic strength the chemical nature of the particle can cause increased interaction with the stationary phase, leading to increased particle retention.

One of the most versatile separation techniques is field-flow fractionation (FFF). It was developed over forty years ago and can be applied to separate particles in the size range of 1 nm up to a few microns.[107] This chromatography-like technique separates particles on the basis of hydrodynamic particle size or in some cases particle mass, but with the advantage of having no

stationary phase and therefore minimizing non-specific sample interactions that could cause artifacts or reduced recovery. The basis of this technique comes from sample elution in a thin, ribbon-like channel with particle separation occurring due to some applied perpendicular field.[107] Several sub-techniques were developed through varying the type of applied field; electrical (El-FFF), sedimentation (Sd-FFF), flow (Fl-FFF), and Thermal (Th-FFF). Particle separation is created in Fl-FFF by applying a secondary flow of liquid perpendicular to the carrier flow. This application has been divided into symmetrical and asymmetrical Fl-FFF. Asymmetrical flow field-flow fractionation (AF4) has only one wall permeable to eluent flow in the channel instead of two, as is the case for symmetrical Fl-FFF. As a result, AF4 has shorter sample run times and less sample dilution.[108] Overall, the versatility of available FFF techniques makes them ideal for dealing with the wide range of MNP sample types.

Asymmetrical flow field-flow fractionation

AF4 theory is described thoroughly elsewhere,[107,109] but a brief overview is given here. As mentioned, in AF4 particles are separated in a thin (200-500 µm) channel which runs over an ultrafiltration membrane with some designated size cut-off value[110] (**Figure 1-1**). It is important to note that membrane and eluent composition can both be altered to adapt to variations in sample type. Following sample injection onto the AF4 membrane, the carrier solution transports the sample through the channel in a laminar flow. Particles are first focused into a narrow band near the channel inlet before elution. An applied perpendicular cross flow concentrates the particles near the ultrafiltration membrane, while the diffusion of the particles opposes this force. Smaller particles have a faster rate of diffusion than larger particles and thus a higher average height in the channel profile. Since the laminar flow sub-layers towards in the center of the channel are faster than those near the channel walls, smaller particles elute faster than larger particles. The size selectivity is related to the ratio of cross flow to channel flow. Increasing the crossflow will provide a better separation of particles, but possibly at the expense of causing irreversible

adherence of particles to the membrane surface. AF4 theory or calibration of the instrument with size standards, paired with particle retention time allows for the determination of the hydrodynamic size of eluted particles.

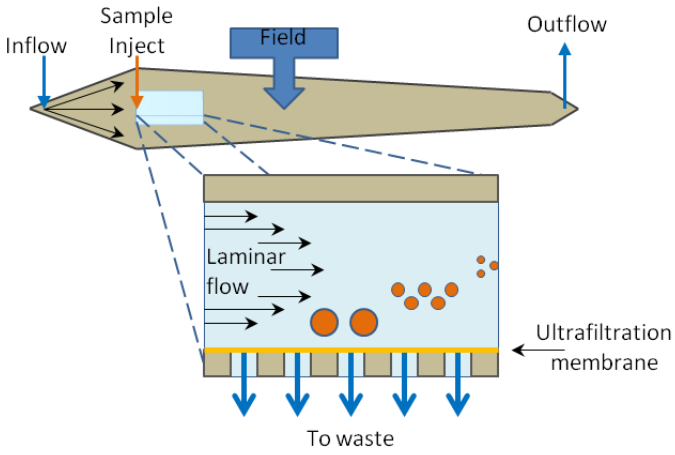

Figure 1-1. Schematic showing asymmetrical flow field-flow fractionation of colloids through the channel in normal mode.

AF4 has been used for analysis in several fields including medical, biological and environmental studies[107] and in the past decade has become increasingly popular for nanoparticle size characterization.[47,110,111,112,113] In order to distinguish between MNPs and other sample constituents, AF4 is often paired to quantitative elemental instrumentation. A wide range of techniques are available, but some are superior for detecting Ag MNPs. Specifically, an ultraviolet-visible (UV-Vis) diode array detector (DAD) can confirm the presence of several types of MNPs including Ag by monitoring the surface plasmon resonance. [98] Typically a band occurs around 400-450 nm for Ag MNPs, however, homoaggregation will lead to a red-shift of the band.[114] Pairing AF4 to light scattering detectors like DLS and MALLS can also overcome the problem of sample polydispersity that limits light scattering techniques. Following AF4 separation, DLS/MALLS measurements are performed on similarly sized particle populations and

can therefore provide more reliable particle size characterization. Parameters including d_h (for DLS) and r_g (MALLS) can then be determined to provide insight on particle size and in some cases shape.[98]

Generally, the most widely used technique for elemental identification and quantitative information is inductively coupled plasma mass spectrometry (ICP-MS). Coupling AF4 to ICP-MS allows for determination of elemental content as a function of particle size. AF4-ICP-MS has been used to analyze samples including MNPs, humic substances, complex food and natural colloids.[110,113,115,116] However, limited studies have developed repeatable, reliable methods for analyzing MNPs in complex media. A recent study used AF4 to examine Ag MNP aggregation and dissolution behavior in aquatic microcosms comprised of water only, water and sediment, water and plants, or water, sediment and plants.[47] Differences in Ag MNP dissolution behavior were observed for differently coated Ag MNPs as a result of organics released from plants. Poda et al. also used this technique to determine change in Ag MNP size in biological tissues upon uptake by an oligochaete, but did not provide any quantitative recovery data.[111] With increasing studies utilizing AF4-ICP-MS, there will be a growing library of unique sample running conditions (e.g., carrier solution, injection amount) available for reference.

1.3 Objectives and Research Outline

The purpose of this research was to develop a method to systematically detect and characterize silver manufactured nanoparticles (Ag MNPs) in soil pore water using asymmetrical flow field-flow fractionation (AF4) coupled to inductively coupled plasma mass spectrometry (ICP-MS) and to use the method to examine the behavior of Ag MNPs having different surface coatings in soil and soil amended with differing levels of sewage sludge biosolids upon aging for different time periods. Surface coating is expected to dictate Ag MNP behavior in the

environment. Specifically, non-ionic, polyvinyl pyrrolidone (PVP) coated Ag MNPs are expected to partition and remain more stable within soil pore water than citrate (CIT) coated Ag MNPs which exhibit a negative surface charge which could easily be destabilized by soil solution cations. Additionally, the low molecular weight CIT coating may more easily be desorbed or exchanged for organics compared to the high molecular weight PVP which could also have multiple sites of attachment to the Ag MNP surface. In soils treated with sewage sludge biosolids we expect sulfidation of Ag MNPs to determine Ag behavior. Sulfidation has already been shown to be a major environmental transformation of Ag MNPs, regardless of the presence of a surface coating. Aging soils treated with Ag MNPs should result in decreased Ag MNPs stabile within pore water due to environmental transformations including extensive sulfidation, oxidative dissolution, and adsorption to immobile colloids.

There is likely an influx of Ag MNPs being introduced into agricultural soils via sewage sludge biosolids, yet there are no systematic methods to detect Ag MNP aggregation state in complex matrixes like soil. Asymmetrical flow field-flow fractionation has been used for various sample types in the past, but has rarely been used for complex matrixes and to date there are no published studies where it was used to detect Ag MNPs in the aqueous phase of soil (e.g., soil pore water). This technique will allow for size characterization of Ag containing particles able to easily partition into the aqueous phase of soil. Such information will be vital in determining Ag MNP behavior, potential mobility in and bioavailability from agricultural soils.

Chapter 2: Optimization of carrier solution composition for analyzing silver nanoparticles and soil colloids using asymmetrical flow field-flow fractionation

Annie R. Whitley[†, ‡], Frank von der Kammer[§], Paul M. Bertsch [†,‡], Jason M. Unrine [†,‡,*]

[†] University of Kentucky, Department of Plant and Soil Sciences, Lexington, KY 40546, United States

[‡] Center for the Environmental Implications of Nanotechnology, Duke University, Durham, NC, 27708, United States

[§] Department of Environmental Geosciences, University of Vienna, Althanstrasse 14, A-1090 Vienna, Austria

2.1 Introduction

With advances in nanotechnology and the increased of production of nanomaterials,[1] it is projected that concentrations of manufactured nanoparticles (MNPs) released into natural waters, soil, and air will continue to increase.[117,118] In the past decade, research on transport, transformations, and toxicity of MNPs in complex matrices, such as soil, has been hampered due to a lack of adequate *in situ* detection and characterization techniques.[89] Elemental quantification is possible with some instruments (e.g., inductively couple plasma mass spectrometry, ICP-MS; atomic absorption spectroscopy, AAS), but there is no distinction between MNPs and their bulk or ionic counterparts. While microscopy is an excellent tool for characterizing MNPs, it is challenging to employ for samples generated under environmentally realistic conditions.[67]

Flow field-flow fractionation (F4) coupled to inductively coupled plasma mass spectrometry (ICP-MS) detection has recently emerged as a promising technique for characterizing MNPs in environmental matrices. Flow field-flow fractionation has the ability to separate heterogeneous particulate phases based on particle hydrodynamic size or molecular weight (in the case of molecules and polymers) and can be paired with ICP-MS to determine the elemental content of particles having a known hydrodynamic size.[67,89,108] It is a chromatography-like technique, but has the advantage of not possessing a stationary phase, therefore minimizing the surface area available for nonspecific sample interactions, as seen with other separation techniques including size exclusion chromatography.[103] A wide range of particle sizes (1 nm-10 µm) may be separated and minimal sample is required.[107] Two main types of F4 techniques that have been commonly applied thus far are symmetrical and asymmetrical (AF4). Symmetrical F4 contains a semi-permeable wall on either side of the sample flow to allow the crossflow to perpendicularly cross the sample flow.[109] Conversely, AF4 has only one permeable wall and maintains a pressure difference between the channel flow and the waste flow, creating the crossflow which leads to sample separation.[108] A narrower channel is therefore used in AF4 to sustain a consistent crossflow. The main advantages of AF4 are less sample dilution and shorter analysis time.[107]

Asymmetrical F4 -ICP-MS may be applied to a wide range of sample types including biological, environmental, and industrial. In many cases AF4-ICP-MS has been used to determine associations between trace metals and environmental colloids[119,120,121,122,123] and the number of studies applying the technique to separate metal and metal oxide nanomaterials in the environment are increasing.[47,89,111,124]

There are many advantages to using AF4 analysis over other separation techniques, but method development is necessary and to develop optimized conditions that are particle and matrix specific.[107] Failure to properly optimize methods could result in decreased recovery, increased nonspecific sample interactions, or even sample transformations during analysis.[108,125] Several reviews have outlined F4 parameters used in recent studies.[108,126] There is an increased need for reliable techniques for *in situ* detection of Ag MNPs and possible Ag derivatives within the complex soil environment.[7,117] The array of different sample types examined in past studies using AF4 suggest that this technique could be instrumental in characterizing Ag MNPs in complex matrices, specifically in soil pore water. For proper sample separation, good recovery, and measurement repeatability using AF4, it is necessary to evaluate and optimize separation parameters for both Ag MNPs and naturally occurring colloids which are likely to be present in soil pore water.[108,120]

The objective of this study was to develop and optimize an AF4 separation method with high separation efficiency and recovery for Ag MNPs and environmental colloids in soil pore water. Various AF4 operating conditions were evaluated, including variations in carrier solution, injection volume, and crossflow, to determine optimal AF4 parameters for the separation of mixed Ag MNP/ environmental colloid suspensions reflective of actual soil pore water. The experimental strategy included analyzing stable soil colloids and Ag MNPs individually under varying AF4 operating conditions to determine conditions optimized for both particle types. To evaluate realistic pore water conditions, Ag MNPs having different surface coatings were mixed with soil and sewage sludge derived colloids and analyzed using AF4-ICP-MS. The operating

parameters used resulted in good repeatability, separation efficiency, and recovery of Ag MNPs and environmental colloids, further supporting AF4-ICP-MS as a viable technique for monitoring Ag MNP behavior in soils amended with sewage sludge biosolids.

2.2 Experimental

Silver nanoparticles

Manufactured silver nanoparticles (Ag MNPs) having two different surface coatings were used in this study; 80 nm diameter polyvinyl pyrrolidone coated Ag MNPs (PVP-Ag MNPs) and 60 nm citrate coated Ag MNPs (CIT-Ag MNPs). PVP-Ag MNPs were synthesized according to Cheng et al., 2011.[127] CIT-Ag MNPs were made in house by reducing silver nitrate ($AgNO_3$) in the presence of sodium citrate.[128] Hydrodynamic radii and electrophoretic mobility of the Ag MNPs and environmental colloids was determined via batch dynamic light scattering (DLS) using a Malvern Zeta-Sizer Nano-ZS (Malvern Instruments, Malvern, UK). Transmission electron microscopy (TEM) was used to assess primary particle size and shape of Ag MNPs using a Jeol 2010 F field emission gun electron microscope (Tokyo, Japan).

Environmental colloid generation

Soil colloids were isolated from Yeager sandy loam (YSL) soil collected from Estill County, KY following a procedure outlined by Plathe et al., (2011).[123] A full description of the procedure is outlined elsewhere, but briefly, soil cations were exchanged for Na by shaking soil with 0.1 M NaOH in a 1:2 mixture for 4 hours. The solution was centrifuged to remove particles > 200 nm based on Stoke's law, assuming a density of 2.68 g cm^{-3} (average soil particle density).[129] The supernatant was decanted and disposed of. Remaining soil solids were combined with 18 MΩ deionized water in a 1:2 ratio and centrifuged to remove particles > 200 nm. The supernatant was collected and the process was repeated until the supernatant returned

clear. All supernatants were combined and stored at 4˚ C. Soil colloids were dried at 60˚ C to determine the total suspended solids in solution.

Sewage sludge biosolids (sludge) were obtained from a municipal wastewater treatment facility in KY. Extraction of sludge colloids is similar to previously used techniques.[130,131] Sludge colloids were obtained by shaking the sludge in a 1:10 ratio with18 MΩ deionized water for 4 hours followed by centrifugation to a > 200 nm cut-off, based on a particle density of 2.69 g cm^{-3}. The procedure was repeated and supernatants were collected, combined and stored at 4˚ C.

Combined environmental colloids and Ag MNPs

After separate AF4 method development with soil colloids and Ag MNPs, soil and sludge colloids were combined with PVP and CIT-Ag MNPs to mimic realistic soil pore waters from biosolids amended soils. The environmental colloid-Ag MNP mixtures were analyzed via AF4-ICP-MS to determine the efficiency of the proposed AF4 separation parameters. Environmental colloids were combined with PVP-Ag MNPs or CIT-Ag MNPs to achieve 25 mg Ag L^{-1}. First, Ag MNP stock solutions were diluted to 500 mg Ag L^{-1}. Then 0.5 mL of 500 mg Ag L^{-1} was diluted with 9.5 mL suspension of soil or sludge colloids. Environmental colloid-Ag MNP mixed suspensions were stored in the dark at 4° C.

AF4 and online detectors

Soil colloids, Ag MNPs, and mixed environmental colloid-Ag MNP samples were separated using asymmetrical flow field-flow fractionation (AF4; Wyatt Eclipse 3, Santa Barbara, CA, USA). Operating parameters used for AF4 analysis are summarized in **Table 2-1**. Soil colloids were analyzed with a crossflow gradient of 0.3-0.03 ml min^{-1}, decreasing over 30 minutes. The concentration of total solids for extracted soil colloids was 2 g L^{-1}. Therefore, several injection volumes were tested (15- 100 µL), with corresponding injection masses of 30, 50, 100, 150, and 200 µg soil colloid. Analysis of PVP and CIT-Ag MNPs also used crossflow gradient of 0.3-0.03 ml min^{-1}, decreasing over 30 minutes. Injection mass of Ag MNPs varied from 0.375, 0.500, 0.625 and 1 µg Ag. Injection amounts used for soil colloid and Ag MNP

recovery analyses (no crossflow) were 20 and 25 µg, respectively. Mixed soil colloid-Ag MNP samples were analyzed with 0.05% FL-70 using a crossflow of 0.3-0.03 ml min^{-1}. A stronger crossflow was required to separate mixtures containing sludge. Therefore, sludge-Ag MNP and soil-Ag MNP mixtures were also separated using an initial crossflow gradient of 1.5- 0.3 ml min^{-1} up to a retention time of 15 minutes, followed by a gradient of 0.3- 0.03 ml min^{-1} over the next 30 minutes. An injection volume of 25 µL was used for all mixed samples, based on optimal injection of soil colloids (50 µg = 25 µL).

Table 2-1: Summary of operating conditions used for asymmetrical flow field-flow fractionation. An asterisk indicates that 200 mg L^{-1} of sodium azide was added.

Membrane	5 kDa regenerated cellulose
Spacer (µm)	350
Channel flow rate (mL min^{-1})	1.0
Focus flow (mL min^{-1})	0.5
Cross flow rate (mL min^{-1})	
Rate 1	Gradient of 0.30- 0.03 (over 30 min)
Rate 2	Gradient of 1.5- 0.30 (over 10 min) then decreasing from 0.30- 0.03 (over 30 min)
Injection amount	30- 200 µg (soil particles) 0.375- 1 µg (Ag MNPs)
UV wavelength (nm)	420
Carrier solution	
Trial 1	Water*
Trial 2	0.05% Sodium dodecyl sulphate (SDS)*
Trial 3	0.5mM Na pyrophosphate (NaPP)
Trial 4	0.05% SDS and 0.5mM NaPP*
Trial 5	0.05% FL-70
Trial 6	0.05% FL-70*
Fractogram time (min)	60

Following AF4 separation, the eluent from the AF4 channel entered an in-line ultraviolet-visible (UV-Vis) diode array detector (DAD) (Agilent 1200 series) which monitored Ag MNP absorbance at 420 nm, which is in the surface plasmon absorption band for Ag MNPs in this size range. In-line flow was then directed to a multi angle/ dynamic laser light scattering

(MALLS/DLS) detector (Wyatt DAWN HELEOS-II) which measured light scattering intensity at 18 angles with DLS measured at 100.3º. Light scattering at 90º was used to monitor the concentration of soil colloids because the particles did not absorb strongly at any UV-Vis wavelength. MALLS was also used to determine the root mean square radius of particles (r_{rms}) using the Berry model.[132] The r_{rms}, also known as the radius of gyration, is a measure of the radius based on the average mass distribution within a particle. The r_{rms} is not equivalent to the geometric radius, being slightly less for a solid sphere.[133] Both the UV-Vis absorbance at 420 nm and light scattering at 90º were monitored for mixed environmental colloid-Ag MNP samples. Lastly, for environmental colloid -Ag MNP samples, in-line flow was directed to an ICP-MS system to detect Ag (m/z =107, 109) in case primary particle size was compromised via dissolution or aggregation as a result of mixing particle types. Agilent Chemstation software was used to collect UV-Vis data, Wyatt ASTRA version 5.3.4.11 was used to process light scattering data and Agilent ICP-MS chromatographic software version C.01.00 was used to process the distribution of Ag in mixed samples.

AF4 Carrier Solution Composition

Several different carrier solutions were tested to separate either soil colloids or Ag MNPs using AF4. In principle, an ideal carrier solution should not alter the aggregation state of suspended sample particles.[120] For that reason, 18 M Ω DI water with the addition of 200 mg L^{-1} sodium azide (MP Biomedicals, LLC, Solon, OH), resulting in pH 7.15 was tested for PVP-Ag MNPs. Water has been used previously as a carrier solution in an attempt to minimize non-ideal interactions between the sample and the carrier solution which cause sample aggregation, disaggregation, or adsorption to the AF4 membrane.[134] Sodium azide was added to water in the carrier solution to prevent bacterial growth in the AF4 system.[115,135] However, sodium azide increases background absorbance below 280 nm, thus disallowing monitoring particles which absorb in that range.[123] The second carrier solution evaluated to separate soil colloids, PVP-Ag

MNPs and CIT-Ag MNPs was 0.05% sodium dodecyl sulfate (SDS; Sigma Aldrich) containing 200 mg L^{-1} sodium azide, with a of pH of 8.66, was used to separate soil colloids, PVP-Ag MNPs and CIT-Ag MNPs. Sodium dodecyl sulfate is an anionic surfactant previously used as a carrier solution for analyzing natural colloids,[133] proteins,[136] sediments/soils, [137] and Ag MNPs.[138]

The third carrier solution evaluated is 0.5 mM sodium pyrophosphate (NaPP) (Fisher Scientific, Fair Lawn, NJ) at pH 8, which is a traditionally employed dispersing agent for isolating natural colloids[139] and colloid associations with trace elements.[123] For this study we used NaPP to analyze soil colloids and PVP-Ag MNPs. Based on mixed results for PVP-Ag MNPs and soil colloids using SDS and NaPP carrier solutions, we tested a mixture of 0.05% SDS, 0.5 mM NaPP, and 200 mg L^{-1} sodium azide, resulting in a final solution pH of 8.16 as a carrier solution for the elution of soil colloids. Lastly, 0.05% FL-70 detergent (Fisher Scientific, Fair Lawn, NJ) with and without 200 mg L^{-1} sodium azide, with final solution pH values of 9.5 and 10.09, respectively, were used based on previous successes[111,140] in dispersing colloidal suspensions and preventing aggregation [141]. Both PVP-Ag MNPs and CIT-Ag MNPs and the soil colloids were analyzed using FL-70 only. Sodium azide was added to FL-70 to analyze PVP-Ag MNPs, but due to decreased recovery, Na azide was not added for the analysis of other particle types. Like SDS, FL-70 is an anionic surfactant commonly used during F4 analyses.[140] The components of FL-70 include 3.0% oleic acid, 3.0% sodium carbonate, 1.8% Tergitol (a non-ionic alcohol ethoxylate surfactant), 1.4% tetrasodium ethylene diamine tetraacetic acid (EDTA), 1.3% triethanolamine and 1.0% polyethylene glycol, in water (MSDS, Fischer Scientific). Previous studies have observed increased recovery of organic soil colloids with FL-70 compared to other carrier solutions, likely as a result of decreased sample membrane fouling due to the nature of the FL-70 surfactant.[142,143]

Recovery and sample injection amount

Sample recovery was calculated based on four separate AF4 sample injections. For the initial injection minimal crossflow (0.03 ml min^{-1}) was applied to ensure complete sample elution through the channel. The subsequent three sample injections used one of the crossflows specified previously to achieve sample separation. Peak areas determined using ASTRA software were used to calculate average sample recovery using **Equation 1**

(1) $$Rec\ (\%) = \frac{S}{S_o} \times 100$$

where S is the peak area from a sample injection with crossflow and S_o represents the peak area having limited crossflow. Recoveries for Ag MNPs were calculated using absorbance at 420 nm and soil colloid recovery was calculated using light scattering at 90˚. For mixed environmental colloid-Ag MNP samples recovery was calculated using the ICP-MS signal for Ag (m/z = 107). Triplicate injections were also used to investigate fractionating repeatability.

Validation of AF4

To validate AF4 separation we analyzed NIST traceable polystyrene latex spheres (20, 46, Thermo Scientific), bovine serum albumin (MW 66,463; 3.5 nm r_h, Sigma), alcohol dehydrogenase (MW 150,000; 9.2 nm diameter, Sigma), standard reference Au nanoparticles (22 nm nominal diameter, Nanocomposix, San Diego, CA; 30 and 60 nm nominal diameters, NIST SRMs 8012 and 8013) and Au particles (80 and 98 nm nominal diameter British Biocel International (Cardiff, United Kingdom)) using 0.05% FL-70 as the carrier solution. Channel thickness due to membrane swelling was estimated with 60 nm Au spheres using AF4 theory.[144] Wyatt Chromatogram version 1.04 was used to determine particle size based on fractogram retention time. Calibration curves of retention time versus the hydrodynamic diameter of reference particles were used to validate particle size (**Figure 2-1**). For a crossflow gradient of 0.3- 0.03 ml min^{-1}, the hydrodynamic diameter of the standards was closely correlated with

retention time (r^2=0.9636). Two separate calibration curves were necessary for the next crossflow evaluated to account for the initial gradient of 1.5- 0.3 ml min-1 up to a retention time of 15 minutes and a second gradient of 0.3- 0.03 ml min^{-1} from 15- 45 minutes. Resulting r^2 values were 0.9847 and 0.9848, respectively. Resulting size values were cross validated with values obtained using DLS/MALLS.

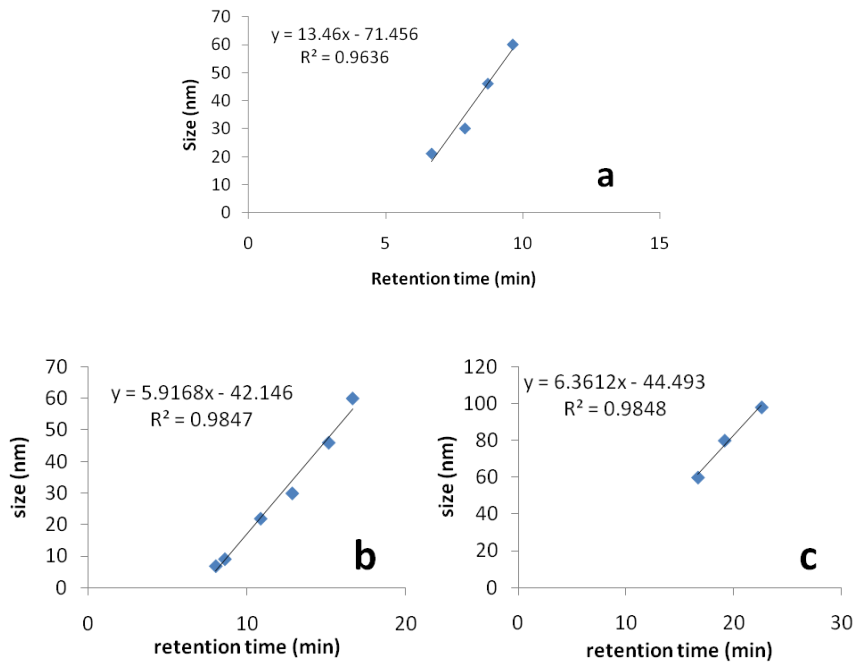

Figure 2-1: Calibration of the AF4 channel with size standards for a crossflow of (**a**) 0.3- 0.03 ml min^{-1} over 30 min and (**b**) decreasing from 1.5-0.3 ml min^{-1} up to a retention time of 15 min followed by (**c**) a gradient of 0.3-0.03 ml min^{-1} from 15- 45 min.

2.3 Results and Discussion

The parameters used during AF4 sample analysis can determine the accuracy and efficiency of particle separation and the resulting observed size distributions.[107] The carrier solution is vital in the separation and recovery of a sample and must be selected based on sample type.[89,120,135] During sample transport the carrier solution prevents interaction with the tubing,

membrane and other particles which could otherwise cause decreased recovery, aggregation, or desegregation of a sample. The resulting fractogram peak(s) can indicate discrepancies in carrier solution composition, injection volume or crossflow rate. Resulting sample sizes should be cross validated with size standards, DLS/MALLS, batch DLS and TEM. For this study, the primary particle size of PVP and CIT-Ag MNPs determined by TEM were 53±1 and 84±24 for PVP and CIT-Ag MNPs, respectively (**Figure 2-2).**

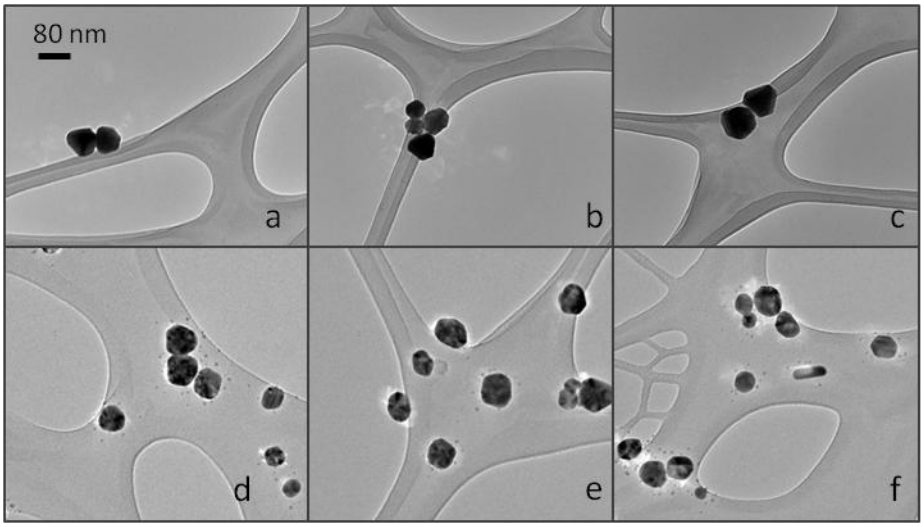

Figure 2-2. Transmission electron microscopy images display the size of the CIT-Ag MNPs (a-c) and PVP-Ag MNPs (d-f).

DLS and PALS data

Mean hydrodynamic radii (r_h) and zeta potential of PVP-Ag MNPs, CIT-Ag MNPs, and soil colloids suspended in18 M Ω DI water and various carrier solutions used during AF4 analysis are shown in **Table 2-2**. Combining the soil colloids with AF4 carrier solutions tended to decrease the average r_h 6-12 nm. However, such decreases are insignificant considering the polydisperse nature of the soil colloids and the incapability of DLS to account for this due to

increased light scattering observed for larger particles which leads to a bias towards larger size measurements.[145] Additionally, particle suspensions in DI water tend to appear larger due to decreased particle diffusion as a result of drag caused by the expanded electrostatic double layer in such low ionic strength media.[145] The addition of salt to a solution (e.g., carrier solution) decreases the thickness of the electrostatic double layer, thereby also increasing the diffusion coefficient for a particle which results in smaller size measurements. A better measurement of alterations in soil colloid particle size is r_{rms}, measured on-line using MALLS, following AF4 separation. Comparably, PVP-Ag MNPs and CIT-Ag MNPs had slight increased or decreased average r_h values, but nothing suggested particle aggregation or desegregation.

Table 2-2. Mean hydrodynamic radius (**r_h** ± standard deviation) and corresponding zeta potential (ZP) are shown for soil colloids, polyvinylpyrrolidone (PVP) coated Ag MNPs, and citrate (CIT) coated Ag MNPs suspended in18 M Ω DI water and AF4 carrier solutions to observe effects of carrier solution. Acronyms indicate sodium dodecyl sulfate (SDS) and sodium pyrophosphate (NaPP) and the asterisk (*) indicates the addition of 200 mg L^{-1} sodium azide. Measurements not available are represented by NA.

	Particle type					
Solution Composition	**Soil colloids**		**PVP-Ag MNPs**		**CIT-Ag MNPs**	
	r_h (nm)	*ZP (mV)*	*r_h (nm)*	*ZP (mV)*	*r_h (nm)*	*ZP (mV)*
Water	101.9 (0.21)	-56.4	42.2 (0.24)	-46.2	30.7 (0.04)	-78.9
Water*	95.65 (0.82)	-47.2	41.9 (0.01)	-11.8	NA	NA
0.05% SDS*	95.95 (0.43)	-49.3	44.6 (0.25)	-20.1	33.85 (0.07)	-51.9
0.5mM NaPP	95.0 (0.21)	-57.5	43.35 (0.08)	-35.8	NA	NA
0.05% SDS and 0.5mM NaPP*	89.5 (0.04)	-56.3	43.3 (0.02)	-12.6	NA	NA
0.05% FL-70	89.95 (0.6)	-60.1	39.5 (0.43)	-31.7	28.6 (0.12)	-71.0
0.05% FL-70*	92.8 (0.96)	-50.5	42.25 (0.25)	-16.7	NA	NA

Electrophoretic mobility measurements in the various carrier solutions indicate minimal changes for soil colloids, but decreased stability in some solutions for Ag MNPs. Electrophoretic mobility measures particle zeta potential or the potential difference between the particle surface charge and the dispersant.[146] Typically, a value of < -25 mV or >25 mV indicates particle stability against aggregation in solution.[147] Slight variations were observed for soil colloids dispersed in each carrier solution, but zeta potential remained indicative of stabilized particles. Likewise, zeta potential indicated consistent stability of CIT-Ag MNPs in all solutions tested. Conversely, several carrier solutions resulted in decreased zeta potential for the PVP-Ag MNPs. The only carrier solutions that did not compromise PVP-Ag MNP stability (based on zeta potential) were 0.5 mM NaPP and 0.05% FL-70, although each decreased zeta potential (made less negative) compared to particle suspensions in DI water by 10.4 and 14.5 mV, respectively.

AF4 using different carrier solutions

Carrier solution had a large impact on the recovery of Ag MNPs during AF4 analysis. Two of the tested carrier solutions, 0.05% SDS with 200 mg L^{-1} azide and 0.05% FL-70 resulted in > 95% recovery for both PVP and CIT-Ag MNPs (**Table 2-3**). Water was tested as a carrier solution for PVP-Ag MNPs to preserve the original sample matrix and thus minimize particle aggregation or desegregation that can result from addition of salt or surfactant.[134,148] Although, poor recovery of PVP-Ag MNPs with water suggests the presence of a surfactant is required for separation.[138] In addition to a weak UV-Vis signal, water also resulted in a light scattering signal too low to make DLS measurements. Elution of PVP-Ag MNPs with 0.05 mM NaPP caused recovery to be < 60%. In addition to NaPP often being used in carrier solutions for fractionating natural colloids,[123,139] NaPP is also often used for the extraction of organics from soils.[149] This suggests highly charged particles like soil colloids or organics (e.g., soil humus) may be more effectively stabilized by NaPP than Ag MNPs which were observed to fluctuate in stability based solely on carrier solution composition (**Table 2-2**). Lastly, the addition of sodium azide to FL-70 decreased sample recovery by 27% for PVP-Ag MNPs. This was likely the result of increased

carrier solution ionic strength which caused a decrease in the zeta potential and electrical double layer thickness for PVP-Ag MNPs, increasing particle interaction with the AF4 membrane.[120] Similar surface charge shielding effects have been observed for natural organic matter exposed to high ionic strength solutions.[150]

Table 2-3: Recovery and retention time of each sample peak are shown as a result of changing AF4 carrier solution composition and holding all other AF4 parameters constant including a sample injection mass of 50 µg for soil colloids and 0.625 µg for PVP and CIT-Ag MNPs. Separation was performed with a crossflow of 0.3 ml min^{-1} ramped down to 0.03 ml min^{-1} over 30 min for all samples. An asterisk (*) indicates the addition of 200 mg L^{-1} sodium azide; NA = not available.

Particle type	Carrier solution	Retention time (min)	% Recovery (stdev)
Soil colloids	500 mg L^{-1} SDS	18.3	54 (5)
	223 mg L^{-1} NaPP	20.5	93 (2)
	500 mg L^{-1} SDS and 223 mg L^{-1} NaPP*	18.8	69 (5)
	500 µl L^{-1} FL-70	16.0	96 (3)
PVP-Ag NPs	Water*	12.1	8 (NA)
	500 mg L^{-1} SDS*	12.4	100 (4)
	223 mg L^{-1} NaPP	11.4	59 (NA)
	500 µl L^{-1} FL-70	11.4	100 (2)
	500 µl L^{-1} FL-70*	13.5	73 (7)
CIT-Ag NPs	500 mg L^{-1} SDS*	12.5	98 (NA)
	500 µl L^{-1} FL-70	11.0	96 (6)

As observed for Ag MNPs, soil colloid recovery was dependent on carrier solution composition. Fractionation with 0.5mM NaPP and 0.05% FL-70 resulted in average sample recoveries of 93 and 96%. Poor recovery (~54%) of soil colloids was observed when 0.05% SDS was used as the carrier solution. This is in agreement with previous work which observed SDS to have minimal to no stabilization effects for clay containing soil suspensions [135]. Attempts at

mixing NaPP and SDS to achieve acceptable sample recovery (> 90%) for both Ag MNPs and soil colloids resulted in < 70% recovery of soil colloids. Mixed NaPP/SDS carrier solutions were therefore not applied to the separation of Ag MNPs.

In addition to recovery, peak shape and time of elution are important for confirming sample separation while avoiding non-ideal sample interactions.[151] More efficient separation can be accomplished at a higher crossflow, but at the expense of peak broadening[111] and can sometimes lead to decreased recovery. For particles normally distributed, such as the Ag MNPs, the ideal peak shape is expected to resemble a Gaussian curve.[140] Previous studies have observed sample overload to lead to peak distortion.[140,152] Therefore, several different injection rates were tested for both PVP-Ag MNPs and soil colloids. An injection mass of 0.625 µg Ag MNPs was observed to give a sufficient signal to achieve a measurable absorbance at 420 nm. Higher injection amounts could lead to carryover effects. Soil colloids were monitored using the light scattered at 90°. The ideal range observed was 15- 25 µL soil colloids (30- 50 µg total solids) to avoid overloading the channel.

The best resolution of PVP-Ag MNPs was observed with either 0.05% FL-70 or 0.5 mM NaPP as the carrier solution. Conversely, peak broadening was observed when PVP-Ag MNPs were eluted with either 0.05% SDS with azide or 0.05% FL-70 with azide (**Figure 2-3**). Poor recovery of PVP-Ag MNPs, delayed peak retention time, and peak broadening observed when 0.05% FL-70 with azide was used as the carrier solution suggests this carrier solution was not effective at preventing non-specific sample interactions such as membrane adsorption. Increased elution time was observed for PVP-Ag MNPs when 0.05% SDS with azide was used as the carrier solution compared to peak position when eluted with 0.05% FL-70. Although good recovery of PVP-Ag MNPs was observed for both solutions, peak broadening and increased retention time resulting from elution with SDS suggest 0.05% SDS with azide may cause shielding of particle surface charges, resulting in increased van der Waals interactions between PVP-Ag MNPs and the ultrafiltration membrane.[120]

Peak shape for soil colloids was observed to be slightly shifted with variation in AF4 carrier solution (**Figure 2-4**). As seen for PVP-Ag MNPs, 0.05% SDS with azide caused increased particle retention compared to elution with 0.05% FL-70. Although, contrary to elution of PVP-Ag MNPs, soil colloid recovery was also reduced 42% using 0.05% SDS with azide. The same shift was observed for the carrier solution containing 0.5mM NaPP with 0.05% SDS and azide and a slightly greater retention was observed when 0.5mM NaPP was used to elute soil colloids. Compared to PVP-Ag MNPs, soil colloid peaks were 3-4 times wider due to the large size distribution of particles in the soil extract. This is typical of fractionated peaks for soil and organic acids which tend to be monomodal, yet polydisperse, as has been observed previously for natural samples.[153]

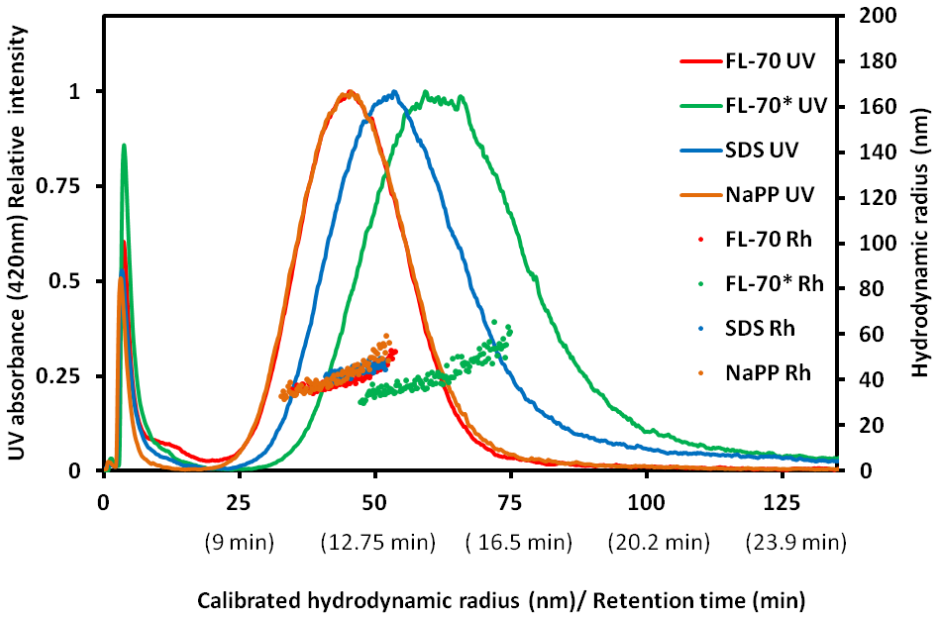

Figure 2-3: Combined AF4 fractograms show the size distribution of 0.625 µg PVP-Ag NPs eluted with different carrier solutions including 500 µl L^{-1} FL-70 (* including 200 mg L^{-1} azide), 500 mg L^{-1} sodium dodecyl sulfate (SDS)*, or 223 mg L^{-1} sodium pyrophosphate (NaPP). The UV trace, calibrated and measured hydrodynamic radii (r_h) of particles are shown. Crossflow was a gradient of 0.3- 0.03 ml min^{-1} over 30 min.

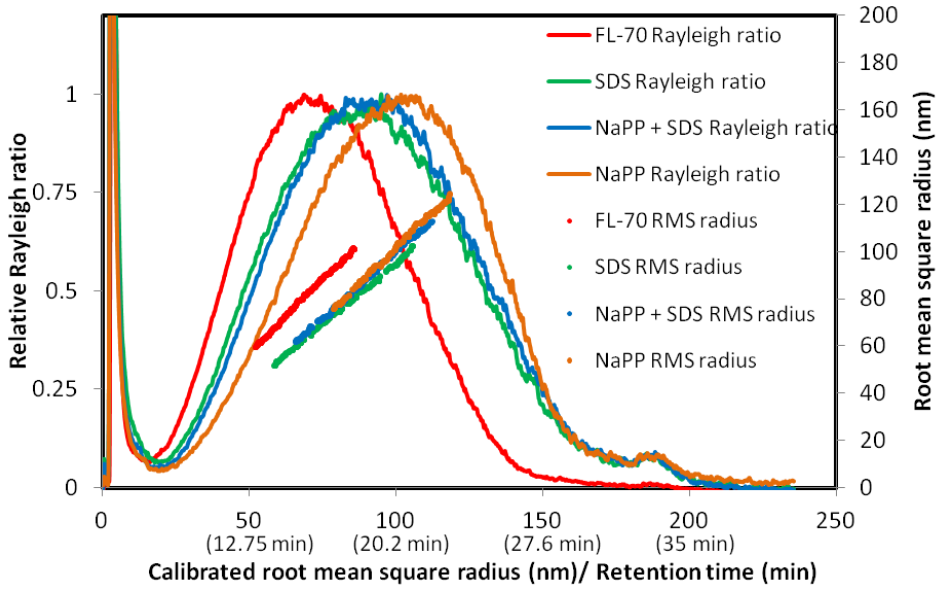

Figure 2-4: Combined AF4 fractograms show the size distribution of 50 µg soil colloids when particles are eluted with different carrier solutions including 500 µl L^{-1} FL-70 (red), 500 mg L^{-1} sodium dodecyl sulfate (SDS) and mg L^{-1} azide (green), 223 mg L^{-1} sodium pyrophosphate (NaPP; orange) or a combination of 500 mg L^{-1} SDS , 223 mg L^{-1} NaPP and mg L^{-1} azide (blue). Light scattering at 90° (solid line), calibrated and measured root mean square radii of particles (dots) are shown for each run. Crossflow was a gradient of 0.3- 0.03 ml min^{-1} over 30 min.

Particle size was determined using the hydrodynamic radius (r_h) for Ag MNPs and root mean squared radius (r_{rms}) for soil colloids. Dynamic light scattering in flow mode works best for smaller particles (r_h < 30 nm) since the motion of the particles causes fluctuations in scattering intensity over longer time scales than the Brownian motion of the smaller particles. Also, static light scattering is not applicable to metal nanoparticles because they cause depolarization of the laser light with respect to the scattering plane leading to non-ideal angular dependence of the scattering. Batch DLS measurements of r_h for PVP-Ag MNPs and soil colloids suspended in DI water were determined to be 42.2 nm and 101.9 nm, respectively. The r_h of PVP-Ag MNPs determined by on-line DLS following AF4 separation was, on average, 42 nm for all carrier

solutions tested, excluding water. Minimal deviations were observed among carrier solution. Conversely, the r_{rms} of soil colloids was more strongly affected by changes in carrier solution composition. The average r_{rms} for soil colloids eluted with 0.05% FL-70 and 0.5 mM NaPP were 165 nm and 200 nm, respectively. This could have been due to the increased ionic strength of FL-70 compared to NaPP which resulted in decreased electrostatic double layer thickness, increased particle diffusion and therefore an overall decrease in observed particle size,[113,151] or simply due to prevention of particle aggregation during the focusing step. The geometric radius of a sphere with an r_{rms} of 165 nm is 213 nm. Note that the DLS measurements are intensity weighted, while the mean r_{rms} values from AF4-MALLS are mass weighted. Elution with 0.05% SDS with azide reveal an average r_{rms} of 150 nm while elution with 0.05% SDS with 0.5 mM NaPP and azide had an average particle size of 175 nm, respectively. This study showed no change in observed r_h for PVP-Ag MNPs with changes in carrier solution. Likewise, the large polydispersivity and non-uniform shape of the soil colloids warrants the minimal differences in observed r_{rms}.

By altering sample injection mass and carrier solution composition for AF4 separation of Ag MNPs and soil colloids, a method was produced to use for the characterization of samples containing Ag MNPs and environmental colloids. The most effective carrier solution for repeatable AF4 separation and good recovery (> 95%) of CIT-Ag MNPs, PVP-Ag MNPs and soil colloids was 0.05% FL-70 (**Figure 2-5**). Injection mass which yielded good peak shape and recovery of Ag MNPs and soil colloids were observed to be 0.625 µg and 50 µg, respectively. Additionally, a crossflow gradient decreasing from 0.3- 0.03 ml min^{-1} over 30 minutes was sufficient for resolving particle from the void peak and getting good separation with short run time.

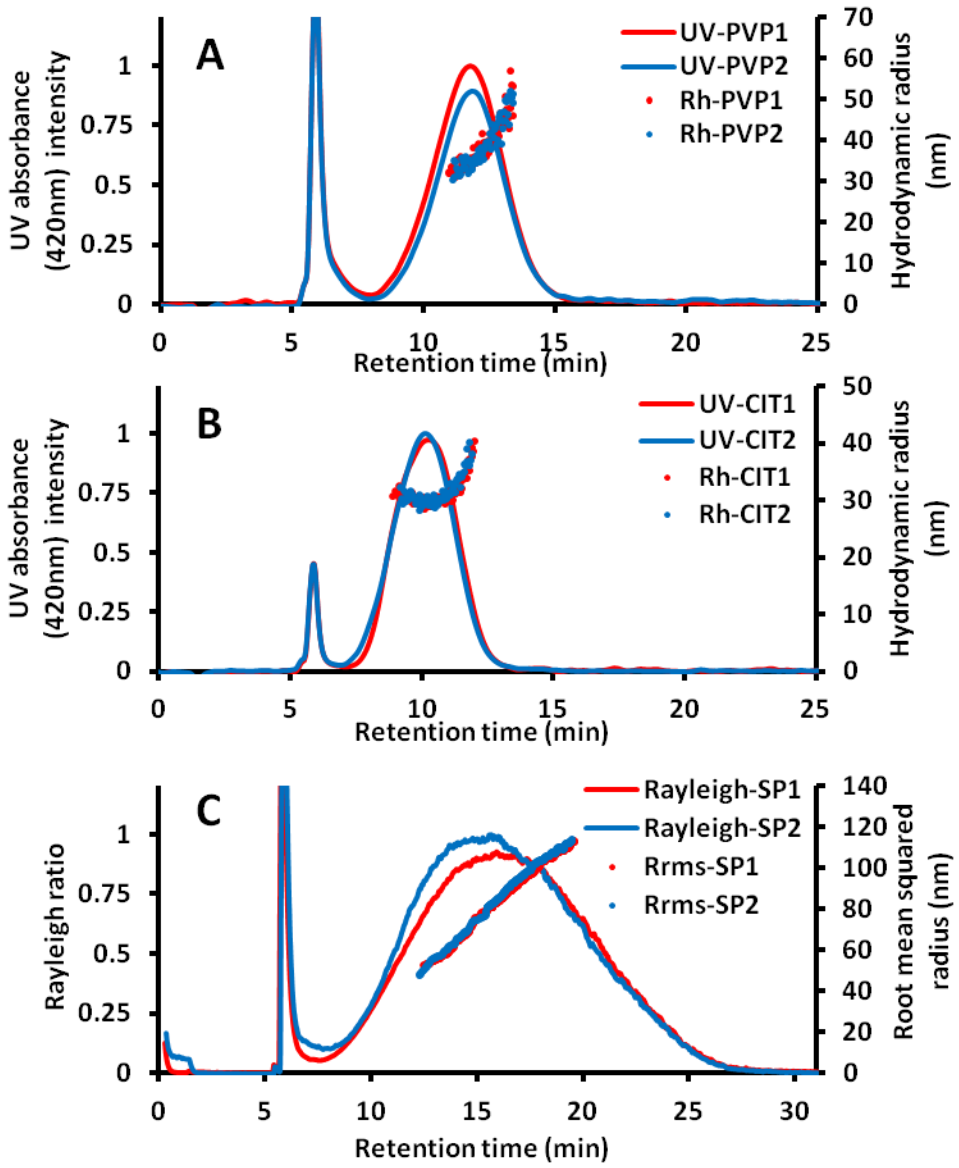

Figure 2-5: Fractogram repeatability is shown for duplicate AF4 sample injections of 0.625 µg (A) polyvinylpyrrolidone (PVP) coated Ag MNPs or (B) citrate (CIT) coated Ag MNPs and for (C) 50 µg soil colloids. Both the UV trace at 420 nm and hydrodynamic radii (R_h) are shown for Ag MNPs. The Rayleigh light scattering trace and root mean squared radii (R_{rms}) are shown for soil colloids. Samples were eluted with 500 µl L^{-1} FL-70 and a crossflow gradient decreasing from 0.3- 0.03 ml min^{-1} over 30 minutes.

Mixtures of environmental colloids and Ag MNPs

The AF4 technique described was subsequently applied to environmental colloid-Ag MNP mixtures using 0.05% FL-70 as the carrier solution, an injection volume of 25 µL (~50 µg), and a crossflow gradient decreasing from 0.3- 0.03 ml min^{-1} over 30 minutes. These parameters were observed to be adequate for the separation of soil colloid-Ag MNP mixtures and resulted in an average sample recovery of 104 ± 9 %, respectively. However, this crossflow rate did not sufficiently provide separation of the sample and void peaks for sludge-Ag MNP mixtures. Therefore, sludge-Ag MNP samples were fractionated using an increased crossflow rate decreasing from 1.5- 0.3 ml min^{-1} over 10 minutes, followed by the gradient of 0.3- 0.03 ml min^{-1} from 15- 45 min (**Figure 2-6**). Soil-Ag MNP samples were also re-evaluated at this crossflow setting. Decreased sample recovery has been observed as a result of increased crossflow,[133] but sample recovery was consistently in the range of 94-100% based on integrated peak areas for all environmental colloid-Ag MNP mixtures. Improved fractionation was observed with an increase in crossflow. Following fractionation, analysis by ICP-MS revealed alterations in the size distribution of Ag MNPs mixed with environmental colloids.

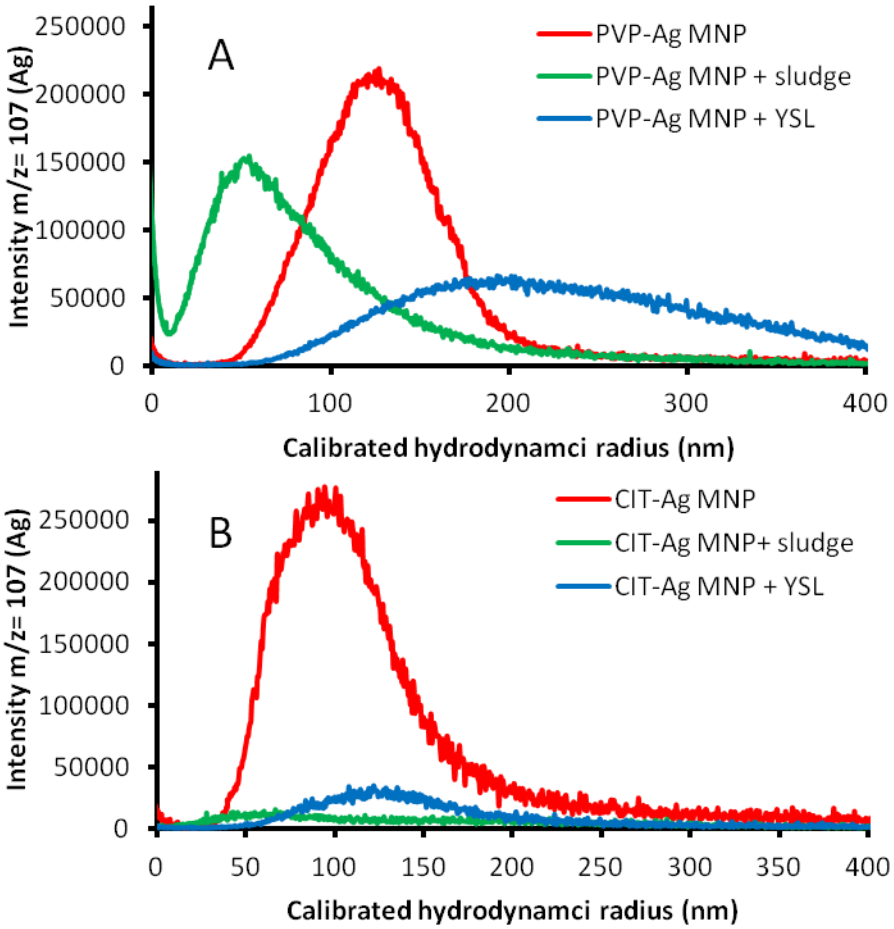

Figure 2-6: Overlaid asymmetrical flow field-flow fractograms using ICP-MS detection of Ag (m/z = 107) for extracted sewage sludge biosolids (sludge) or Yeager Sandy Loam (YSL) soil colloids combined with (**A**) polyvinylpyrrolidone coated (PVP) Ag MNPs or (**B**) citrate coated (CIT) Ag MNPs. The x-axis displays calibrated hydrodynamic diameters. Initial cross flow was 1.5 ml min-^{1}. Cross flow was decreased to 0.3 ml min-^{1} from 5-15min and decreased to 0.03 from 15-45 min.

Through the application of sewage sludge biosolids to agriculture soils, Ag MNPs are expected to enter terrestrial environments, yet risk assessment is lacking reliable *in situ* methods for detecting Ag MNP contaminants in soil. The application of AF4-ICP-MS for the analysis of soil pore waters has been proposed as a valuable technique. This work investigated the role of injection mass, carrier solution composition, and crossflow rate and found that all were important for the separation of Ag MNPs and environmental colloids. This study outlines AF4 parameters for the analysis of soil pore water, based on efficient separation, high recovery and excellent repeatability observed for the analysis of Ag MNPs mixed with environmental colloids.

Chapter 3: Behavior of Ag Nanoparticles in Soil Pore Water: Effects of Particle Surface Coating, Aging and Sewage Sludge Amendment

Annie R. Whitley[†, ‡], Clément Levard [‡, δ], Emily Oostveen[†, ‡], Paul M. Bertsch [†,‡] , Chris J. Matocha[†], Frank von der Kammer[§], Jason M. Unrine [†,‡,*]

[†] University of Kentucky, Department of Plant and Soil Sciences, Lexington, KY 40546, United States

[‡] Center for the Environmental Implications of Nanotechnology, Duke University, Durham, NC, 27708, United States

[§] Department of Environmental Geosciences, University of Vienna, Althanstrasse 14, A-1090 Vienna, Austria

[δ] Surface and Aqueous Geochemistry Group, Department of Geological & Environmental Sciences, Stanford University, Stanford, California 94305-2155, United States

*To whom correspondence may be addressed (jason.unrine@uky.edu)

3.1 Introduction

The growth of nanotechnology has raised public concern about potential environmental and human health effects of manufactured nanoparticles (MNPs) released to the environment.[154,155] Production of consumer products containing MNPs continues to increase despite the lack of sufficient knowledge concerning how they may affect the environment**.** The lack of detection and *in situ* characterization capabilities for nanomaterials in complex biological and environmental matrices also hinders the development of regulations for MNPs in the environment.[89,102] One major class of MNPs currently being used is Ag MNPs, due to their antimicrobial properties.[156] However, Ag MNP containing products, such as paint and textiles have already been shown to release Ag MNPs through normal use.[13,14,15] Silver MNPs are predicted to enter wastewater treatment plants (WWTP) via sewage streams where they are likely to efficiently partition to the sewage sludge and be sulfidized.[17,63] In the United States and elsewhere, the majority of sewage sludge is applied to agricultural lands as biosolids.[157] Because of this, agricultural soils are expected to be a major repository for MNPs. It has been shown that aggregation and dissolution behavior of Ag MNPs can have important implication for environmental fate and toxicity.[47,158] Ag MNP behavior in soil has not been widely investigated,[34,53] in part due to difficulties associated with tracking MNPs in the complex soil matrix. To our knowledge, no studies have been published that attempt to characterize Ag MNP aggregation/dissolution behavior in soil pore water.

Changes in Ag MNP behavior due to modification by the manufacturer (e.g., surface coating) or transformations in the environment via contact with naturally occurring minerals or organic matter (NOM), as well as other ligands further increases difficulties associated with assessing the risk of MNPs to human health and the environment. Differences in surface coating alone can affect Ag MNP aggregation and dissolution behavior under differing environmental conditions.[31,41,45,47] Likewise, environmental constituents such as NOM have been shown to promote particle stability for both MNPs and naturally occurring particles,[49] in some cases by

coating the particle surface.[21,61,77,159] In wastewater treatment plants, Ag MNPs are likely sulfidized which significantly reduces Ag solubility and mobility, resulting in decreased toxicity.[5,17,63,69,81] However, little is known of Ag MNP behavior following application of sewage sludge to agricultural soils including the influence of sulfidation and surface coating.

The objective of this study was to determine the aggregation and dissolution behavior of Ag MNPs soluble in soil pore water as a function of surface chemistry, sewage sludge biosolids pre-incubation and amendment rate as well as soil aging. To observe effects of Ag MNP surface coating and biosolids pre-incubation, we aged soils containing Ag MNPs having different surface coatings and under controlled laboratory conditions with various incubation times between 1 week and 6 months. The Ag MNPs were introduced to the soil either directly or through amendment of sewage sludge containing the Ag MNPs which was pre-incubated for 1 week. We expected differences in surface coating to result in dissimilar Ag MNP behavior, with sterically stabilized PVP Ag MNPs being more stable against aggregation than the low molecular weight organic acid (citrate, CIT) coated particles which would be subject to removal of coating through desorption as well as screening of surface charge by cations in soil solution. Further, we expected sulfidation to negate the effects of manufactured coating[56] within pore waters and aging to yield a decline in pore water Ag.

To accomplish this objective we extracted pore water from soils and analyzed them using asymmetrical flow field-flow fractionation (AF4) coupled to multiple in-line detectors (static/dynamic multi-angle laser light scattering (MALLS/DLS), ultraviolet-visible (UV-vis) diode array (DAD), and an inductively coupled plasma mass spectrometer (ICP-MS)). Ultrafiltration and ultracentrifugation were also used to assess the proportion of dissolved Ag in pore waters. Knowledge of Ag MNP aggregation and dissolution behavior will be vital in tracking Ag MNP mobility and toxicity in soils and ultimately regulating Ag MNP release through application of sewage sludge biosolids.

3.2 Experimental

Silver nanoparticles synthesis and characterization

Two types of Ag MNPs were used having differing surface coatings. First, 60 nm nominal diameter polyvinylpyrrolidone (PVP) Ag MNPs were synthesized as previously described.[127] We also used 60 nm nominal diameter citrate (CIT) coated Ag MNPs made via reduction of $AgNO_3$ by boiling in sodium citrate.[128] Primary particle size and shape was examined using transmission electron microscopy (TEM) using a Jeol 2010 F field emission gun electron microscope (Tokyo, Japan). $AgNO_3$ was used to compare the MNP treatments with ionic Ag behavior. Size distributions were verified in triplicate for both types of Ag MNPs and soil nanoparticles via batch dynamic light scattering (DLS) with a Malvern Zeta-Sizer Nano-ZS (Malvern Instruments, Malvern, UK). Intensity weighted hydrodynamic diameters (d_h) are reported. Electrophoretic mobility was also determined at pH 6 in 18 MΩ deionized water using phase analysis light scattering (PALS).

Soil preparation and aging

Yeager sandy loam (YSL) soil from Estill County, KY was air-dried and sieved to < 1 mm. This soil has already been thoroughly characterized with respect to pH, composition, and cation exchange capacity (**Table A-1**).[50] Determination of soil field capacity, outlined in the appendix, was found to be 19% w/w. Sewage sludge biosolids (sludge) were obtained from a municipal wastewater treatment facility (Winchester, KY). Chemical composition of the sludge is reported in **Table A-2**.

Sludge was spiked with Ag MNP suspensions or $AgNO_3$ solution to obtain a final concentration of 200 mg Ag kg^{-1} solid (soil + sludge) when combined with soil. The Ag MNPs were synthesized in the colloidal phase, so no dispersion step was necessary. Spiked sludge was incubated for 1 week in an environmental chamber at 20° C and rewetted daily to maintain

constant moisture content. Sludge was then combined with 10 g YSL to achieve either 1 or 3% sludge dry mass. Soil samples without sludge were spiked directly with 200 mg Ag kg^{-1} soil for each treatment. Soil mixtures were prepared in 20 mL glass scintillation vials. Blank samples consisted of YSL at 0, 1, and 3% sludge with no Ag addition. Samples were maintained at 19% (v/w) moisture content in an environmental chamber at 20° C in the dark for 1 week, 2 months or 6 months. Soils were rewetted as necessary every three days to maintain constant moisture content. Three replicates were included for each Ag treatment at each time point.

Soil pore water extraction and Ag dissolution measurements

To extract soil pore water, we added a volume of 18 MΩ deionized (DI) water equivalent to 2.5X the moisture content of the soils. The soil slurry was added to a 20 mL syringe plugged with borosilicate glass wool pre-wetted with DI water. The syringe was suspended in a 50 mL centrifuge tube and centrifuged 8 min (25 ºC) at 1000 rpm to allow the pore water to elute into the centrifuge tube. We measured 73±13%, 81±10% and 68±12% recovery of PVP-Ag MNPs, CIT-Ag MNPs and Ag ions for the pore water extraction apparatus. Pore water extracts were filtered with 30 mm, 1.0 µm borosilicate glass fiber syringe filters (GE Osmonics, Fairfield, CT, USA) prior to analysis. We obtained 95±2%, 107±5% and 49±2% recovery of PVP-Ag MNPs, CIT-Ag MNPs and Ag ions after filtering. This step was required to remove particles larger than 1 µm prior to AF4 analysis to avoid steric inversion where particles larger than 1 µm elute in the reverse order of particles smaller than 1 µm.[160] Total Ag in pore water was determined by digesting samples in 7.5 M concentrated trace-metal grade HNO_3 followed by dilution and ICP-MS (Agilent Technologies 7500cx; Santa Clara, CA, USA) analysis. Total organic carbon (TOC) and nitrogen (TN) in pore waters were determined using a FlashEA 1112 elemental analyzer (ThermoFisher Scientific Inc., Waltham, MA, USA). Anion (Fl^-, Cl^-, NO_2^-, Br^-, NO_3^{2-}, PO_4^-, and SO_4^-) concentrations in pore waters extracted from blank soil samples (0, 1, and 3% sludge) and sludge were measured at experiment start and after aging using a Metrohm 792 Basic ion

chromatograph (Herisau, Switzerland) having a MetroSep RP guard disc holder and a MetroSep A column. The eluent was 3.2 mmol L^{-1} $NaCO_3$ and 1 mmol L^{-1} HCO_3^-. Cations (Na^+, Mg^{2+}, Al^{3+}, K^+, Ca^{2+}, Mn^{2+}, Fe) were also determined via ICP-MS analysis. Pore water pH was determined immediately after 1µm filtration**.**

After pore water extraction, 200 mg dried sample soil was digested in 9 mL trace-metal grade HNO_3 and 3 mL HCl using a MARS Express microwave digestion system (CEM, Matthews, NC) according to USEPA method 3052.[161] Total Ag in the digestates was determined using ICP-MS following USEPA method 6020[162] including blanks, duplicate digestions, and standard reference materials (SRM 2711a Montana II soil and 2781 Domestic sludge, National Institute of Standards and Technology). Recovered acid leachable Ag in the SRMs was 93± 3.2% and 93±1.5 %, respectively (n=8). Pore waters were analyzed for dissolved Ag using 3 kDa molecular weight cutoff (MWCO) regenerated cellulose ultrafiltration devices in addition to ultracentrifugation at 239,311 x g for 60 min to account for Ag bound to DOM > 3 kDa that would not have passed through the ultrafiltration membranes. Ultrafiltrates and ultrasupernatants were acidified 0.15 M HNO_3 to preserve for analysis. Recovery of Ag for ultrafiltration and ultracentrifugation was 52 ± 1% and 79 ± 0.4% (mean ± standard deviation), respectively. Ag concentrations were corrected for recovery in subsequent analyses.

Statistical analyses

For statistical comparison among Ag concentrations we tested homoscedasticity using the Bartlett test and Normality using the Shapiro-Wilk test. Since the data were non-normally distributed and had nonhomogeneous variance we used the Kruskal-Wallace test to determine differences in mean Ag concentrations. Individual differences among means were determined with the Wilcoxon Rank-Sum test ($p < 0.05$).

AF4-ICP-MS analysis

An asymmetrical flow field-flow fractionation (AF4) system was used to separate samples based on hydrodynamic radius (Wyatt Eclipse 3, Santa Barbara, CA, USA). All samples were analyzed within 12 hours of extraction because extended storage at 4˚ C beyond this time led to decreased intensity of Ag-containing particles within fractograms, likely resulting from the aggregation of particles. Parameters used for AF4 are shown in **Table A-3**. The eluent from the AF4 channel entered an on-line DAD (Agilent 1200 series) used to monitor Ag MNP absorbance at 420nm, to MALLS/DLS detector (Wyatt DAWN HELEOS-II) which measured light scattering intensity at 18 angles with DLS measured at 100.3º and finally to an ICP-MS system used for element specific detection. Masses monitored on the ICP-MS included Ag (m/z =107, 109), Al (m/z=27), Fe (m/z=56), Mn (m/z=55), and Si (m/z=28). Agilent Chemstation software was used to collect UV-Vis data, Wyatt ASTRA version 5.3.4.11 was used to process light scattering data and Agilent ICP-MS chromatographic software version C.01.00 was used to process elemental distribution fractograms collected via the ICP-MS. A flow splitter diverted a portion of the sample flow to waste to reduce the eluent flow rate to the optimal flow rate for the ICP-MS nebulizer (0.25 ml min^{-1}). The portion diverted to the waste was also diverted to a fraction collector (Agilent 1200 series), with fractions collected for additional analyses including TEM. For TEM analysis, particles from AF4 fractions were deposited onto TEM grids placed on 3 kDa ultrafiltration membranes within centrifugal filtration devices. The devices were centrifuged allowing the solutes to pass through the ultrafiltration membrane, while particles were deposited onto the grid. Dried grids were analyzed by TEM and energy dispersive X-ray spectroscopy (EDS) for elemental identification.

Validation of AF4-separations

To validate AF4 separation we analyzed bovine serum albumin (MW 66,463; 7 nm d_h, Sigma), National Institute of Standards and Technology (NIST) traceable polystyrene latex

spheres (20 and 46 nm diameters, Thermo Scientific), alcohol dehydrogenase (MW 150,000; 9.2 nm diameter, Sigma), standard reference Au nanoparticles (22 nm nominal diameter, Nanocomposix, San Diego, CA; 30 and 60 nm nominal diameters, NIST Standard Reference Materials (SRM) 8012 and 8013) and Au particles (80 and 98 nm diameter, British Biocell International, Cardiff, United Kingdom). Calibration curves of retention time versus diameter of reference particles were used to determine particle size. Calibration curves are shown in **Figure A-1**. These values were cross validated with values obtained using DLS/MALLS. Pore water particle sizes were also validated using DLS/MALLS for soils not amended with sludge (**Figure A-2**). Sewage sludge particles strongly absorbed at 658 nm (the wavelength of the MALLS laser) so data from DLS/MALLS was not valid for soils amended with 1 and 3% sludge and TEM was instead used to confirm calibrated particle sizes for samples containing sludge.

EXAFS

Following extraction of pore waters, 1 week soils treated with $AgNO_3$, PVP-Ag MNP and CIT-Ag MNP and soils amended with 3% sludge and treated likewise were analyzed by Extended X-Ray Absorption Fine Structure (EXAFS) spectroscopy using linear combination fits of model compounds to determine speciation of Ag retained in the soils. Details of the EXAFS data collection and analysis can be found in the Appendix.

3.3 Results

TEM, EXAFs and Pore Water Chemistry

Pore water chemistry and Ag speciation in soils are largely altered following the addition of sludge to soil. Zeta potentials of PVP-Ag MNPs and CIT-Ag MNPs were -46.2±14.4mV and -78.9±17mV (Hückel approximation), respectively. Pore waters from sludge amended soils have

increased amounts of Na^+, Ca^{2+}, Cl^-, Br^-, SO_4^{2-}, and most notably K^+ and PO_4^{2-} (**Table A-4,5**), in addition to increased organic carbon concentration (**Figure A-4**). Aging resulted in increased concentrations of SO_4^{2-}, Mg^{2+}, Ca^{2+}, and Fe^{2+}, decreased Cl^- and decreased organic carbon On average, pore waters from 0%, 1%, and 3% sludge amended soils had 2.0, 5.3 and 5.6 g L^{-1} total suspended solids, respectively. The best linear combination fits (LCF) of EXAFS data suggests that Ag speciation in $AgNO_3$ treated soil without sludge contains Ag_2S (33%), AgCl (30%), Ag-acetate (25%), and Ag metal (13%). The best fit for soils amended with 3% sludge treated with $AgNO_3$ has an increased proportion of Ag_2S (52%) as well as Ag-glutathione (36%), while the proportion of Ag metal (12%) changed little. In soils without sludge, 100% of Ag in PVP-Ag MNP and CIT-Ag MNP remained as Ag metal, while incubation in sludge amended soil led to significant transformations to Ag_2S (70% and 78%, respectively).

Total and Dissolved Ag in Pore Waters

Total pore water Ag concentrations are expressed as the % Ag in soil present within the pore water to account for slight differences between total Ag concentrations in soil. Aging soils (un-amended with sludge) for 1 week resulted in pore water Ag concentrations as high as 41% (190 mg Ag L^{-1}) and as low as 1% (4.4 mg Ag L^{-1}) of the total added Ag for CIT-Ag MNP and PVP-Ag MNP treatments, respectively. Soils treated with $AgNO_3$ and PVP-Ag MNPs had significantly higher Ag concentrations in pore waters from sludge amended soils, compared to non-amended soils. Addition of sludge had no impact on Ag pore water concentrations for CIT-Ag MNP soils. In comparison to $AgNO_3$ and PVP-Ag MNP treated soils, CIT-Ag MNP treated soil had over 35% more pore water Ag after 1 week in non-amended soils (**Figure 3-1**).

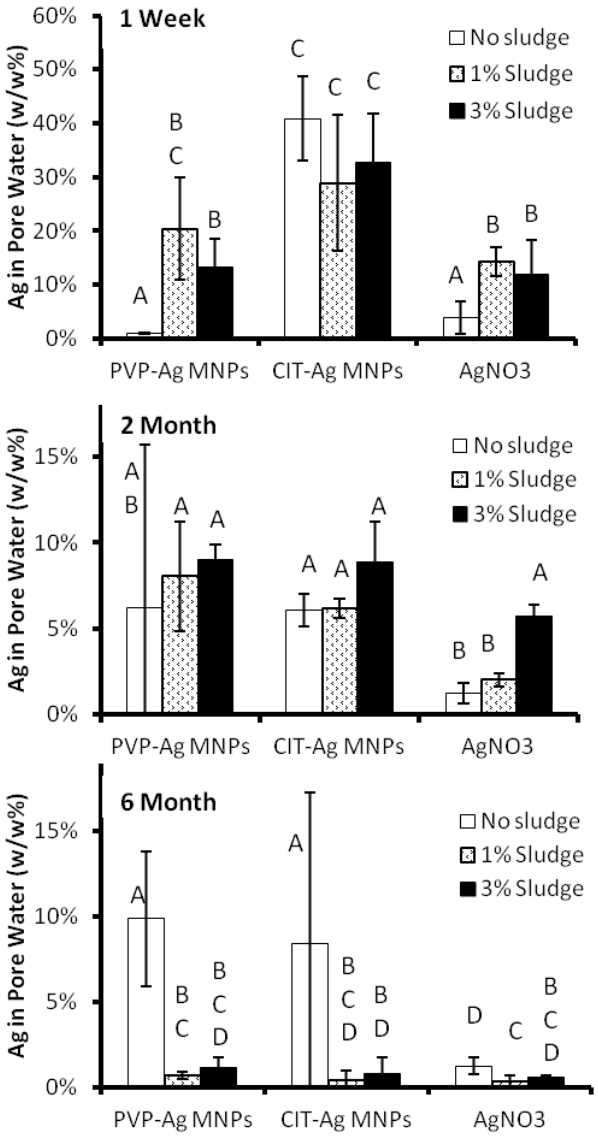

Figure 3-1. Total Ag expressed as a percentage of the soil concentration (w/w%) contained within filtered (1.0 µm) pore water samples from soils treated with silver nitrate ($AgNO_3$), polyvinylpyrrolidone coated Ag nanoparticles (PVP-Ag MNP), or citrate coated Ag nanoparticles (CIT-Ag MNP) amended with 0, 1, or 3% sludge (w/w; dry mass) and aged for 1 week, 2 or 6 months. Bars with the same letter are not significantly different among treatments ($AgNO_3$, PVP-Ag MNP, CIT-Ag MNP) for a given incubation time (1 week, 2 or 6 months). All treatments were significantly different than control samples amended with 0, 1, or 3% sludge and aged for 1 week, 2 or 6 months.

In most cases, less Ag is observed in soil pore waters following 2 months of aging. Pore water Ag in the $AgNO_3$ treated, non-amended soil was comparable to the 1% sludge treatment, although both had significantly less Ag than the 3% sludge treatment. Non-amended and 1% sludge soils treated with $AgNO_3$ had significantly less pore water Ag than all other soils with the exception of non-amended PVP-Ag MNP treated soil which displayed a wide range of variability among replicates. Contrary to other Ag treatments, non-amended PVP-Ag MNP treated soil had higher pore water Ag concentrations after 2 months of aging than observed after 1 week. In addition, after aging 2 months, sludge had no effect on PVP-Ag MNP Ag pore water concentrations. Pore water Ag for CIT-Ag MNP treatments decreased from 1 week to 2 months of aging, but there was still no effect due to sludge amendment.

Ag was still present in all soil pore waters following 6 months of aging. However, less than 2% Ag was recovered in pore waters from non-amended $AgNO_3$ treated soils and all Ag treatments amended with sludge. Significantly more Ag partitioned to pore waters in non-amended Ag MNP treatments; approximately 9.9% and 7.1% total Ag were measured for PVP-Ag MNP and CIT-Ag MNP treatments. Unlike $AgNO_3$ and CIT-Ag MNP treated soils, pore water Ag concentrations increased with aging for non-amended PVP-Ag MNP soil.

The proportion of total pore water Ag that was dissolved was determined by ultrafiltration and ultracentrifugation. Dissolved species bound to NOM larger than 3 kDa but less than 7-10 nm (equivalent to about 100 kDa)[163] may be retained in the filtrate during ultrafiltration, but remain in the supernatant following ultracentrifugation.[47,143] The Ag concentration is typically greater in the ultrasupernatant than the ultrafiltrate for all samples (**Figure 3-2**). One exception to this is the non-amended $AgNO_3$ treated soils aged for 1 week and 2 months. All of the Ag in pore water from $AgNO_3$ treated soils is accounted for in the dissolved form (< 3 kDa; 0.9 nm) from both ultrafiltrates and ultrasupernatants. Following 6 months only 15% and 21% total pore water Ag is accounted for in the ultrafiltrate and ultrasupernatant of the

non-amended $AgNO_3$ treated soil. In $AgNO_3$ soils amended with sludge, dissolved Ag accounts for an increased proportion of the total pore water Ag with increased aging time. For the 1% and 3% sludge amended soils approximately 6% and 1% dissolved Ag present after 1 week increased to 45% and 30% total Ag after 6 months. Since less than 4% dissolved Ag is accounted for in the ultrafiltrate for all sludge amended $AgNO_3$ treatments, most dissolved Ag is likely bound to NOM or colloids that have a d_h between 1 nm and 10 nm.

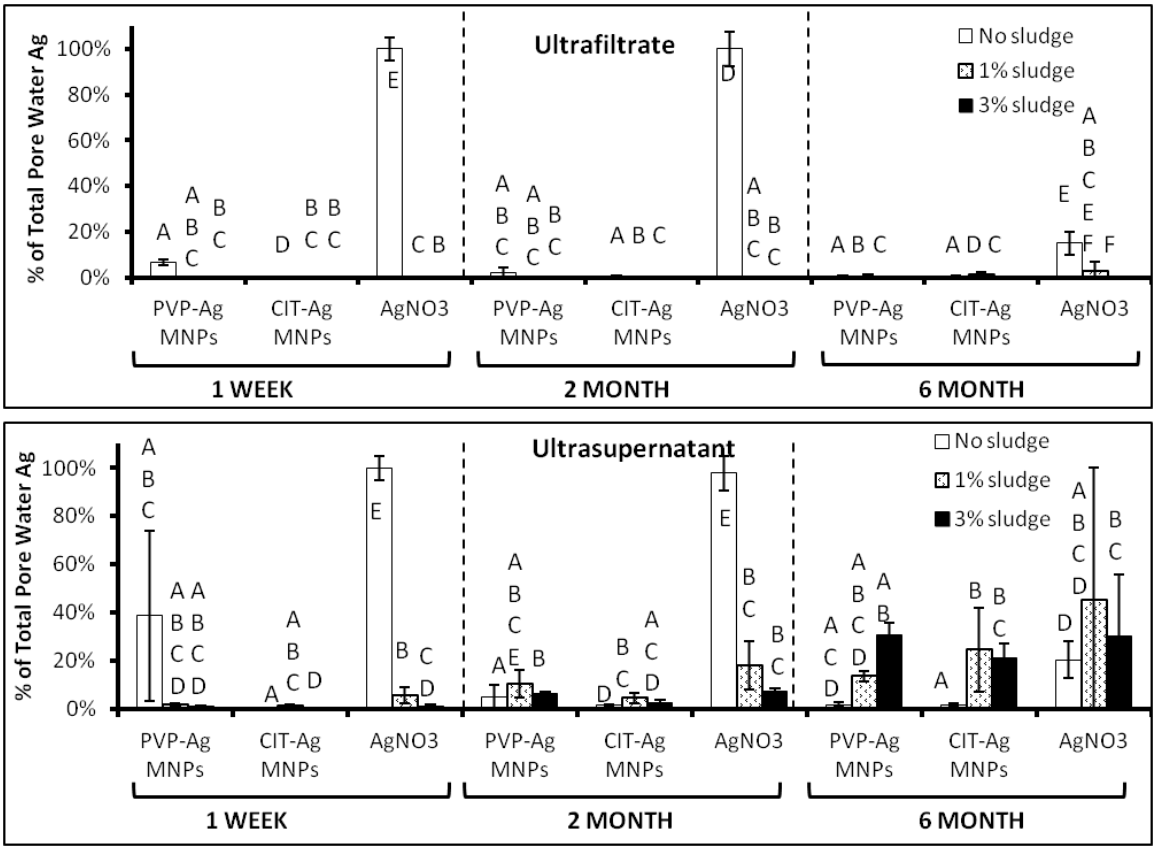

Figure 3-2. Dissolved Ag in filtered (1.0 µm) pore water samples from soil treated with silver nitrate ($AgNO_3$), polyvinylpyrrolidone coated Ag nanoparticles (PVP-Ag MNP), or citrate coated Ag nanoparticles (CIT-Ag MNP) amended with 0, 1, or 3% sludge (w/w; dry mass) and aged for 1 week, 2 or 6 months following ultracentrifugation (ultrasupernatant) or ultrafiltration (ultrafiltrate). Bars with the same letter are not significantly different among treatments ($AgNO_3$, PVP-Ag MNP, CIT-Ag MNP) for a given incubation time (1 week, 2 or 6 months).

The proportion of dissolved Ag in soil pore waters was similar for both Ag MNP treatments with aging. At 1 week there was 40 % more dissolved Ag in non-amended PVP-Ag MNP treated soil than CIT-Ag MNP; however there was no statistically significant difference due to variation among PVP-Ag MNP soil replicates. Less than 3% of pore water Ag was accounted for in ultrasupernatants from sludge amended Ag MNP soils at 1 week. Following 6 months aging, dissolved Ag in ultrasupernatants of Ag MNP pore waters is comparable to $AgNO_3$ treatments (on average, approximately 28% of total Ag in pore water).

AF4 Multidetection Analysis

The size distribution and quantity of Ag containing particles from $AgNO_3$ treated soils was altered with addition of sewage sludge. In pore water from the non-amended $AgNO_3$ treated soil, Ag is only observed in fractograms at the first time point (1 week; **Figure 3-3**). The average d_h is approximately 250 nm. Following aging, Ag is absent from fractograms and is likely immobilized due to binding to the soil solids. It is important to note that any Ag complexes < 5 kDa (~ 1 nm) would permeate the AF4 membrane and would not appear in the fractograms.[143] Measurements of total and dissolved Ag account for such losses. Addition of sludge to $AgNO_3$ treated soils decreased the average particle size to < 90 nm. In several fractograms, what appears to be tailing of the void peak at 15 nm is likely Ag bound to NOM (~ 5 nm), which can be resolved from the void peak at a higher crossflow (**Figure A-5**). With the addition of sludge Ag appears in this portion of the fractogram even after aging soils for 2 months.

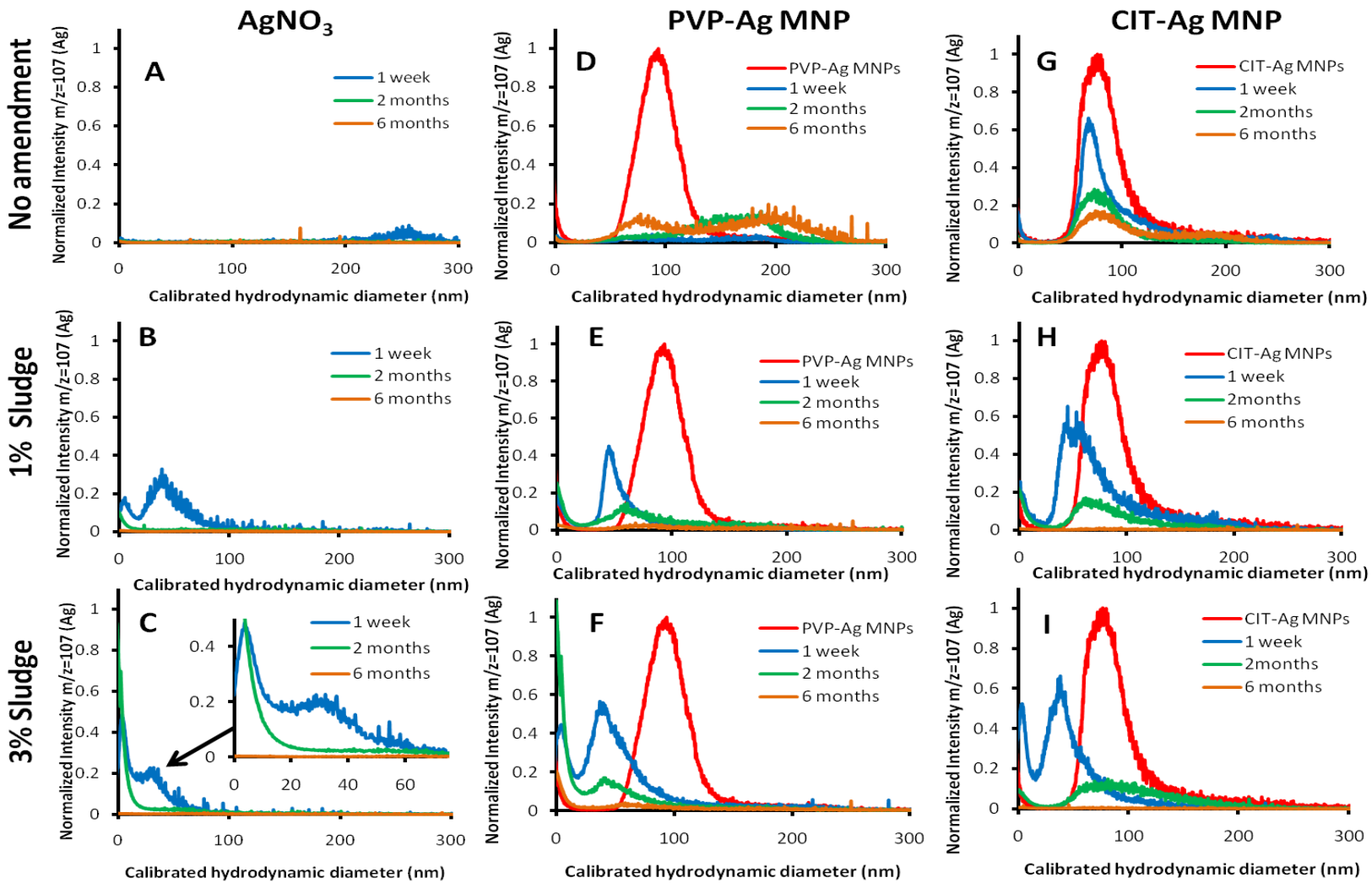
AgNO3
PVP-Ag MNP
CIT-Ag MNP
No amendment
1% Sludge
3% Sludge
A
B
C
D
E
F
G
H
I
1 week
2 months
6 months
PVP-Ag MNPs
CIT-Ag MNPs
2months
Normalized Intensity m/z=107 (Ag)
Calibrated hydrodynamic diameter (nm)

Figure 3-3. Asymmetrical flow field-flow fractograms using ICP-MS detection of Ag (m/z= 107) for pore waters extracted from polyvinylpyrrolidone coated Ag nanoparticles (PVP-Ag MNP; **A-C**), citrate coated Ag nanoparticles (CIT-Ag MNP; **D-F**) or silver nitrate ($AgNO_3$; **G-I**) treated soils amended with 0% (**A, D, G**), 1% (**B, E, H**), or 3% (**C, F, I**) sludge (w/w; dry mass) and aged for 1 week, 2 or 6 months. The y-axis displays the normalized Ag intensity. The x-axis displays calibrated hydrodynamic diameters.

Soils treated with PVP-Ag MNP typically had more Ag containing particles in soil pore water than $AgNO_3$ treatments. After 1 week, pore water Ag from non-amended PVP-Ag MNP treated soil was present in only small quantities, yet with aging a larger peak (2 months) or peaks (6 months) were observed (**Figure 3-3**). As observed for $AgNO_3$, the size distribution of Al and Si containing particles, which may be alluminosilicate clay particles, was slightly different than the trace for Ag (**Figure 3-4**). Particles containing Ag recovered in sludge amended PVP-Ag MNP soils exhibit size distributions that were slightly larger than the particles observed in the $AgNO_3$ sludge treatments at 1 week. Peak intensities decrease with aging, but Ag containing particles are still present in sludge amended PVP-Ag MNP soils after 6 months. Average Ag containing particle sizes are approximately 75 nm and 55 nm for 1% and 3% sludge PVP-Ag MNP soils at 6 months.

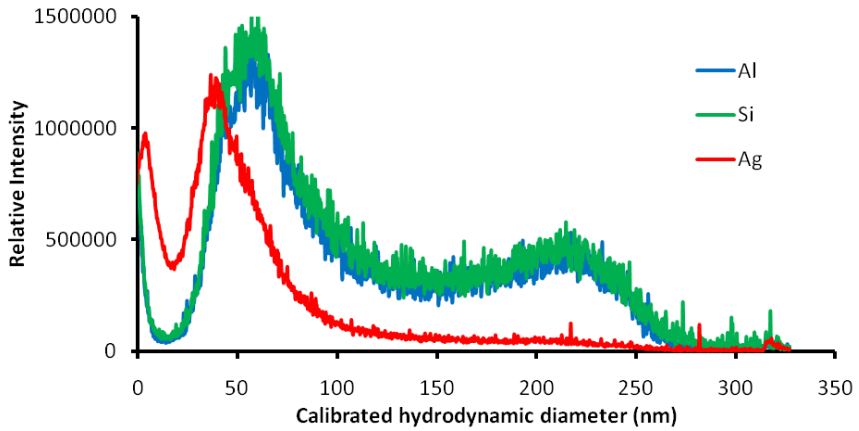

Figure 3-4. Representative asymmetrical flow field-flow fractogram using ICP-MS detection of Al (m/z = 27), Si (m/z = 28) and Ag (m/z = 107) for pore water extracted from soil amended with 3% sludge containing PVP-Ag MNP (w/w; dry mass). The y-axis displays the relative peak intensities because concentrations of Al and Si in soil pore waters were exponentially higher than Ag concentrations. The x-axis displays calibrated hydrodynamic diameter determined from reference particles.

Fractograms for non-amended CIT-Ag MNP treated soils display Ag containing peaks comparable in size to the original particles (80 nm). Such particles were extractable even after aging soils for 6 months. Addition of sludge decreased the average Ag containing particle size distribution to < 80 nm, comparable to the $AgNO_3$ and PVP-Ag MNP treatments with sludge. While the 1% sludge CIT-Ag MNP treatment had a wider size distribution than the other treatments, almost all Ag MNP treatments display more intense peaks than observed for $AgNO_3$. At 6 months of aging, Ag appeared to be absent in pore waters extracted from CIT-Ag MNP soils with sludge.

Validity of AF4 Separation

Retention time of standard reference materials using UV absorbance and light scattering data validated our calibration curve. Calculated sizes closely corresponded to nominal particle sizes. Average Ag recovery was 100 ± 8% for samples at all time points. Fractograms from replicate microcosms slightly varied in intensity; representative samples are shown in **Figure 3-3** and individual replicates are available in the Appendix (**Figure A-7**). Data from Fe and Mn are not shown due to low intensity, although size distributions generally followed those seen for Al and Si. In addition, light scattering data from MALLS indicated that particle sizes were similar to calibrated particle sizes (**Figure A-2**), although some differences were observed. Further validation of AF4 separation was provided through TEM analysis of collected fractions as described below.

TEM

The primary particle size of PVP and CIT-Ag MNPs determined by TEM were 53±1 and 84±24 for PVP-Ag MNPs and CIT-Ag MNPs, respectively (**Figure A-8**). TEM was also used to validate AF4 particle size distributions and characterize Ag containing particles in 1 week treatments for select soil-sludge samples. Intact Ag MNPs similar in size to the original particles are verified in pore water extracted from non-amended CIT-Ag MNP treated soil in AF4 fractions that corresponded to the pristine primary particle size (**Figure 3-5**). EDS analysis confirmed the composition of these particles as primarily containing Ag with some traces of S (**Figure A-10**). No Ag nanoparticles are observed via TEM in pore water from non-amended PVP-Ag MNP soil from the size fraction that corresponded to the original particle size; however, actual concentrations are very low. In both PVP-Ag MNP and CIT-Ag MNP soils amended with 3% sludge, a collection of smaller Ag nanoparticles were observed with sizes corresponding to calibrated sizes from AF4. These were confirmed with EDS to contain Cl and in some cases S

(**Figure A-10**), although some particles appeared to be unaltered judging from the electron density and morphology of the particles.

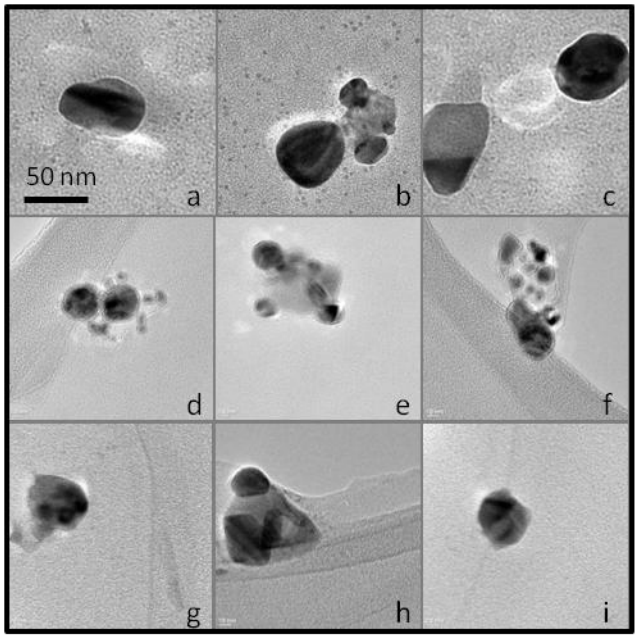

Figure 3-5. Transmission electron microscopy (TEM) images confirming the presence of Ag nanoparticles in pore waters extracted after 1 week from non-amended CIT-Ag MNP treated soil (a-c), 3% sludge (w/w; dry mass) CIT-Ag MNP treated soil (d-f) and 3% sludge amended PVP-Ag MNP treated soil (g-i). Accompanying energy dispersive spectra (EDS) can be found in the Appendix **(Figure A-10**).

3.4 Discussion

Surface coating was demonstrated to influence Ag MNP stability in pore water extracted from non-amended soil for up to six months. Relatively high concentrations of intact CIT-Ag MNPs are observed in pore water while PVP-Ag MNPs were absent and likely bound to solid phases in the soil. This finding is in agreement with another study which observed PVP-Ag MNPs to have a high affinity for soil solids in a sandy loam soil.[164] Other work has predicted that

PVP-Ag MNPs would be among the most mobile Ag MNP under environmental conditions compared to several other capped Ag MNPs, including CIT-coated.[31,43] However, our results suggest that after 1 week electrostatically stabilized CIT-Ag MNPs were more stable in soil pore water than sterically stabilized PVP-Ag MNPs. It is likely that the uncharged PVP coating has a relatively high affinity for the soil solid phases, while the CIT coating, possessing a net negative charge would repel soil surfaces. It is also possible that CIT, having a lower molecular weight, more readily exchanges with dissolved organic matter (DOM) than the high molecular weight PVP. Previous studies have shown DOM to have a stabilizing effect on Ag MNPs.[47,49]

Pre-incubation of Ag with sludge and subsequent amendment to soils had a large effect on the ensuing behavior of Ag and seemed to negate the effect of initial Ag MNP coating. Surface coating had little effect on Ag MNP aggregation state in pore waters in soils amended with Ag containing sludge, as evidenced by similarity of the fractograms for CIT-Ag MNPs and PVP-Ag MNPs. Comparatively, non-amended soils had higher pore water Ag concentrations at six months for Ag MNP treatments compared to $AgNO_3$, likely as a result of increased stability of Ag MNPs compared to Ag ions which had a strong affinity for the immobile soil solids. Application of Ag to soil through sludge resulted in similar total Ag pore water concentrations in all treatments, likely due to extensive sulfidation of the particles. While Ag speciation in YSL soil was found to be 100% Ag (0) for both Ag MNP treatments, introduction of Ag MNP to sludge transformed the particles resulting in extensive sulfidation. Results from EXAFS LCF are in agreement with previous studies showing sulfidation of Ag MNP as a major environmental transformation.[56,63,165] Levard et al. observed that the PVP surface coating did not inhibit sulfidation or subsequent aggregation.[56] Comparable results among PVP and CIT-Ag MNPs suggest that the CIT coating also does not inhibit sulfidation. A small fraction of Ag (0) was observed in sludge treatments for both $AgNO_3$ and Ag MNPs. It is possible that this is the result of formation of a core-shell Ag(0)-Ag_2S structure as previously described.[56] Conversely, one

study observed ionic Ag reduced to Ag(0) as a major pathway for the removal of free Ag^+ ions from solution when exposed to an anaerobic soil with organic matter.[166]

Interestingly, the proportion of dissolved Ag in pore water based on ultracentrifugation increased with aging for all sludge amended soils, despite this sulfidation. This was not apparent in ultra-filtered samples, suggesting that Ag in sludge amended soils is exchangeable with organic molecules that have between 1 nm and 10 nm d_h. This fraction is observed eluting near the void volume in the AF4-ICP-MS fractograms and may potentially be separated from the void at higher cross-flows (**Figure A-5**). This has extremely important implications because it suggests that ionic Ag, which has the potential to cause toxicity, is present within the pore water of sludge amended soils, despite extensive sulfidation and aging for 6 months. We postulate that this is due to exchange of Ag between Ag_2S and sulfhydryls on macromolecules originating from the sludge. Increases in the concentration of SO^{3-} over time indicated that oxidizing conditions may have existed in the soils during aging, perhaps facilitating this process. These sulfhydryl bound Ag moieties would not be observed in the EXAFS since the fraction is less than 5% of the total Ag.

In soils amended with sludge containing Ag MNPs at 1 week, a sharp, tailing, Ag peak appeared in the fractograms with a peak particle size around 35 nm. Analysis of fractions collected from this peak by TEM confirmed the presence of Ag rich particles in the Ag MNP treatments. Some of the particles appeared intact while others appeared to have been partially converted to Ag_2S or AgCl. We propose three possibilities to explain this observation: (1) a smaller sub-population of particles is preferentially dispersed, (2) some of the observed particles have been precipitated from the release of dissolved Ag from oxidative dissolution, and/or (3) some of the particles that appear untransformed have actually been weathered to a smaller size through dissolution processes. At week one, we also observed Ag within a similar size range in the $AgNO_3$ treatment when sludge was added. These could have also been precipitated Ag_2S particles. The similarity in size between these particles and the particles in the Ag MNP

treatments suggests that they originate from dissolution of the Ag MNPs and subsequent re-precipitation of Ag_2S and AgCl. We observed more of these particles in the Ag MNP treatments than the $AgNO_3$, although the particles diminished with aging time in all treatments. After six months of aging, few particles were observed in pore waters from any sludge amended soil, regardless of Ag form.

This study suggests that surface coating dictates Ag MNP mobility when directly exposed to soil, but initial Ag MNP coating has less relevance on aging or when added via sewage sludge amendment. Non-amended soil treated with CIT-Ag MNPs has ten-fold more Ag in soil pore water after 1 week than soil treated directly with PVP-Ag MNP or $AgNO_3$. In sludge amended soils, similar pore water Ag concentrations and size distributions of Ag containing particles are observed for both Ag MNP and $AgNO_3$ treatments; although fractograms revealed more Ag in the colloidal phase for Ag MNP treatments. In all sludge amended soils, regardless of Ag sulfidation, a steady release of Ag was observed up to 6 months of aging.

We believe this to be the first report examining Ag MNP dissolution and aggregation behavior in soils amended with sewage sludge pretreated with Ag MNPs. Using AF4-ICP-MS combined with TEM and EDS analyses we have characterized Ag particles in pore waters extracted from sludge amended soils. Although total Ag concentrations used in this work exceed projected concentrations of Ag MNPs in sewage sludge amended soils, they are similar to the upper 99th percentile of Ag observed in a survey of sewage sludge in the United States.[6] It appears that despite extensive sulfidation of the particles, slow dissolution and release of Ag ions is expected to occur and this has the potential to cause toxicity.

Acknowledgement

This research was supported by the United States Environmental Protection Agency (U.S. EPA) and National Science Foundation (NSF) through cooperative agreements CR-83515701 (Office of Research and Development) and EF-0830093 (Center for Environmental Implications of Nanotechnology) and through the EPA Science to Achieve Results (STAR) program (RD-83485701). It has not been formally reviewed by EPA or NSF. The views expressed in this document are solely those of the authors. EPA and NSF do not endorse any products or commercial services mentioned in this publication. The authors also wish to acknowledge the assistance of J. Ye, S. Hunyadi, S. Marinakos, M. Vandiviere, A. Gondikas and J. Nelson.

Chapter 4: Summary and Conclusions

The use of nanomaterials in consumer products continues to increase [1] without much knowledge of the potential effects nanomaterials could have on environmental or human health. There is increased concern over the effects nanomaterials, like manufactured silver nanoparticles (Ag-MNPs) will have as a result of already observed product leaching and/or disposal.[13,14,15] A large portion of Ag MNPs are likely to end up in the sewage sludge during wastewater treatment,[17] where they are largely sulfidized.[63] As a result of sewage sludge biosolids application, soils have the potential to accumulate Ag MNPs.[7,117] The toxicity of Ag will depend on particle size and speciation, but there are currently no reliable techniques for monitoring the *in situ* characterization of Ag MNPs.[89] For this reason, asymmetrical flow field-flow fractionation (AF4) was coupled to an ultraviolet-visible (UV-Vis), light scattering and inductively coupled plasma mass spectrometer (ICP-MS) detector and has been employed for the characterization of Ag MNP aggregation state within soil pore waters.

The aim of this research was to develop a reliable method for extracting soil pore water and characterizing Ag MNP behavior within pore water. To observe this we set up soils with varying levels of sewage sludge biosolids addition, spiked with differently coated Ag MNPs or ionic Ag, and aged 1 week, 2 or 6 months. We hypothesized that increased sewage sludge would increase Ag MNP partitioning to the pore water, that Ag MNP surface charge would affect the aggregation stability of Ag MNPs in pore water, and that decreased concentrations of Ag would be observed in pore waters with aging.

Past studies have used AF4 for a variety of sample types,[47,115,120,123] but it has not yet been applied for the separation and characterization of Ag MNPs within soil pore waters. The nature of AF4, including minimal sample pretreatment, the lack of a stationary phase (as observed in chromatography techniques), and wide range of size detection make it ideal for characterizing soil

pore water.[8,107] However, the separation parameters used for AF4 are very sample specific and must be used in accordance with sample type.[107,120] To accomplish our objective, Ag MNPs and soil colloids were separately investigated under varying AF4 parameters including injection volume, carrier solution composition and crossflow setting. We determined AF4 parameters which yielded good quality size characterization, separation, sample recovery and repeatability of mixed samples containing Ag MNPs and environmental colloids. The methods that we developed will be invaluable for future studies of the fate of Ag MNPs in soils.

The established AF4 method was then applied to soils containing varying levels of sewage sludge biosolids, differently coated Ag MNPs or ionic Ag and aged for different periods. Surface charge of Ag MNPs strongly affected Ag MNP partitioning to soil pore waters after 1 week in the absence of sewage sludge. Addition of sewage sludge, however, resulted in minimal differences among Ag treatments in terms of dissolved Ag species and in general resulted in increased pore water Ag concentrations at 1 week. All treatments resulted in decreased pore water Ag with aging, although with aging there was also an increased proportion of dissolved Ag in sewage sludge amended soil pore water. These results suggest that a portion of Ag MNPs in sewage sludge applied to soil will partition to the soil pore water following application, but Ag MNP stability in pore water decreases with aging. On the other hand, even though there is extensive sulfidation of the particles, it appears that there is a slow release of dissolved Ag species, which could potentially cause toxicity, over time. Size characterization of Ag containing particles in soil pore water resulted in some differences between $AgNO_3$ and Ag MNP treatments. Most noticeably, after 6 months, soils without sludge had significantly more Ag in the soil pore water when treated with Ag MNPs compared to $AgNO_3$. While the addition of sludge decreased the size distribution of Ag containing particles in both treatments, more Ag was observed in the colloidal phase for Ag MNP treatments.

This work has been novel in the application of AF4 to the detection and characterization of Ag MNPs in soil pore water. In the absence of reliable *in situ* techniques for characterizing MNPs in soil, AF4-ICP-MS will be an asset for investigating this behavior. In this study, Ag MNPs had the highest concentrations in pore water from sludge amended soils after 1 week of aging, suggesting that Ag MNP mobility and transport within a soil may be greatest within the first week following sewage sludge biosolids application to soil. Regardless of the apparent sulfidation of Ag MNPs in soil, Ag was measured in pore water after aging 6 months, suggesting that the soil-sludge environment could influence the dissolution of immobilized Ag species within soil and potentially increase the potential for toxicity.

The results from this study pave the way for more like it, addressing other types of MNPs, as well as illustrate Ag MNP transformations in soil which will be important for ultimately determining toxicity. This technique and the discussed AF4 parameters are applicable to other relevant MNPs, but some method development may be necessary to ensure repeatability, recovery and good size characterization. Variations in AF4 crossflow rate will be necessary for separating particles smaller than 10 nm and it may also be beneficial to investigate alternative methods for extracting soil pore water to minimize the loss of dissolved metal ions. Future studies should also investigate MNP behavior in other soil types, including the long-term role soil type could have on MNP availability in soil pore water. Aging experiments could be used to approximate the time for Ag MNPs to reach a semblance of steady state in soil. Likewise, aging Ag MNPs in soil generally decreased observed concentrations, but did not alter the size distributions of Ag containing particles in the pore water. Aging MNPs for extended periods in a particular medium (e.g., soil, sewage sludge) and then monitoring organism toxicity over time could provide data on potential effects of persistent MNPs within that medium. Since aging and organic matter (sewage sludge) content were both observed to affect Ag MNP aggregation state in soil, it will be important to address the toxicity of the observed Ag sized particles and species.

Appendix A

Table A-1. Analysis of Yeager Sandy Loam (table adopted from Shoults-Wilson et al.).[50]

Property	Yeager Sandy Loam
pH (in H_20)	5.17
Cation exchange capacity, cmol kg^{-1}	
Total	9.18
K	0.11
Ca	0.91
Mg	0.27
Na	0.05
Composition, %	
Sand	76.34
Silt	16.53
Clay	7.13
Organic Matter	1.77

Yeager Sandy Loam Field Capacity

Soil field capacity (FC) was determined with a pressure plate apparatus, keeping saturated soil at a specific pressure (-0.33 bar) until no water release from the pressure plate was observed. Water content (19% w/w) was then determined gravimetrically after drying at 105°C for 24 hours.

Table A-2. Chemical composition of the sewage sludge biosolids collected from a wastewater treatment plant in Winchester, KY.

Analysis	**Dry weight %**
Solids, Total for dry weight	35.7
Solids, Volatile	19
Calcium Carbonate	79
	Dry weight (mg kg^{-1})
Nitrogen, nitrate	12
Nitrogen, ammonia	1500
Ammonium	1900
Nitrogen, total	31000
Phosphorus	8800
Arsenic	12
Cadmium	0.36
Calcium	330000
Chromium	5.7
Copper	98
Lead	4.1
Mercury	< 0.14
Molybdenum	3.8
Nickel	8.7
Potassium	7200
Selenium	< 3.4
Silver	1.7
Zinc	110

Table A-3. AF4 operating conditions used for the analysis of soil pore water.

Membrane	5kDa regenerated cellulose
Spacer (µm)	350
Channel flow rate (mL min $^{-1}$)	1.0
Cross flow rate (mL min $^{-1}$)	Gradient of 1.5 – 0.3 (10 min), 0.3- 0.03 (15-45 min)
Injection volume (µl)	15
UV wavelength (nm)	420,
Carrier solution	0.05% FL-70
Approximate fractogram time (min)	60

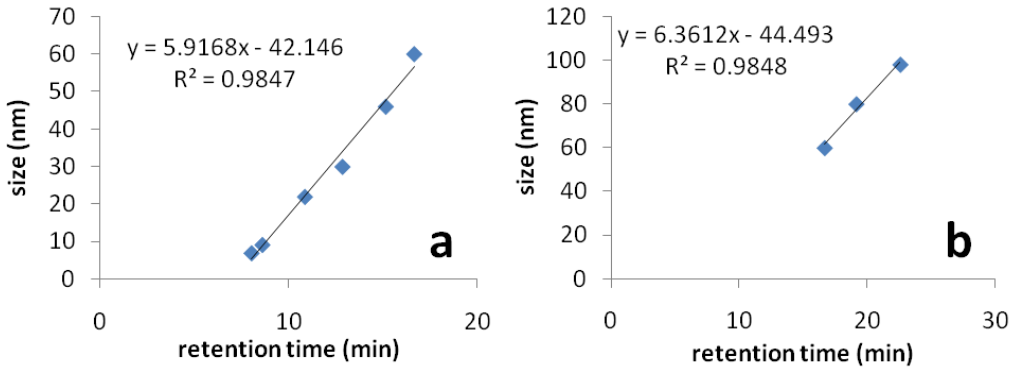

Figure A-1. AF4 calibration curve with size standards for (a) up to 15 minutes and (b) 15-45 min of the calibration curve.

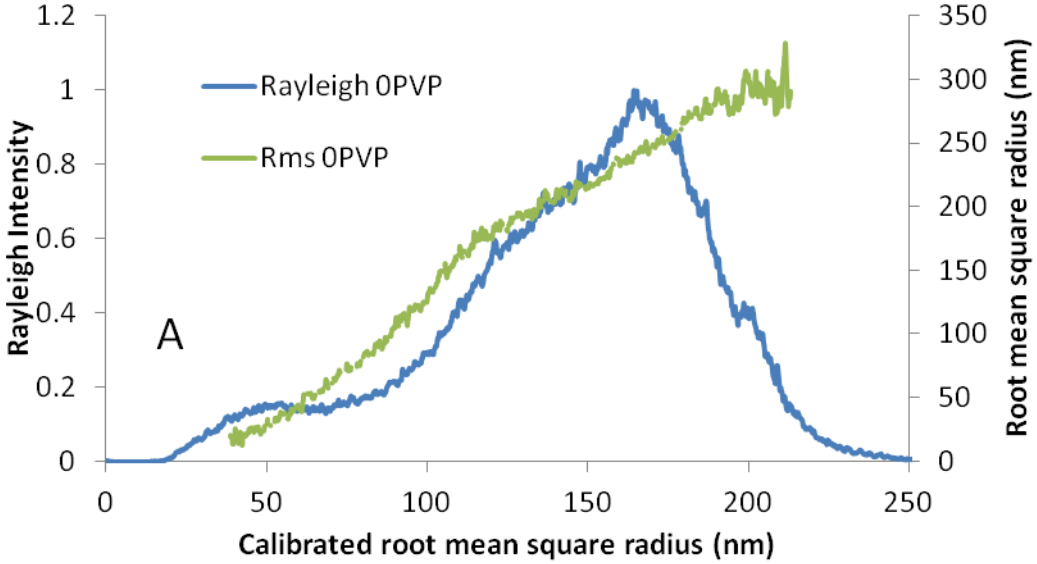

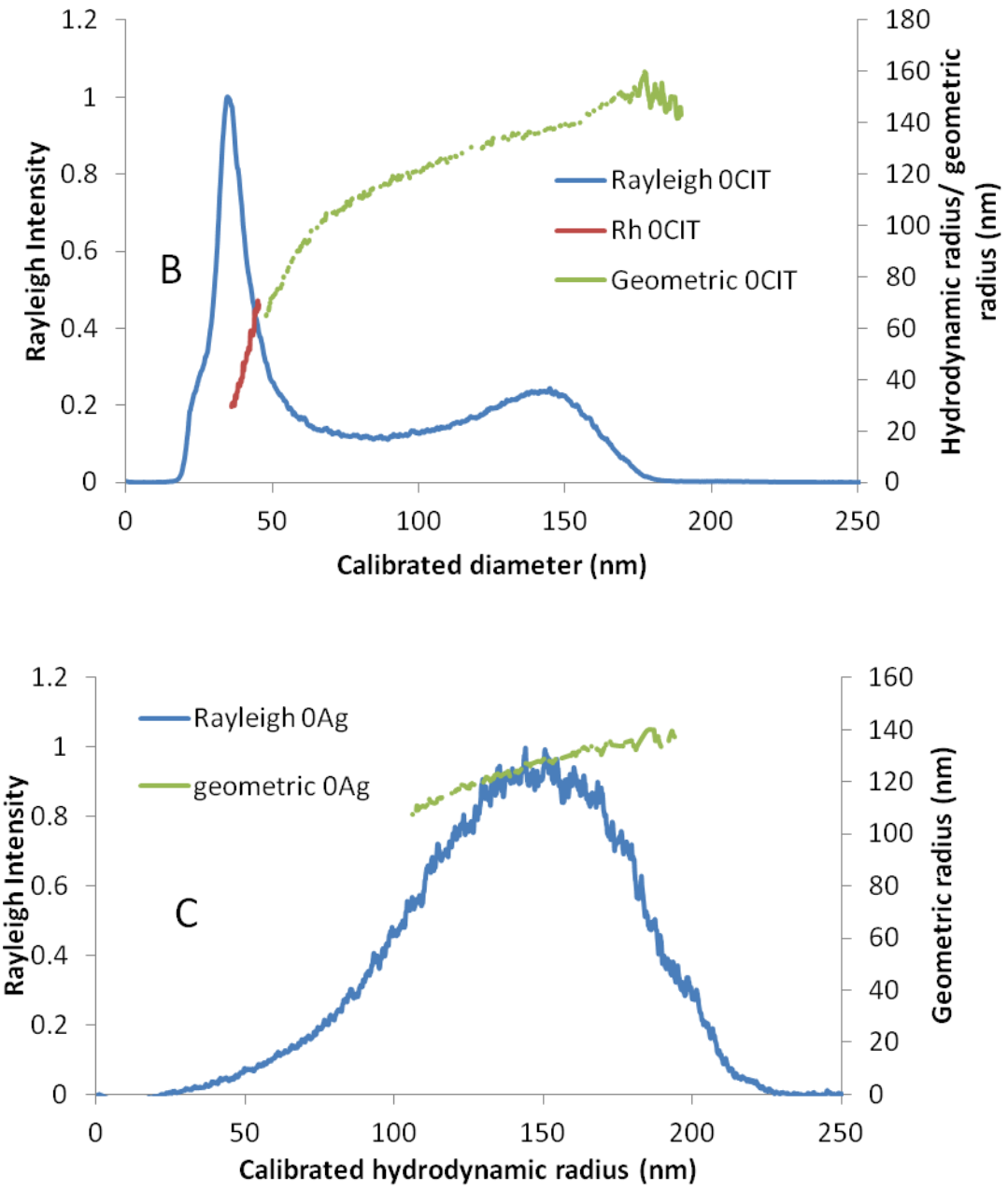

Figure A-2. To validate calibrated particle size, DLS/MALLS was used to determine the root mean square (rms), hydrodynamic (Rh) and geometric radii of particles in soil pore waters. These analyses was only used for pore water samples from non-amended soils because sludge was observed to strongly absorb at 658 nm. Representative samples are shown for the non-amended (a) PVP-Ag MNP, (b) CIT-Ag MNP, and (c) $AgNO_3$ treatments.

EXAFS Analysis

Silver K-edge EXAFS spectra were collected at the Stanford Synchrotron Radiation Lightsource (SSRL) on beamline 4-1. A N_2-cooled Si(220) ($\Phi = 90$) double crystal monochromator was used and detuned by 20% for harmonic rejection. Energy calibration was monitored with a Ag metal foil placed after the I1 transmitted beam detector. The samples were run in fluorescence mode using a 13-elements Ge detector in a N_2-cooled cryostat to reduce potential beam damage and noise due to thermal motion. EXAFS spectra of the following reference compounds were also collected in transmission mode under liquid N_2-cooled cryostat: AgNPs, AgCl, $AgNO_3$, Ag_2S, Ag_2SO_4, Ag-Acetate, Ag_2O, Ag_3PO_4, Ag_2CO_3 and Ag-glutathione (Ag-GSH) as a simple proxy for Ag bound to thiol-containing organics. Model compounds were diluted with glucose powder to achieve an optimized edge step of 1. Linear combination fitting (LCF) of the EXAFS data was performed using the SIXPack interface to the IFEFFIT XAFS analysis package.

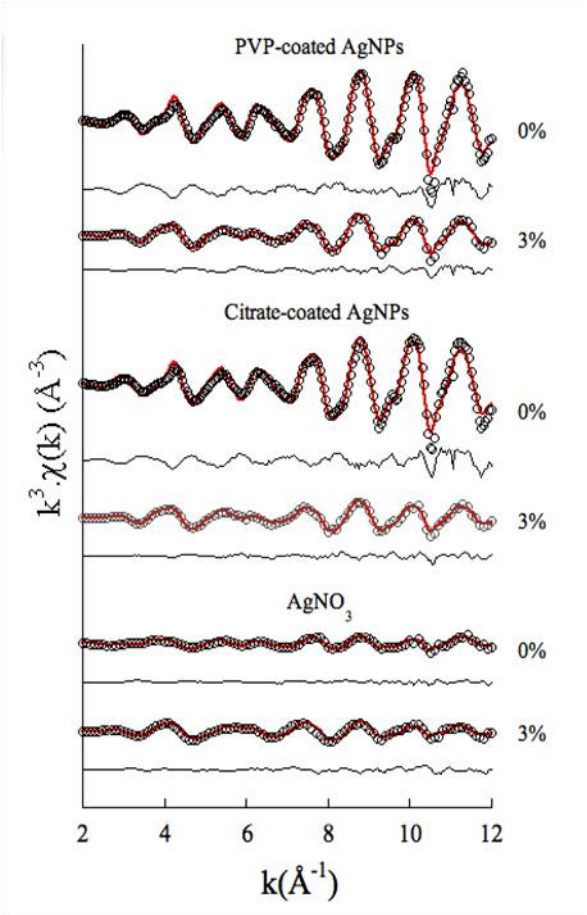

Figure A-3. Linear combination fitting of the EXAFS data measured from soils following the extraction of pore water. Representative samples are shown from soils amended with no sewage sludge (0%) or 3% sewage sludge (w/w%) and treated with PVP or citrate coated Ag MNPs or silver nitrate ($AgNO_3$).

Table A-4. Ion chromatography analysis of the concentration (mg L^{-1}) of anions extractable after (1) 24 hours and (2) 3 months from 10 g of Yeager Sandy loam (YSL) soil, YSL amended with sludge (1% sludge or 3% sludge) or (24 hours only) an amount of sludge equivalent to the amount added to the 3% sludge microcosm. (mean ± standard deviation, n=16)

	(1) 24 hours						
	Fl^-	Cl^-	$N0_2^-$	Br^-	NO_3^-	PO_4^{2-}	SO_4^{-2}
Sludge	0.92 (0.06)	14.17 (0.82)	0.20 (0.34)	2.39 (0.31)	0.80 (0.36)	438.61 (6.36)	23.54 (0.26)
3% sludge	3.61 (0.39)	18.05 (0.39)	1.48 (0.05)	2.44 (0.79)	2.95 (0.38)	240.59 (25.54)	30.39 (3.60)
1% sludge	3.02 (0.05)	11.24 (3.57)	1.49 (0.04)	1.06 (0.03)	4.14 (0.24)	76.42 (5.59)	20.61 (0.23)
YSL	1.13 (0.01)	2.12 (0.05)	0.81 (0.01)	0.00	3.22 (0.11)	0.65 (0.02)	5.62 (0.13)

	(2) 3 Months						
	Fl^-	Cl^-	$N0_2^-$	Br^-	NO_3^-	PO_4^{2-}	SO_4^{-2}
3% sludge	3.42 (0.20)	11.22 (4.40)	3.26 (2.47)	0.86 (0.16)	2.26 (0.64)	111.88 (75.49)	113.39 (61.30)
1% sludge	3.43 (0.07)	6.61 (0.45)	1.37 (0.47)	0.86 (0.12)	1.35 (0.47)	29.10 (6.59)	80.26 (6.51)
YSL	0.94 (0.02)	1.18 (0.10)	0.54 (0.01)	0.00	2.28 (1.32)	3.69 (0.05)	16.99 (0.44)

Table A-5. ICP-MS analysis of the concentration (mg L^{-1}) of cations extractable after (1) 24 hours and (2) 3 months from 10 g of Yeager Sandy loam (YSL) soil, YSL amended with sludge (1% sludge or 3% sludge) or (24 hours only) an amount of sludge equivalent to the amount added to the 3% sludge microcosm. (mean ± standard deviation, n=16)

	(1) 24 hours						
	Na^+	Mg^{2+}	Al^{3+}	K^+	Ca^{2+}	Mn^{2+}	Fe^{2+}
Sludge	10.89 (0.98)	0.11 (0.01)	0.84 (0.17)	92.65 (10.05)	4.02 (0.49)	0.05 (0.01)	1.04 (0.17)
3% sludge	11.05 (0.88)	1.24 (0.22)	5.35 (0.99)	54.85 (6.32)	11.16 (5.93)	0.88 (0.13)	8.13 (1.69)
1% sludge	5.69 (1.92)	1.07 (0.70)	4.58 (0.34)	14.77 (0.89)	5.21 (0.42)	0.71 (0.07)	5.82 (0.50)
YSL	3.85 (0.07)	0.08 (0.05)	1.90 (0.09)	6.51 (0.71)	5.24 (0.37)	1.53 (0.15)	0.68 (0.20)

	(2) 3 Months						
	Na^+	Mg^{2+}	Al^{3+}	K^+	Ca^{2+}	Mn^{2+}	Fe^{2+}
3% sludge	2.61 (1.11)	2.15 (1.11)	5.84 (0.75)	35.96 (5.93)	132.23 (4.79)	1.36 (0.21)	10.50 (2.15)
1% sludge	6.01 (3.50)	3.54 (1.78)	5.91 (0.32)	21.20 (8.67)	509.46 (325.64)	1.66 (0.04)	10.07 (0.95)
YSL	7.88 (0.66)	2.86 (0.58)	5.72 (1.19)	6.53 (0.41)	534.51 (94.37)	0.83 (0.10)	8.87 (1.68)

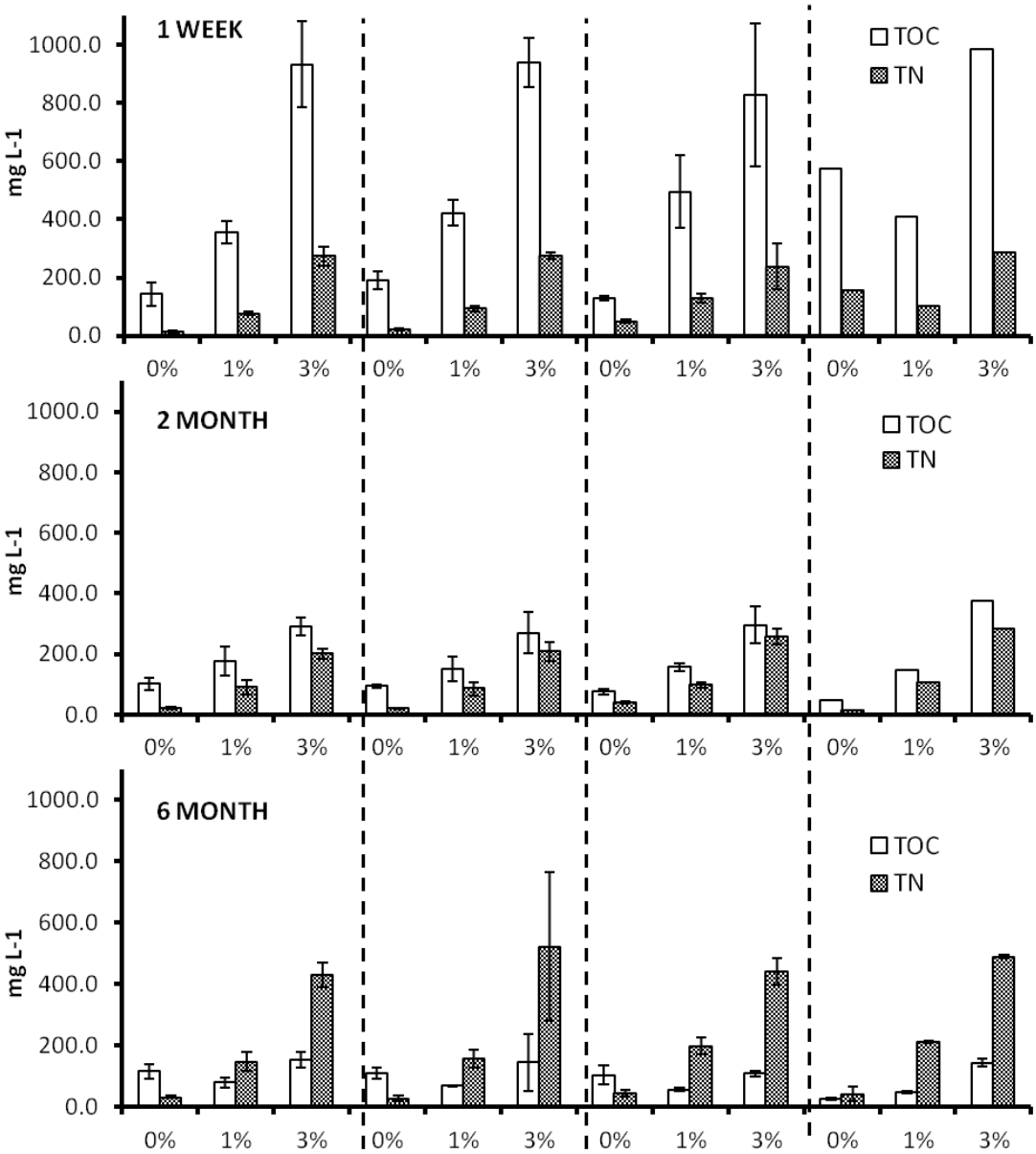

Figure A-4. Total organic carbon (TOC) and nitrogen (TN) analysis of pore waters extracted from polyvinylpyrrolidone coated Ag MNPs (PVP-Ag MNP), citrate coated Ag MNPs (CIT-Ag MNP), silver nitrate ($AgNO_3$), or control soil microcosms amended with 0, 1 or 3 % sewage sludge biosolids and aged for 1 week, 2 months or 6 months.

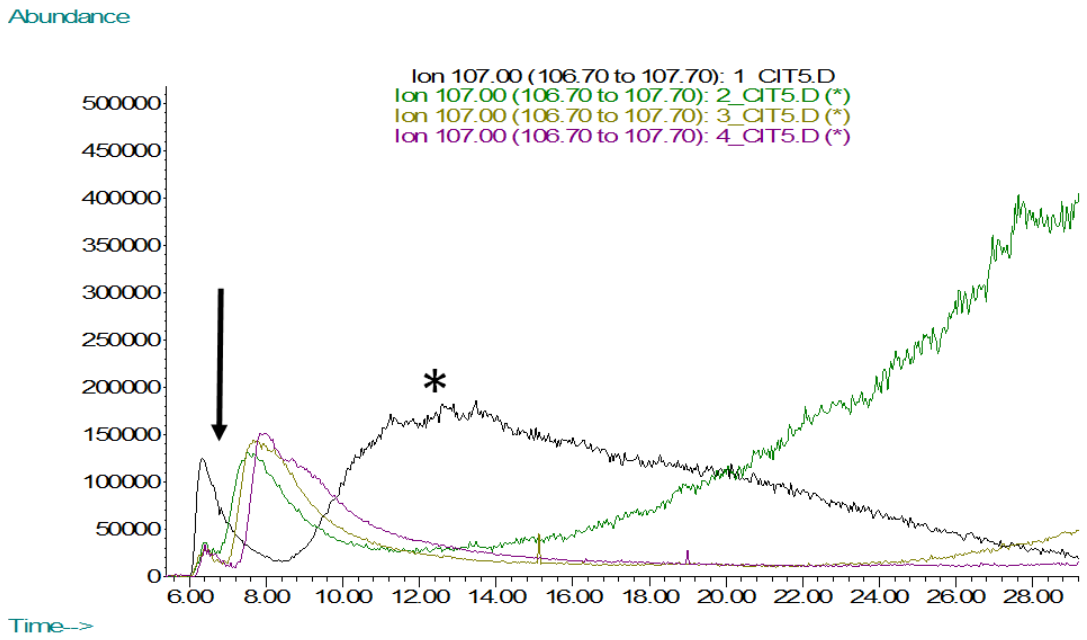

Figure A-5. AF4-ICP-MS fractogram showing resolution of the void peak and sample peak, most likely Ag bound to natural organic matter. The black, green, yellow, and magenta traces represent four tested constant crossflow rates of 1, 2, 3, and 4 ml min^{-1} for pore water extracted from 3% sludge soil treated with citrate coated (CIT) Ag MNPs and aged 1 week. The asterisk indicates the sample peak with the lowest crossflow rate (1ml min^{-1}) that does not provide resolution of the smaller (1-10nm) peak and the arrow indicates the specific site of separation.

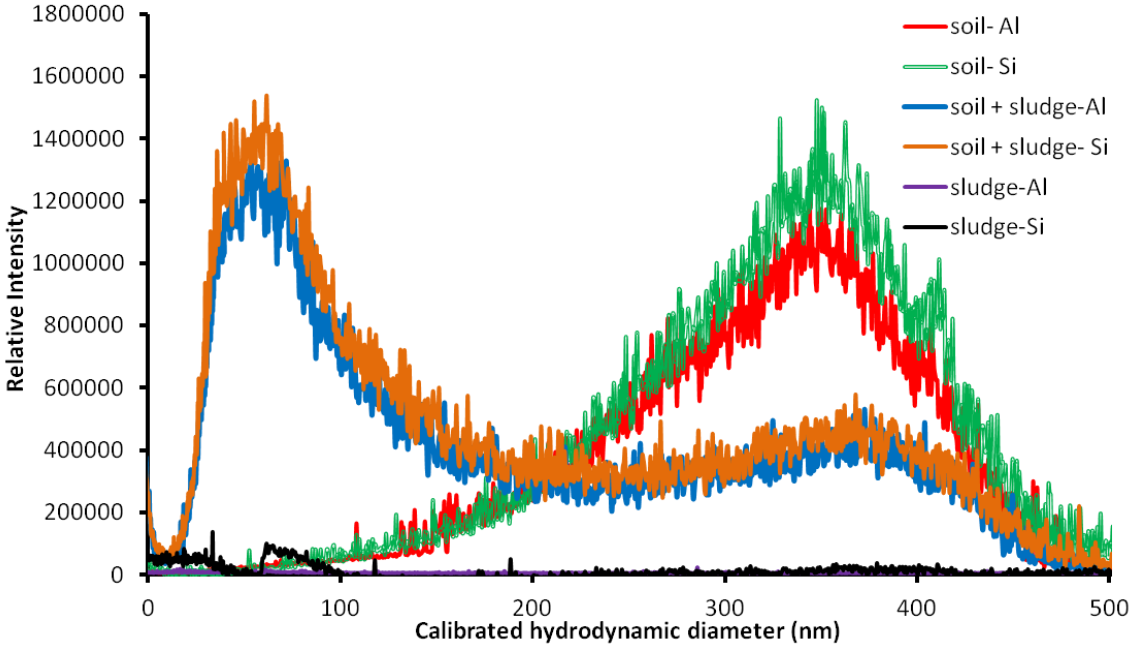

Figure A-6. AF4-ICP-MS representative fractogram showing the shift in Al (m/z=27) and Si (m/z= 28) size distribution in pore water with the addition of sewage sludge biosolids to soil.

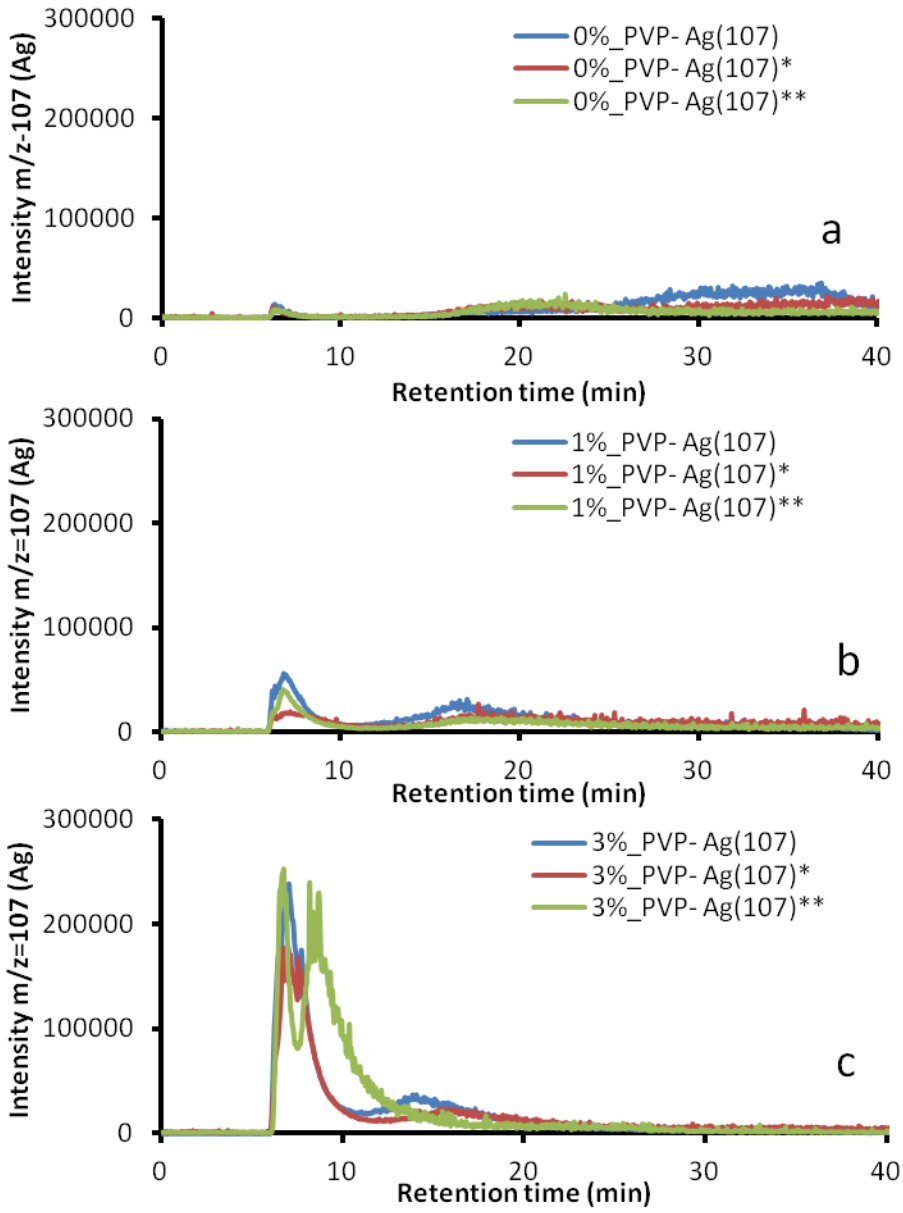
300000
200000
100000
0
Intensity m/z-107 (Ag)
0%_PVP- Ag(107)
0%_PVP- Ag(107)*
0%_PVP- Ag(107)**
a
0
10
20
30
40
Retention time (min)
300000
200000
100000
0
Intensity m/z=107 (Ag)
1%_PVP- Ag(107)
1%_PVP- Ag(107)*
1%_PVP- Ag(107)**
b
0
10
20
30
40
Retention time (min)
300000
200000
100000
0
Intensity m/z=107 (Ag)
3%_PVP- Ag(107)
3%_PVP- Ag(107)*
3%_PVP- Ag(107)**
c
0
10
20
30
40
Retention time (min)

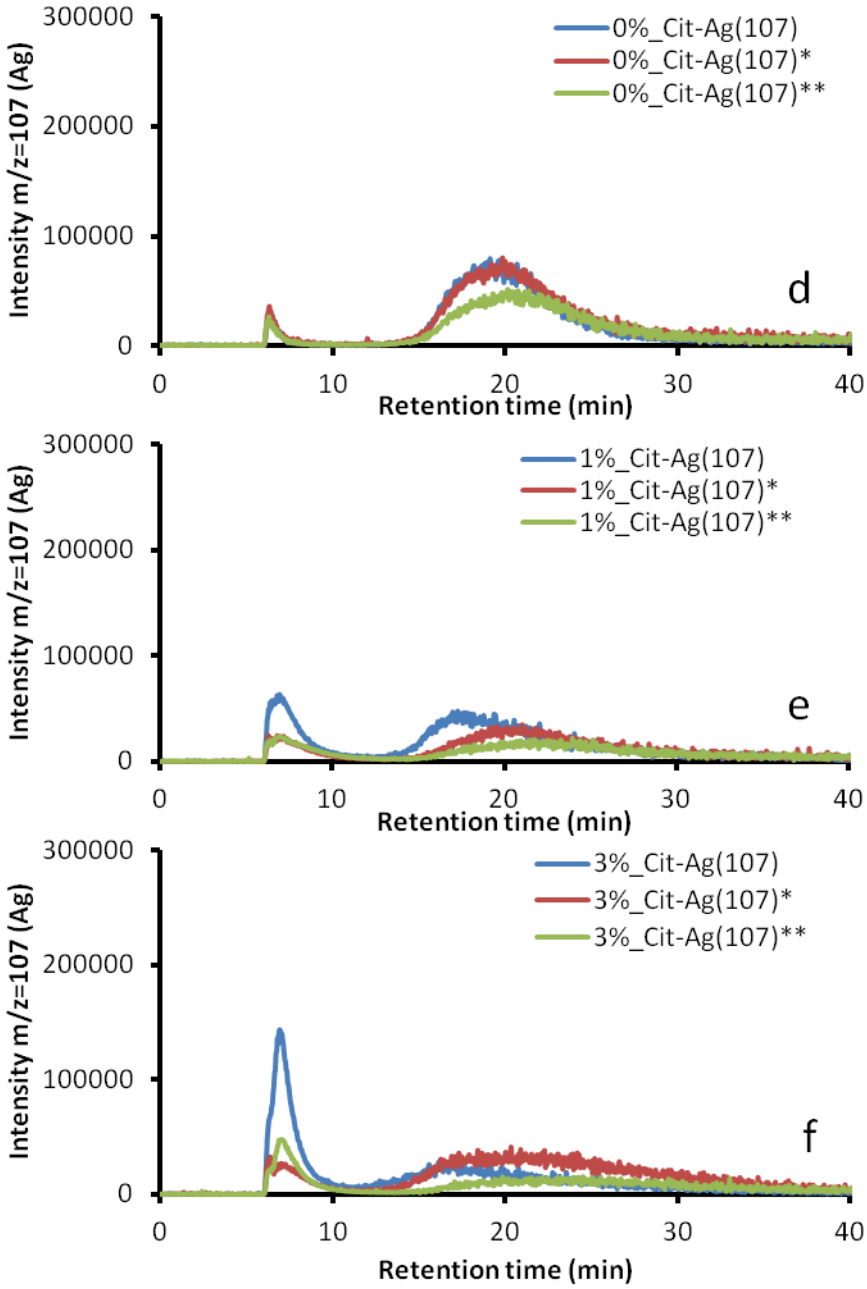
300000
200000
100000
0
Intensity m/z=107 (Ag)
0%_Cit-Ag(107)
0%_Cit-Ag(107)*
0%_Cit-Ag(107)**
d
0
10
20
30
40
Retention time (min)
300000
200000
100000
0
Intensity m/z=107 (Ag)
1%_Cit-Ag(107)
1%_Cit-Ag(107)*
1%_Cit-Ag(107)**
e
0
10
20
30
40
Retention time (min)
300000
200000
100000
0
Intensity m/z=107 (Ag)
3%_Cit-Ag(107)
3%_Cit-Ag(107)*
3%_Cit-Ag(107)**
f
0
10
20
30
40
Retention time (min)

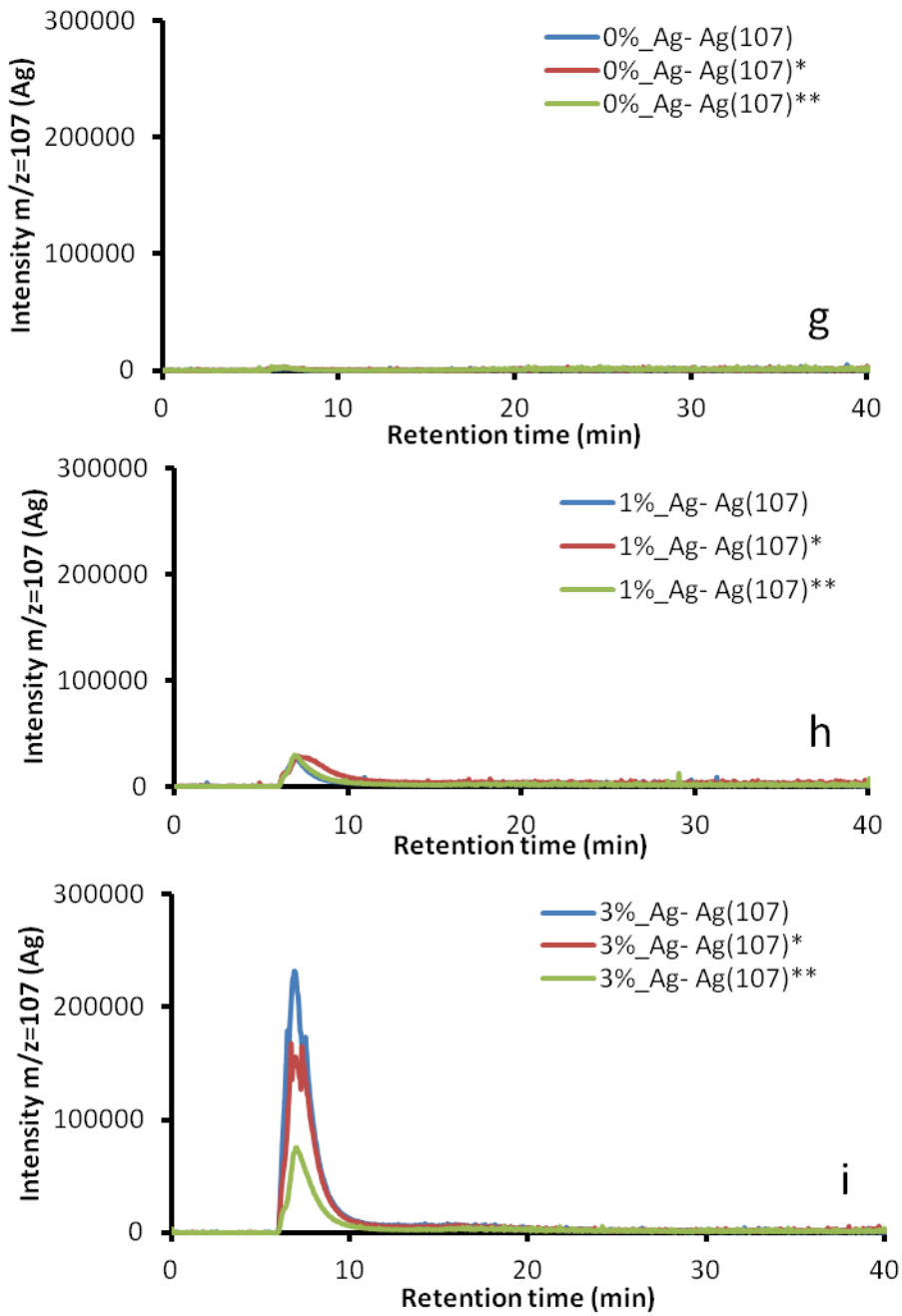

Figure A-7. AF4-ICP-MS fractogram using ICP-MS detection of Ag (m/z= 107) showing consecutive injections of 0, 1, and 3% sludge amended soil treated with (a-c) PVP-Ag MNPs , (d-f) CIT-Ag MNPs or (g-i) $AgNO_3$.

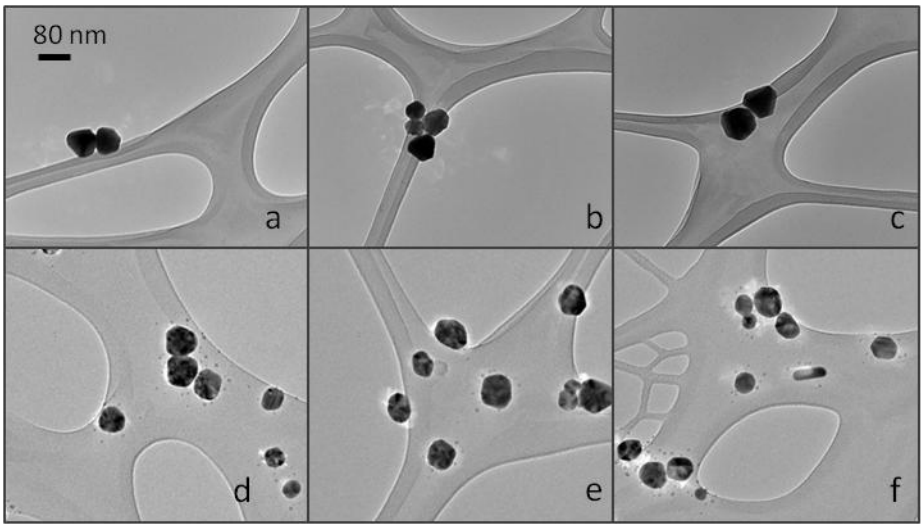

Figure A-8. TEM images of original (a-c) CIT-Ag MNP and (d-f) PVP-Ag MNP particle size distributions.

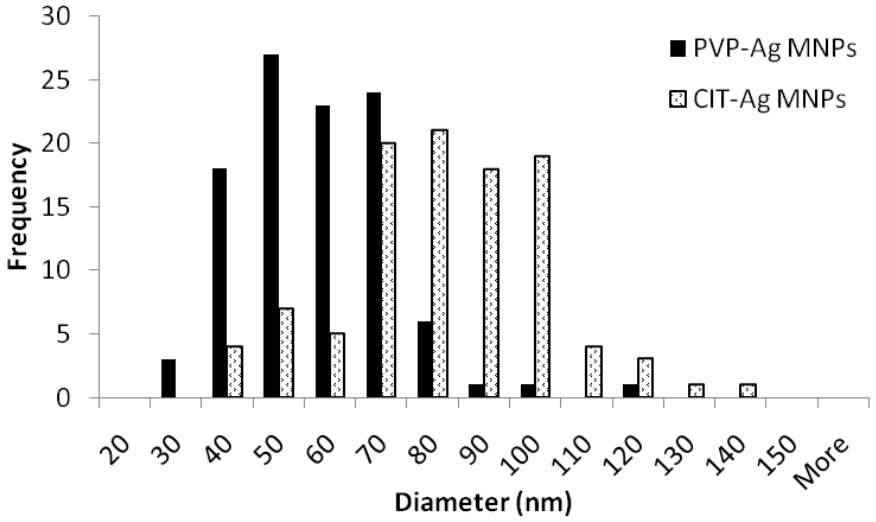

Figure A-9. Overlaying histograms showing size distributions of original (1-4) CIT-Ag MNP and (5-7) PVP-Ag MNP particle size distributions, based on TEM imaging.

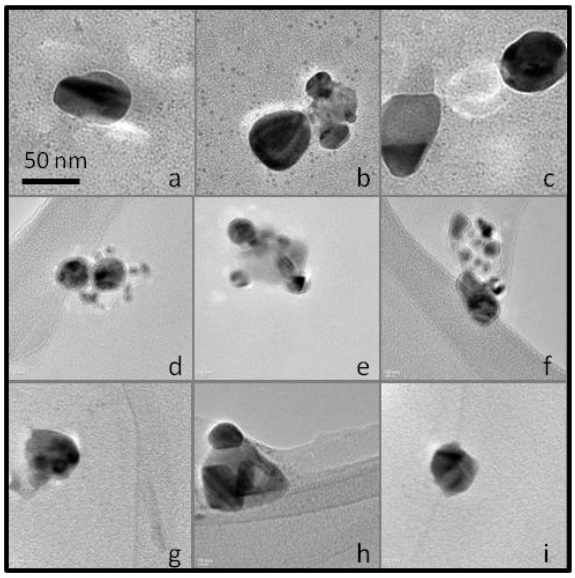
50 nm
a
b
c
d
e
f
g
h
i

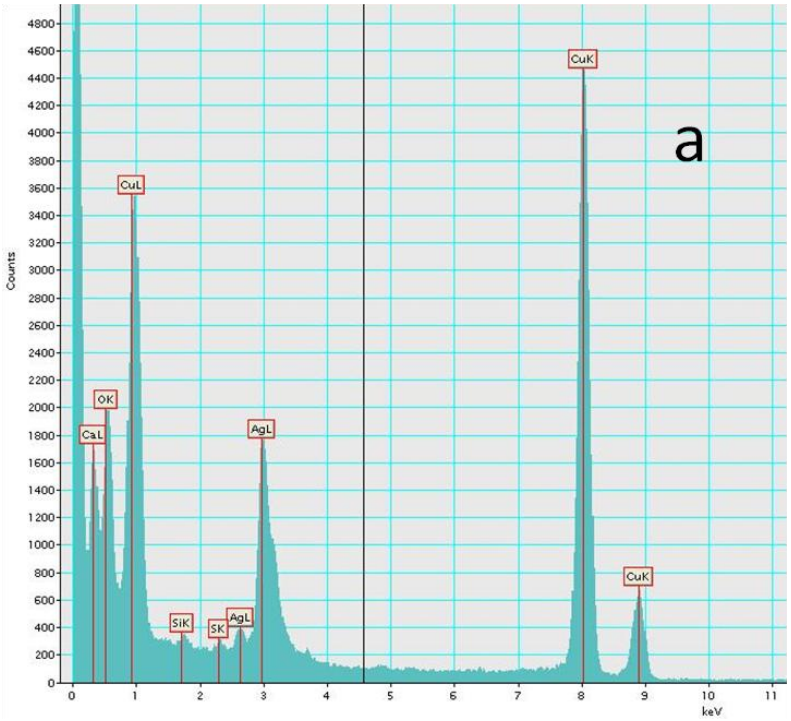
a
Counts
keV
CuK
CuL
OK
CaL
AgL
SiK
SK
AgL
CuK

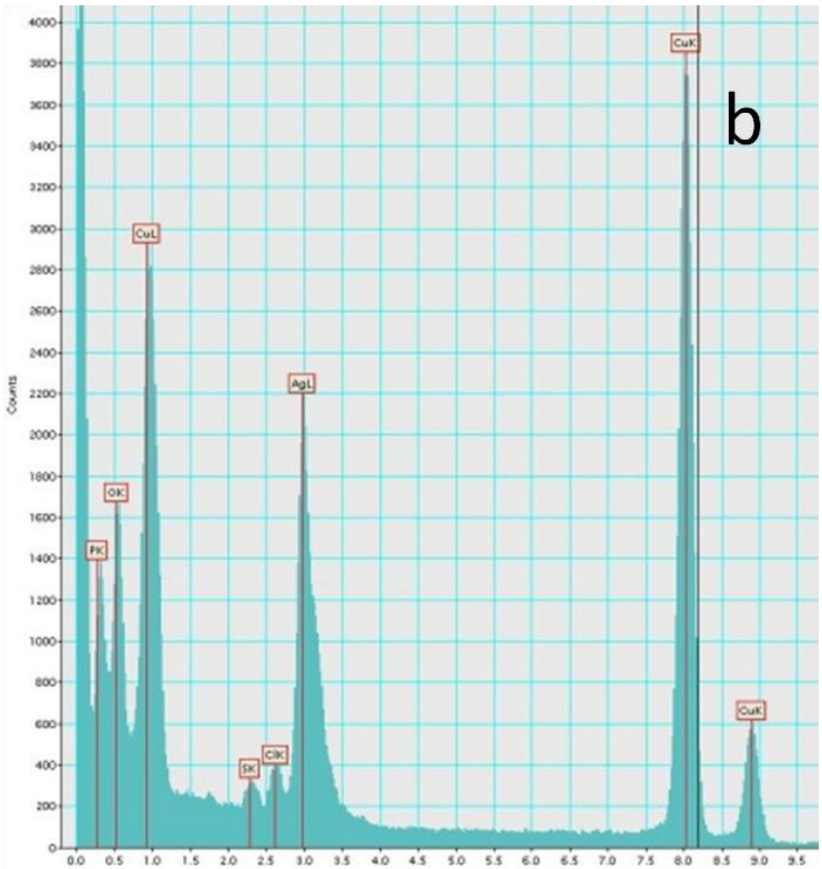
b
Counts
CuK
CuL
AgL
OK
PK
SK
ClK
CuK

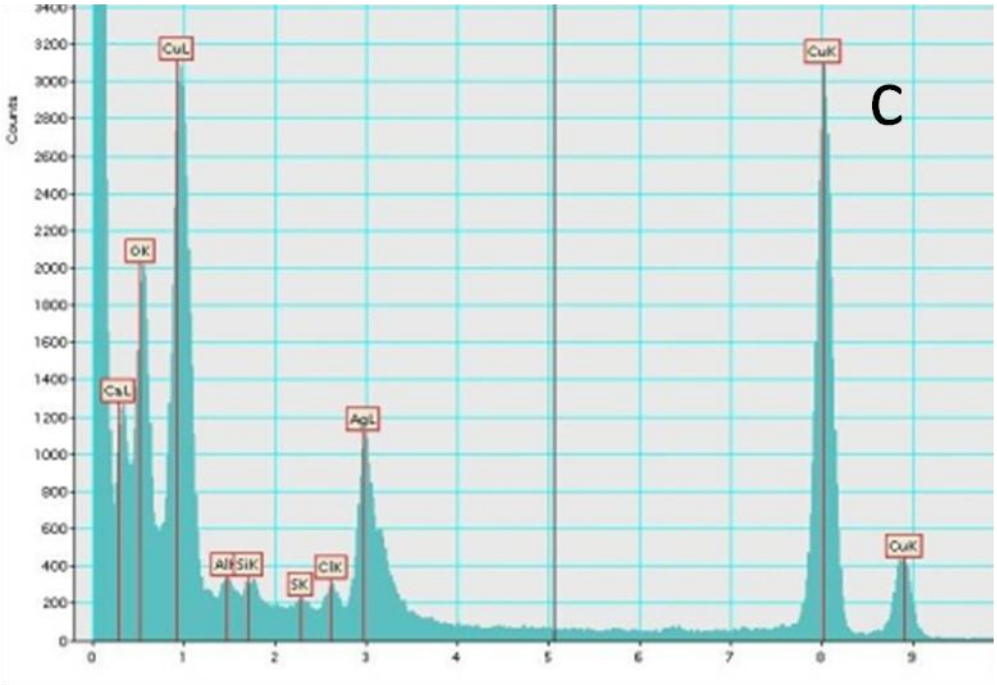
c
Counts
CuL
CuK
OK
CaL
AgL
AlK
SiK
SK
ClK
CuK

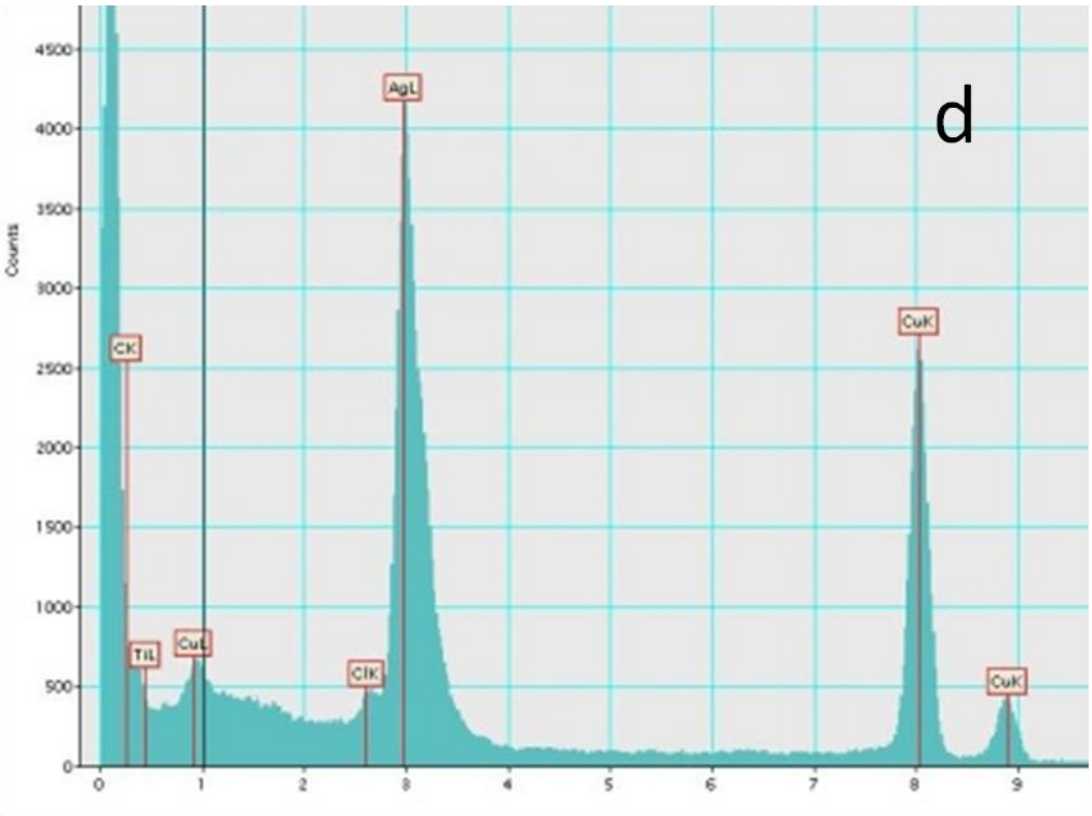
d
Counts
CK
TiL
CuL
ClK
AgL
CuK
CuK

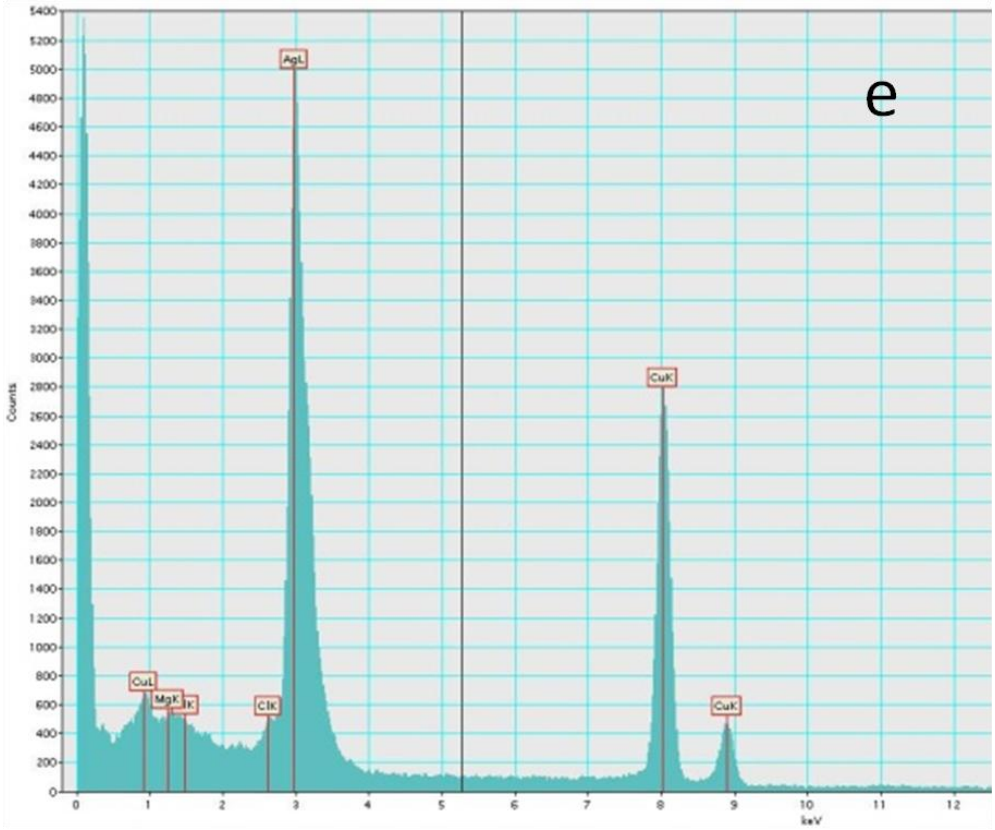
e
Counts
keV
CuL
MgK
ClK
AgL
CuK
CuK

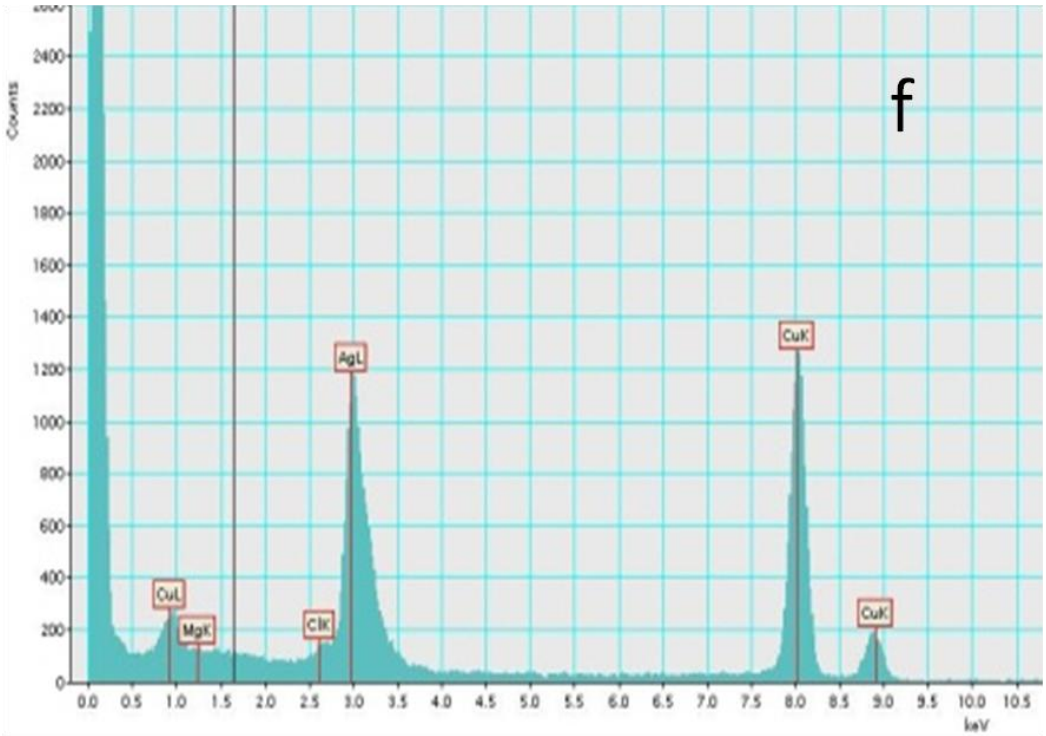
f
Counts
keV
CuL
MgK
ClK
AgL
CuK
CuK

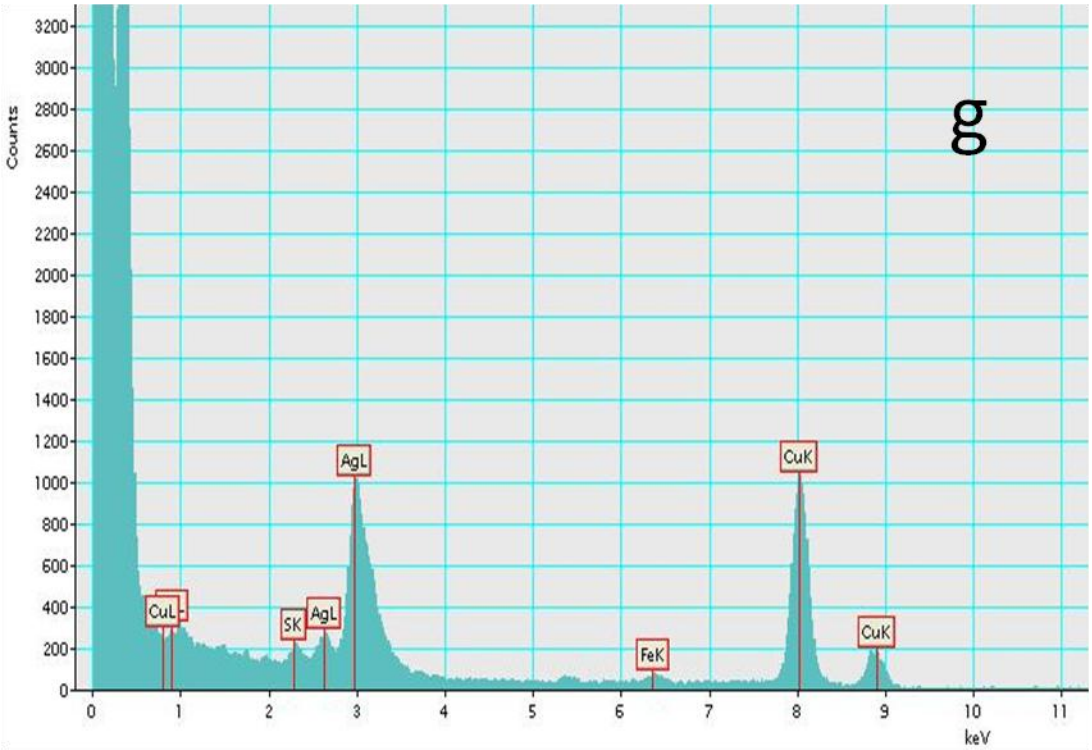
g
Counts
keV
CuL
SK
AgL
AgL
FeK
CuK
CuK

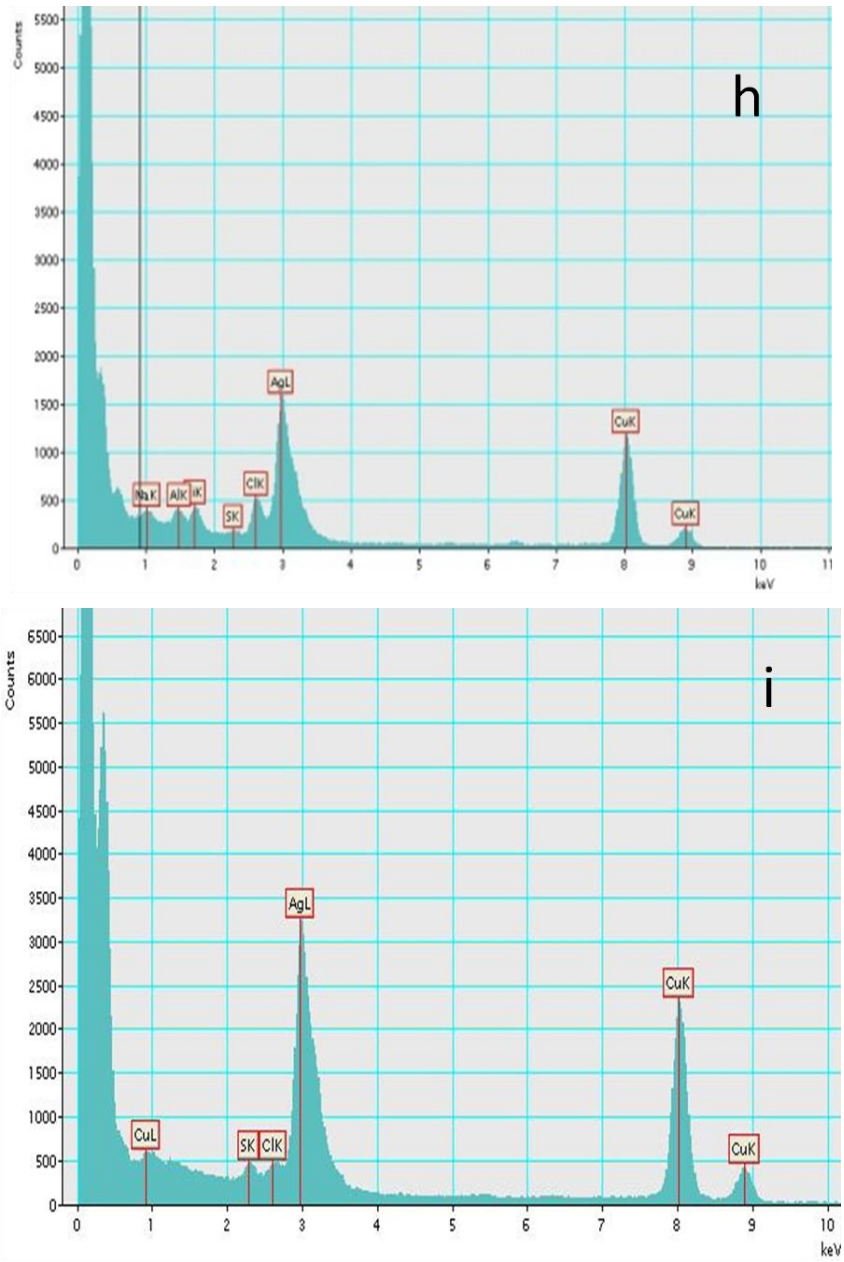

Figure A-10. Images taken from transmission electron microscopy (TEM) and the corresponding energy dispersive spectra (EDS) shown for representative particles imaged in pore water collected from (a-c) non-amended CIT-Ag MNP treated soil and 3% sludge amended soil treated with (d-f) CIT-Ag MNPs or (g-i) PVP-Ag MNPs.

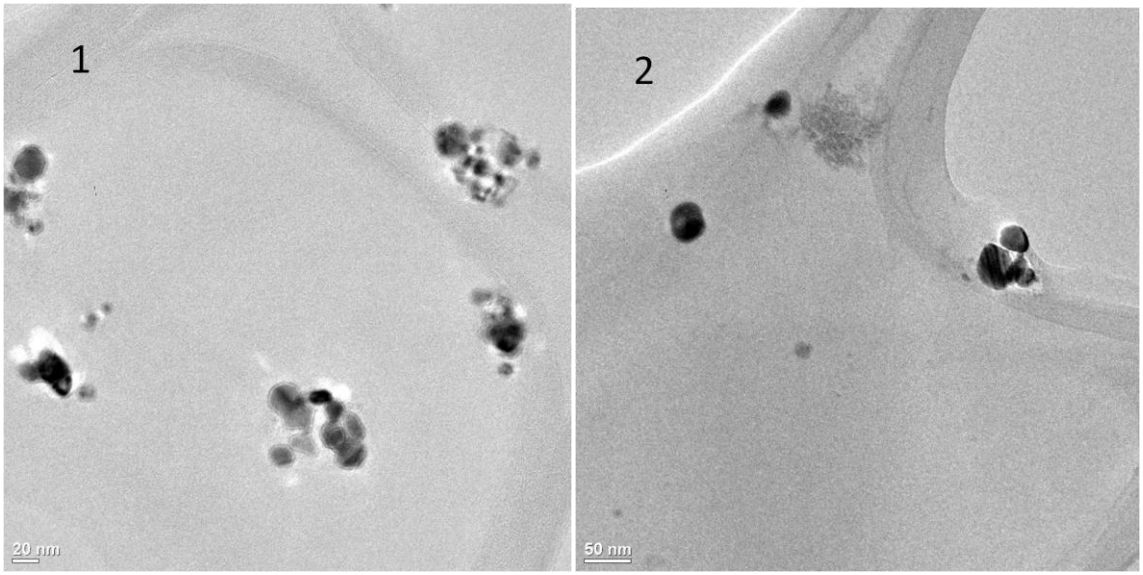

Figure A-11. Representative TEM images capturing several smaller, Ag-rich particles from pore waters extracted from soil amended with 3% sewage sludge and treated with (1) CIT-Ag MNPs and (2) PVP-Ag MNPs.

References

(1) (2012). "Nanotechnology Consumer Product Inventory." Retrieved July, 2012, from http://www.nanotechproject.org/44.
(2) Carson, R. Silent Spring. Boston, Houghton Mifflin. **1962**.
(3) Tanabe, S. PCB problems in the future: Foresight from current knowledge. *Environmental Pollution* **1988**, 50(1–2): 5-28.
(4) El Badawy, A., D. Feldhake and R. Venkatapathy (2010). State of the Science Literature Review: Everything Nanosilver and More. Washington, DC, Environmental Protection Agency**:** 221.
(5) Ratte, H. T. Bioaccumulation and toxicity of silver compounds: A review *Environmental Toxicology and Chemistry* **1999**, 18(1): 89-108.
(6) EPA (2009). "Targeted National Sewage Sludge Survey (TNSSS)." from http://water.epa.gov/scitech/wastetech/biosolids/tnsss-overview.cfm.
(7) Gottschalk, F., T. Sonderer, R. W. Scholz and B. Nowack. Modeled Environmental Concentrations of Engineered Nanomaterials (TiO_2, ZnO, Ag, CNT, Fullerenes) for Different Regions. *Environmental Science & Technology* **2009**, 43(24): 9216-9222.
(8) Handy, R. D., G. Cornelis, T. Fernandes, O. Tsyusko, A. Decho, T. Sabo-Attwood, C. Metcalfe, J. A. Steevens, S. J. Klaine, A. A. Koelmans and N. Horne. Ecotoxicity test methods for engineered nanomaterials: Practical experiences and recommendations from the bench. *Environmental Toxicology and Chemistry* **2012**, 31(1): 15-31.
(9) Klaine, S. J., P. J. Alvarez, G. E. Batley, T. F. Fernandes, R. D. Handy, D. Y. Lyon, S. Mahendra, M. J. McLaughlin and J. R. Lead. Nanomaterials in the environment: behavior, fate, bioavailability, and effects. *Environmental Toxicology and Chemistry* **2008**, 27(9): 1825-1851.
(10) Li, Q., S. Mahendra, D. Y. Lyon, L. Brunet, M. V. Liga, D. Li and P. J. Alvarez. Antimicrobial nanomaterials for water disinfection and microbial control: Potential applications and implications. *Water Research* **2008**, 42: 4591-4602.
(11) Luoma, S. Silver nanotechnologies and the environment: Old problems or new challenges? Philadelphia, PA., The Pew Charitable Trust. **2008**.
(12) Ruparelia, J. P., A. K. Chatterjee, S. P. Duttagupta and S. Mukherji. Strain specificity in antimicrobial activity of silver and copper nanoparticles. *Acta Biomaterialia* **2008**, 4(3): 707-716.
(13) Benn, T. M. and P. Westerhoff. Nanoparticle silver released into water from commercially available sock fabrics. *Environmental Science & Technology* **2008**, 42: 4133-4139.
(14) Kaegi, R., B. Sinnet, S. Zuleeg, H. Hagendorfer, E. Mueller, R. Vonbank, M. Boller and M. Burkhardt. Release of silver nanoparticles from outdoor facades. *Environmental Pollution* **2010**, 158(9): 2900-2905.
(15) Cleveland, D., S. E. Long, P. L. Pennington, E. Cooper, M. H. Fulton, G. I. Scott, T. Brewer, J. Davis, E. J. Petersen and L. Wood. Pilot estuarine mesocosm study on the environmental fate of Silver nanomaterials leached from consumer products. *Science of The Total Environment* **2012**, 421–422(0): 267-272.
(16) Blaser, S. A., M. Scheringer, M. Macleod and K. Hungerbuhler. Estimation of cumulative aquatic exposure and risk due to silver: contribution of nano-functionalized plastics and textiles. *Science of the Total Environment* **2008**, 390(2-3): 396-409.
(17) Kaegi, R., A. Voegelin, B. Sinnet, S. Zuleeg, H. Hagendorfer, M. Burkhardt and H. Siegrist. Behavior of Metallic Silver Nanoparticles in a Pilot Wastewater Treatment Plant. *Environmental Science & Technology* **2011**, 45(9): 3902-3908.
(18) Gottschalk, F., R. W. Scholz and B. Nowack. Probabilistic material flow modeling for assessing the environmental exposure to compounds: Methodology and an application to engineered nano-TiO_2 particles. *Environmental Modelling & Software* **2010**, 25(3): 320-332.

(19) Pérez, S., M. l. Farré and D. Barceló. Analysis, behavior and ecotoxicity of carbon-based nanomaterials in the aquatic environment. *Trends in Analytical Chemistry* **2009**, 28(6): 820-832.
(20) Roco, M. C. National Nanotechnology Initiative- Past, Present, Future *Handbook on Nanoscience, Engineering and Technology* **2006**: 42.
(21) Hotze, E. M., T. Phenrat and G. V. Lowry. Nanoparticle aggregation: challenges to understanding transport and reactivity in the environment. *Journal of Environmental Quality* **2010**, 39(6): 1909-1924.
(22) Saleh, N., H. J. Kim, T. Phenrat, K. Matyjaszewski, R. D. Tilton and G. V. Lowry. Ionic strength and composition affect the mobility of surface-modified Fe0 nanoparticles in water-saturated sand columns. *Environmental Science & Technology* **2008**, 42(9): 3349-3355.
(23) Dahirel, V. and M. Jardat. Effective interactions between charged nanoparticles in water: What is left from the DLVO theory? *Current Opinion in Colloid & Interface Science* **2010**, 15(1–2): 2-7.
(24) He, Y., J. Wan and T. Tokunaga. Kinetic stability of hematite nanoparticles: the effect of particle sizes. *Journal of Nanoparticle Research* **2008**, 10(2): 321-332.
(25) Missana, T. and A. Adell. On the Applicability of DLVO Theory to the Prediction of Clay Colloids Stability. *Journal of Colloid and Interface Science* **2000**, 230(1): 150-156.
(26) Peukert, W., H. C. Schwarzer, ouml, M. tzinger, uuml, L. nther and F. Stenger. Control of particle interfaces-the critical issue in nanoparticle technology. *Advanced Powder Technology* **2003**, 14(4): 411-426.
(27) Azeredo, J., J. Visser and R. Oliveira. Exopolymers in bacterial adhesion: interpretation in terms of DLVO and XDLVO theories. *Colloids and Surfaces B: Biointerfaces* **1999**, 14(1–4): 141-148.
(28) Logan, B. E. Environmental Transport Processes. **1999**.
(29) Schrick, B., B. W. Hydutsky, J. L. Blough and T. E. Mallouk. Delivery Vehicles for Zerovalent Metal Nanoparticles in Soil and Groundwater. *Chemistry of Materials* **2004**, 16(11): 2187-2193.
(30) Kirschling, T. L., P. L. Golas, J. M. Unrine, K. Matyjaszewski, K. B. Gregory, G. V. Lowry and R. D. Tilton. Microbial Bioavailability of Covalently Bound Polymer Coatings on Model Engineered Nanomaterials. *Environmental Science & Technology* **2011**, 45(12): 5253-5259.
(31) El Badawy, A. M., T. P. Luxton, R. G. Silva, K. G. Scheckel, M. T. Suidan and T. M. Tolaymat. Impact of Environmental Conditions (pH, Ionic Strength, and Electrolyte Type) on the Surface Charge and Aggregation of Silver Nanoparticles Suspensions. *Environmental Science & Technology* **2010**, 44: 1260-1266.
(32) Shoults-Wilson, W. A., B. C. Reinsch, O. V. Tsyusko, P. M. Bertsch, G. V. Lowry and J. M. Unrine. Role of particle size and soil type in toxicity of silver nanoparticles to earthworms. *Soil Science Society of America* **2011**, 75.
(33) Zhang, W., Y. Yao, N. Sullivan and Y. Chen. Modeling the Primary Size Effects of Citrate-Coated Silver Nanoparticles on Their Ion Release Kinetics. *Environmental Science & Technology* **2011**, 45(10): 4422-4428.
(34) Coutris, C., E. J. Joner and D. H. Oughton. Aging and soil organic matter content affect the fate of silver nanoparticles in soil. *Science of The Total Environment* **2012**, 420(0): 327-333.
(35) Yin, L., Y. Cheng, B. Espinasse, B. P. Colman, M. Auffan, M. Wiesner, J. Rose, J. Liu and E. S. Bernhardt. More than the Ions: The Effects of Silver Nanoparticles on Lolium multiflorum. *Environmental Science & Technology* **2011**, 45(6): 2360-2367.
(36) Ma, R., C. Levard, S. M. Marinakos, Y. Cheng, J. Liu, F. M. Michel, G. E. Brown and G. V. Lowry. Size-Controlled Dissolution of Organic-Coated Silver Nanoparticles. *Environmental Science & Technology* **2011**, 46(2): 752-759.

(37) Ju-Nam, Y. and J. R. Lead. Manufactured nanoparticles: an overview of their chemistry, interactions and potential environmental implications. *Science of the Total Environment* **2008**, 400(1-3): 396-414.
(38) Qafoku, N. P. (2010). Terrestrial Nanoparticles and Their Controls on Soil-/Geo-Processes and Reactions. Advances in Agronomy. L. S. Donald, Academic Press. **107:** 33-91.
(39) Petosa, A. R., D. P. Jaisi, I. R. Quevedo, M. Elimelech and N. Tufenkji. Aggregation and Deposition of Engineered Nanomaterials in Aquatic Environments: Role of Physicochemical Interactions. *Environmental Science & Technology* **2010**, 44(17): 6532-6549.
(40) Tolaymat, T. M., A. M. El Badawy, A. Genaidy, K. G. Scheckel, T. P. Luxton and M. Suidan. An evidence-based environmental perspective of manufactured silver nanoparticle in syntheses and applications: A systematic review and critical appraisal of peer-reviewed scientific papers. *Science of the Total Environment* **2010**, 408(5): 999-1006.
(41) MacCuspie, R. Colloidal stability of silver nanoparticles in biologically relevant conditions. *Journal of Nanoparticle Research* **2011**, 13(7): 2893-2908.
(42) Huynh, K. A. and K. L. Chen. Aggregation Kinetics of Citrate and Polyvinylpyrrolidone Coated Silver Nanoparticles in Monovalent and Divalent Electrolyte Solutions. *Environmental Science & Technology* **2011**, 45(13): 5564-5571.
(43) Tejamaya, M., I. Römer, R. C. Merrifield and J. R. Lead. Stability of Citrate, PVP, and PEG Coated Silver Nanoparticles in Ecotoxicology Media. *Environmental Science & Technology* **2012**, 46(13): 7011-7017.
(44) Li, X., J. J. Lenhart and H. W. Walker. Aggregation Kinetics and Dissolution of Coated Silver Nanoparticles. *Langmuir* **2011**, 28(2): 1095-1104.
(45) Kittler, S., C. Greulich, J. Diendorf, M. Köller and M. Epple. Toxicity of Silver Nanoparticles Increases during Storage Because of Slow Dissolution under Release of Silver Ions. *Chemistry of Materials* **2010**, 22(16): 4548-4554.
(46) Mudunkotuwa, I. A., J. M. Pettibone and V. H. Grassian. Environmental Implications of Nanoparticle Aging in the Processing and Fate of Copper-Based Nanomaterials. *Environmental Science & Technology* **2012**.
(47) Unrine, J. M., B. P. Colman, A. J. Bone, A. P. Gondikas and C. W. Matson. Biotic and Abiotic Interactions in Aquatic Microcosms Determine Fate and Toxicity of Ag Nanoparticles. Part 1. Aggregation and Dissolution. *Environmental Science & Technology* **2012**, 46(13): 6915-6924.
(48) Liu, J. and R. H. Hurt. Ion Release Kinetics and Particle Persistence in Aqueous Nano-Silver Colloids. *Environmental Science & Technology* **2010**, 44(6): 2169-2175.
(49) King, S. M. and H. P. Jarvie. Exploring How Organic Matter Controls Structural Transformations in Natural Aquatic Nanocolloidal Dispersions. *Environmental Science & Technology* **2012**.
(50) Shoults-Wilson, W. A., B. C. Reinsch, O. V. Tsyusko, P. M. Bertsch, G. V. Lowry and J. M. Unrine. Effect of silver nanoparticle surface coating on bioaccumulation and reproductive toxicity in earthworms (Eisenia fetida). *Nanotoxicology* **2010**, 5(3): 432-444.
(51) Christian, P., F. Von der Kammer, M. Baalousha and T. Hofmann. Nanoparticles: structure, properties, preparation and behaviour in environmental media. *Ecotoxicology* **2008**, 17(5): 326-343.
(52) Kim, H. J., T. Phenrat, R. D. Tilton and G. V. Lowry. Fe0 nanoparticles remain mobile in porous media after aging due to slow desorption of polymeric surface modifiers. *Environmental Science & Technology* **2009**, 43(10): 3824-3830.
(53) Sagee, O., I. Dror and B. Berkowitz. Transport of silver nanoparticles (AgNPs) in soil. *Chemosphere* **2012**, 88(5): 670-675.

(54) Kim, B., C.-S. Park, M. Murayama and M. F. Hochella. Discovery and Characterization of Silver Sulfide Nanoparticles in Final Sewage Sludge Products. *Environmental Science & Technology* **2010**, 44(19): 7509-7514.
(55) Cappel, C. R. (2000). Silver Compounds. Kirk-Othmer Encyclopedia of Chemical Technology, John Wiley & Sons, Inc.
(56) Levard, C. m., B. C. Reinsch, F. M. Michel, C. Oumahi, G. V. Lowry and G. E. Brown. Sulfidation Processes of PVP-Coated Silver Nanoparticles in Aqueous Solution: Impact on Dissolution Rate. *Environmental Science & Technology* **2011**, 45(12): 5260-5266.
(57) Elechiguerra, J. L., L. Larios-Lopez, C. Liu, D. Garcia-Gutierrez, A. Camacho-Bragado and M. J. Yacaman. Corrosion at the Nanoscale: The Case of Silver Nanowires and Nanoparticles. *Chemistry of Materials* **2005**, 17(24): 6042-6052.
(58) Nielsen, A., H. rn, J. Vollertsen, H. S. Jensen, H. I. Madsen and T. Hvitved-Jacobsen. Aerobic and Anaerobic Transformations of Sulfide in a Sewer SystemField Study and Model Simulations. *Water Environment Research* **2008**, 80(1): 16-25.
(59) Levard, C., E. M. Hotze, G. V. Lowry and G. E. Brown. Environmental Transformations of Silver Nanoparticles: Impact on Stability and Toxicity. *Environmental Science & Technology* **2012**, 46(13): 6900-6914.
(60) Li, X., J. J. Lenhart and H. W. Walker. Dissolution-Accompanied Aggregation Kinetics of Silver Nanoparticles. *Langmuir* **2010**, 26(22): 16690-16698.
(61) Bertsch, P. M. and J. C. Seaman. Characterization of complex mineral assemblages: implications for contaminant transport and environmental remediation. *Proceedings of the National Academy of Sciences of the United States of America* **1999**, 96(7): 3350-3357.
(62) Kim, B., M. Murayama, B. P. Colman and M. F. Hochella. Characterization and environmental implications of nano- and larger TiO2 particles in sewage sludge, and soils amended with sewage sludge. *Journal of Environmental Monitoring* **2012**.
(63) Kim, B., C. S. Park, M. Murayama and M. F. Hochella. Discovery and characterization of silver sulfide nanoparticles in final sewage sludge products. *Environmental Science & Technology* **2010**, 44(19): 7509-7514.
(64) Choi, O., T. E. Clevenger, B. Deng, R. Y. Surampalli, L. Ross Jr and Z. Hu. Role of sulfide and ligand strength in controlling nanosilver toxicity. *Water Research* **2009**, 43(7): 1879-1886.
(65) Nolan, A. L., E. Lombi and M. J. McLaughlin. Metal Bioaccumulation and Toxicity in Soils—Why Bother with Speciation? *Australian Journal of Chemistry* **2003**, 56(3): 77-91.
(66) Harmsen, J. Measuring Bioavailability: From a Scientific Approach to Standard Methods. *Journal of Environmental Quality* **2007**, 36(5): 1420-1428.
(67) Handy, R., N. van den Brink, M. Chappell, M. Mühling, R. Behra, M. Dušinská, P. Simpson, J. Ahtiainen, A. Jha, J. Seiter, A. Bednar, A. Kennedy, T. Fernandes and M. Riediker. Practical considerations for conducting ecotoxicity test methods with manufactured nanomaterials: what have we learnt so far? *Ecotoxicology* **2012**, 21(4): 933-972.
(68) Gorth, D. J., D. M. Rand and T. J. Webster. Silver nanoparticle toxicity in Drosophila: size does matter. *International Journal of Nanomedicine* **2011**, 6: 343-350.
(69) Reinsch, B. C., C. Levard, Z. Li, R. Ma, A. Wise, K. B. Gregory, G. E. Brown and G. V. Lowry. Sulfidation of Silver Nanoparticles Decreases Escherichia coli Growth Inhibition. *Environmental Science & Technology* **2012**.
(70) Khaydarov, R. R., R. A. Khaydarov, Y. Estrin, S. Evgrafova, T. Scheper, C. Endres and S. Y. Cho (2009). Silver Nanoparticles Nanomaterials: Risks and Benefits. I. Linkov and J. Steevens, Springer Netherlands**:** 287-297.

(71) Sotiriou, G. A. and S. E. Pratsinis. Antibacterial Activity of Nanosilver Ions and Particles. *Environmental Science & Technology* **2010**, 44(14): 5649-5654.

(72) Clift, M. J. D., F. Blank, P. Gehr and B. Rothen-Rutishauser (2009). Nanotoxicology: A Brief Overview and Discussion of the Current Toxicological Testing In Vitro and Suggestions for Future Research. General, Applied and Systems Toxicology, John Wiley & Sons, Ltd.
(73) Beer, C., R. Foldbjerg, Y. Hayashi, D. S. Sutherland and H. Autrup. Toxicity of silver nanoparticles—Nanoparticle or silver ion? *Toxicology Letters* **2012**, 208(3): 286-292.
(74) Wijnhoven, S. W. P., W. J. G. M. Peijnenburg, C. A. Herberts, W. I. Hagens, A. G. Oomen, E. H. W. Heugens, B. Roszek, J. Bisschops, I. Gosens, D. Van De Meent, S. Dekkers, W. H. De Jong, M. van Zijverden, A. J. A. M. Sips and R. E. Geertsma. Nano-silver – a review of available data and knowledge gaps in human and environmental risk assessment. *Nanotoxicology* **2009**, 3(2): 109-138.
(75) Drake, P. L. and K. J. Hazelwood Exposure-Related Health Effects of Silver and Silver Compounds: A Review. *Annals of Occupational Hygiene* **2005**, 49(7): 575-585.
(76) Colman, B., S.-Y. Wang, M. Auffan, M. Wiesner and E. Bernhardt. Antimicrobial effects of commercial silver nanoparticles are attenuated in natural streamwater and sediment. *Ecotoxicology* **2012**: 1-11.
(77) Fabrega, J., S. R. Fawcett, J. C. Renshaw and J. R. Lead. Silver Nanoparticle Impact on Bacterial Growth: Effect of pH, Concentration, and Organic Matter. *Environmental Science & Technology* **2009**, 43(19): 7285-7290.
(78) Powers, C. M., T. A. Slotkin, F. J. Seidler, A. R. Badireddy and S. Padilla. Silver nanoparticles alter zebrafish development and larval behavior: Distinct roles for particle size, coating and composition. *Neurotoxicology and Teratology* **2011**, In Press, Corrected Proof.
(79) Gao, J., S. Youn, A. Hovsepyan, V. n. L. Llaneza, Y. Wang, G. Bitton and J.-C. J. Bonzongo. Dispersion and Toxicity of Selected Manufactured Nanomaterials in Natural River Water Samples: Effects of Water Chemical Composition. *Environmental Science & Technology* **2009**, 43(9): 3322-3328.
(80) Delay, M., T. Dolt, A. Woellhaf, R. Sembritzki and F. H. Frimmel. Interactions and stability of silver nanoparticles in the aqueous phase: Influence of natural organic matter (NOM) and ionic strength. *Journal of Chromatography A* **2011**, 1218(27): 4206-4212.
(81) Hirsch, M. P. Availability of sludge-borne silver to agricultural crops. *Environmental Toxicology and Chemistry* **1998**, 17(4): 610-616.
(82) Kim, S. W., S.-H. Nam and Y.-J. An. Interaction of Silver Nanoparticles with Biological Surfaces of Caenorhabditis elegans. *Ecotoxicology and Environmental Safety* **2012**, 77(0): 64-70.
(83) Lee, W.-M., J. Kwak and Y.-J. An. Effect of silver nanoparticles in crop plants. *Phaseolus radiatus* and *Sorghum bicolor*: Media effect on phytotoxicity *Chemosphere* **2012**, 86: 491-499.
(84) Lapied, E., E. Moudilou, J.-M. Exbrayat, D. H. Oughton and E. J. Joner. Silver nanoparticle exposure causes apoptotic response in the earthworm Lumbricus terrestris (Oligochaeta). *Nanomedicine* **2010**, 5(6): 975-984.
(85) McGechan, M. B. SW—Soil and Water: Transport of Particulate and Colloid-sorbed Contaminants through Soil, Part 2: Trapping Processes and Soil Pore Geometry. *Biosystems Engineering* **2002**, 83(4): 387-395.
(86) McGechan, M. B. and D. R. Lewis. SW—Soil and Water: Transport of Particulate and Colloid-sorbed Contaminants through Soil, Part 1: General Principles. *Biosystems Engineering* **2002**, 83(3): 255-273.
(87) Heckmann, L.-H., M. Hovgaard, D. Sutherland, H. Autrup, F. Besenbacher and J. Scott-Fordsmand. Limit-test toxicity screening of selected inorganic nanoparticles to the earthworm *Eisenia fetida*. *Ecotoxicology* **2011**, 20(1): 226-233.
(88) Shoults-Wilson, W. A., O. I. Zhurbich, D. H. McNear, O. V. Tsyusko, P. M. Bertsch and J. M. Unrine. Evidence for avoidance of Ag nanoparticles by earthworms (*Eisenia fetida*). *Ecotoxicology* **2011**.

(89) von der Kammer, F., P. L. Ferguson, P. A. Holden, A. Masion, K. R. Rogers, S. J. Klaine, A. A. Koelmans, N. Horne and J. M. Unrine. Analysis of engineered nanomaterials in complex matrices (environment and biota): General considerations and conceptual case studies. *Environmental Toxicology and Chemistry* **2012**, 31(1): 32-49.
(90) Fabrega, J., S. N. Luoma, C. R. Tyler, T. S. Galloway and J. R. Lead. Silver nanoparticles: behaviour and effects in the aquatic environment. *Environ Int* **2011**, 37(2): 517-531.
(91) Domingos, R. F., M. A. Baalousha, Y. Ju-Nam, M. M. Reid, N. Tufenkji, J. R. Lead, G. G. Leppard and K. J. Wilkinson. Characterizing manufactured nanoparticles in the environment: multimethod determination of particle sizes. *Environmental Science & Technology* **2009**, 43(19): 7277-7284.
(92) Balnois, E., K. J. Wilkinson, J. R. Lead and J. Buffle. Atomic Force Microscopy of Humic Substances: Effects of pH and Ionic Strength. *Environmental Science & Technology* **1999**, 33(21): 3911-3917.
(93) Ngo, P. D. (1999). Energy Dispersive Spectroscopy Failure Analysis of Integrated Circuits. L. C. Wagner, Springer US. **494:** 205-215.

(94) Schaffer, B., W. Grogger, G. Kothleitner and F. Hofer. Comparison of EFTEM and STEM EELS plasmon imaging of gold nanoparticles in a monochromated TEM. *Ultramicroscopy* **2010**, 110(8): 1087-1093.
(95) Hemraj-Benny, T., S. Banerjee, S. Sambasivan, M. Balasubramanian, D. A. Fischer, G. Eres, A. A. Puretzky, D. B. Geohegan, D. H. Lowndes, W. Han, J. A. Misewich and S. S. Wong. Near-Edge X-ray Absorption Fine Structure Spectroscopy as a Tool for Investigating Nanomaterials. *Small* **2006**, 2(1): 26-35.
(96) Norman, D. X-ray absorption spectroscopy (EXAFS and XANES) at surfaces. *Journal of Physics C: Solid State Physics* **1986**, 19(18): 3273.
(97) Rehr, J. J. and R. C. Albers. Theoretical approaches to x-ray absorption fine structure. *Reviews of Modern Physics* **2000**, 72(3): 621-654.
(98) Hassellov, M., J. W. Readman, J. F. Ranville and K. Tiede. Nanoparticle analysis and characterization methodologies in environmental risk assessment of engineered nanoparticles. *Ecotoxicology* **2008**, 17(5): 344-361.
(99) Laborda, F., J. Jimenez-Lamana, E. Bolea and J. R. Castillo. Selective identification, characterization and determination of dissolved silver(I) and silver nanoparticles based on single particle detection by inductively coupled plasma mass spectrometry. *Journal of Analytical Atomic Spectrometry* **2011**.
(100) Mitrano, D. M., A. Barber, A. Bednar, P. Westerhoff, C. P. Higgins and J. F. Ranville. Silver nanoparticle characterization using single particle ICP-MS (SP-ICP-MS) and asymmetrical flow field flow fractionation ICP-MS (AF4-ICP-MS). *Journal of Analytical Atomic Spectrometry* **2012**, 27(7): 1131-1142.
(101) Gimbert, L. J., P. M. Haygarth, R. Beckett and P. J. Worsfold. Comparison of Centrifugation and Filtration Techniques for the Size Fractionation of Colloidal Material in Soil Suspensions Using Sedimentation Field-Flow Fractionation. *Environmental Science & Technology* **2005**, 39(6): 1731-1735.
(102) Weinberg, H., A. Galyean and M. Leopold. Evaluating engineered nanoparticles in natural waters. *Trends in Analytical Chemistry* **2011**, 30(1): 72-83.
(103) Dubin, P. L. and J. M. Principi. Failure of universal calibration for size-exclusion chromatography of rodlike macromolecules vs. random coils and globular proteins. *Macromolecules* **1989**, 22(4): 1891-1896.
(104) Williams, A., E. Varela, E. Meehan and K. Tribe. Characterisation of nanoparticulate systems by hydrodynamic chromatography. *International Journal of Pharmaceutics* **2002**, 242(1–2): 295-299.

(105) Tiede, K., A. B. A. Boxall, X. Wang, D. Gore, D. Tiede, M. Baxter, H. David, S. P. Tear and J. Lewis. Application of hydrodynamic chromatography-ICP-MS to investigate the fate of silver nanoparticles in activated sludge. *Journal of Analytical Atomic Spectrometry* **2010**, 25(7): 1149-1154.
(106) Prieve, D. C. and P. M. Hoysan. Role of colloidal forces in hydrodynamic chromatography. *Journal of Colloid and Interface Science* **1978**, 64(2): 201-213.
(107) Schimpt, M., K. Caldwell and J. C. Giddings. Field-Flow Fractionation Handbook. New York, Wiley Interscience. **2000**.
(108) Dubascoux, S., I. Le Hecho, M. Hassellov, F. Von Der Kammer, M. Potin Gautier and G. Lespes. Field-flow fractionation and inductively coupled plasma mass spectrometer coupling: History, development and applications. *Journal of Analytical Atomic Spectrometry* **2010**, 25(5): 613-623.
(109) Giddings, J. C., F. J. Yang and M. N. Myers. Theoretical and experimental characterization of flow field-flow fractionation. *Analytical Chemistry* **1976**, 48(8): 1126-1132.
(110) Dubascoux, S., F. Von Der Kammerb, I. LeHécho, M. P. Pautiera and G. Lespesa. Optimisation of asymmetrical flow field flow fractionation for environmental nanoparticles separation. *Journal of Chromatography* **2008**, (1206): 160-165.
(111) Poda, A. R., A. J. Bednar, A. J. Kennedy, A. Harmon, M. Hull, D. M. Mitrano, J. F. Ranville and J. Steevens. Characterization of silver nanoparticles using flow-field flow fractionation interfaced to inductively coupled plasma mass spectrometry. *Journal of Chromatography A* **2010**.
(112) Baalousha, M., B. Stolpe and J. R. Lead. Flow field-flow fractionation for the analysis and characterization of natural colloids and manufactured nanoparticles in environmental systems: A critical review. *Journal of Chromatography A* **2011**, 1218(27): 4078-4103.
(113) Cumberland, S. A. and J. R. Lead. Particle size distributions of silver nanoparticles at environmentally relevant conditions. *Journal of Chromatography A* **2009**, 1216(52): 9099-9105.
(114) Link, S. and M. A. El-Sayed. Optical properties and ultrafast dynamics of metallic nanocrystals. *Annual Review of Physical Chemistry* **2003**, 54: 331-366.
(115) von der Kammer, F., S. Legros, T. Hofmann, E. H. Larsen and K. Loeschner. Separation and characterization of nanoparticles in complex food and environmental samples by field-flow fractionation. *Trends in Analytical Chemistry* **2011**, 30(3): 425-436.
(116) Bolea, E., M. P. Gorriz, M. Bouby, F. Laborda, J. R. Castillo and H. Geckeis. Multielement characterization of metal-humic substances complexation by size exclusion chromatography, asymmetrical flow field-flow fractionation, ultrafiltration and inductively coupled plasma-mass spectrometry detection: a comparative approach. *Journal of Chromatography A* **2006**, 1129(2): 236-246.
(117) Mueller, N. C. and B. Nowack. Exposure Modeling of Engineered Nanoparticles in the Environment. *Environmental Science & Technology* **2008**, 42(12): 4447-4453.
(118) Gottschalk, F. and B. Nowack. The release of engineered nanomaterials to the environment. *Journal of Environmental Monitoring* **2011**, 13(5): 1145-1155.
(119) Jackson, B. P., J. F. Ranville and A. L. Neal. Application of flow field flow fractionation-ICPMS for the study of uranium binding in bacterial cell suspensions. *Analytical Chemistry* **2005**, 77(5): 1393-1397.
(120) Bolea, E., F. Laborda and J. R. Castillo. Metal associations to microparticles, nanocolloids and macromolecules in compost leachates: Size characterization by asymmetrical flow field-flow fractionation coupled to ICP-MS. *Analytica Chimica Acta* **2010**, 661(2): 206-214.
(121) Claveranne-Lamolère, C., G. Lespes, S. Dubascoux, J. Aupiais, F. Pointurier and M. Potin-Gautier. Colloidal transport of uranium in soil: Size fractionation and characterization by field-flow fractionation-multi-detection. *Journal of Chromatography A* **2009**, 1216(52): 9113-9119.

(122) Stolpe, B., L. Guo, A. M. Shiller and M. Hassellöv. Size and composition of colloidal organic matter and trace elements in the Mississippi River, Pearl River and the northern Gulf of Mexico, as characterized by flow field-flow fractionation. *Marine Chemistry* **2010**, 118(3-4): 119-128.
(123) Plathe, K. L., F. von der Kammer, M. Hassellov, J. Moore, M. Murayama, T. Hofmann and M. F. Hochella. Using FlFFF and aTEM to determine trace metal-nanoparticle associations in riverbed sediment. *Environmental Chemistry* **2010**, 7(1): 82-93.
(124) Paterson, G., A. Macken and K. V. Thomas. The need for standardized methods and environmental monitoring programs for anthropogenic nanoparticles. *Analytical Methods* **2011**, 3(7): 1461-1467.
(125) Bouby, M., H. Geckeis and F. W. Geyer. Application of asymmetric flow field-flow fractionation (AsFlFFF) coupled to inductively coupled plasma mass spectrometry (ICPMS) to the quantitative characterization of natural colloids and synthetic nanoparticles. *Analytical and Bioanalytical Chemistry* **2008**, 392(7-8): 1447-1457.
(126) Baalousha, M., B. Stolpe and J. R. Lead. Flow field-flow fractionation for the analysis and characterization of natural colloids and manufactured nanoparticles in environmental systems: a critical review. *J Chromatogr A* **2011**, 1218(27): 4078-4103.
(127) Cheng, Y., L. Yin, S. Lin, M. Wiesner, E. Bernhardt and J. Liu. Toxicity Reduction of Polymer-Stabilized Silver Nanoparticles by Sunlight. *The Journal of Physical Chemistry C* **2011**, 115(11): 4425-4432.
(128) Turkevich, J., P. C. Stevenson and J. Hillier. A study of the nucleation and growth processes in the synthesis of colloidal gold. *Discussions of the Faraday Society* **1951**, 11: 55-75.
(129) Gee, G. W. and J. W. Bauder. Particle Size Analysis By Hydrometer: A Simplified Method For Routine Textural Analysis And A Sensitivity Test Of Measurement Parameters. *Soil Sci. Soc. Am. J.* **1979**, 43(5): 1004-1007.
(130) Karathanasis, A. D. and D. M. C. Johnson. Stability and transportability of biosolid colloids through undisturbed soil monoliths. *Geoderma* **2006**, 130(3–4): 334-345.
(131) Karathanasis, A. D., D. M. C. Johnson and C. J. Matocha. Biosolid Colloid-Mediated Transport of Copper, Zinc, and Lead in Waste-Amended Soils. *Journal of Environmental Quality* **2005**, 34(4): 1153-1164.
(132) Wyatt, P. J. Light scattering and the absolute characterization of macromolecules. *Analytica Chimica Acta* **1993**, 272(1): 1-40.
(133) Baalousha, M., F. V. Kammer, M. Motelica-Heino, H. S. Hilal and P. Le Coustumer. Size fractionation and characterization of natural colloids by flow-field flow fractionation coupled to multi-angle laser light scattering. *Journal of Chromatography A* **2006**, 1104(1-2): 272-281.
(134) Amarasiriwardena, D., A. Siripinyanond and R. M. Barnes. Trace elemental distribution in soil and compost-derived humic acid molecular fractions and colloidal organic matter in municipal wastewater by flow field-flow fractionation-inductively coupled plasma mass spectrometry (flow FFF-ICP-MS). *Journal of Analytical Atomic Spectrometry* **2001**, 16(9): 978-986.
(135) Dubascoux, S., F. Von Der Kammer, I. Le Hécho, M. P. Gautier and G. Lespes. Optimisation of asymmetrical flow field flow fractionation for environmental nanoparticles separation. *Journal of Chromatography A* **2008**, 1206(2): 160-165.
(136) Giddings, J. C., F. J. Yang and M. N. Myers. Flow field-flow fractionation as a methodology for protein separation and characterization. *Analytical Biochemistry* **1977**, 81(2): 395-407.
(137) von der Kammer, F., M. Baborowski and K. Friese. Field-flow fractionation coupled to multi-angle laser light scattering detectors: Applicability and analytical benefits for the analysis of environmental colloids. *Analytica Chimica Acta* **2005**, 552(1-2): 166-174.

(138) Bolea, E., J. Jiménez-Lamana, F. Laborda and J. Castillo. Size characterization and quantification of silver nanoparticles by asymmetric flow field-flow fractionation coupled with inductively coupled plasma mass spectrometry. *Analytical and Bioanalytical Chemistry* **2011**: 1-10.
(139) Ranville, J. F., D. J. Chittleborough, F. Shanks, R. J. S. Morrison, T. Harris, F. Doss and R. Beckett. Development of sedimentation field-flow fractionation-inductively coupled plasma mass-spectrometry for the characterization of environmental colloids. *Analytica Chimica Acta* **1999**, 381(2–3): 315-329.
(140) Siripinyanond, A. and R. M. Barnes. Flow field-flow fractionation-inductively coupled plasma mass spectrometry of chemical mechanical polishing slurries. *Spectrochimica Acta Part B: Atomic Spectroscopy* **2002**, 57(12): 1885-1896.
(141) Zanardi-Lamardo, E., C. D. Clark and R. G. Zika. Frit inlet/frit outlet flow field-flow fractionation: methodology for colored dissolved organic material in natural waters. *Analytica Chimica Acta* **2001**, 443(2): 171-181.
(142) Moon, J., S. Lee, J.-H. Song and J. Cho. Membrane fouling indicator of effluent organic matter with nanofiltration for wastewater reclamation, as obtained from flow field-flow fractionation. *Separation and Purification Technology* **2010**, 73(2): 164-172.
(143) Moon, J., S.-H. Kim and J. Cho. Characterizations of natural organic matter as nano particle using flow field-flow fractionation. *Colloids and Surfaces A: Physicochemical and Engineering Aspects* **2006**, 287(1–3): 232-236.
(144) Wahlund, K. G. and J. C. Giddings. Properties of an asymmetrical flow field-flow fractionation channel having one permeable wall. *Analytical Chemistry* **1987**, 59(9): 1332-1339.
(145) NIST-NCL (2007). Measuring the size of nanoparticles in aqueous media using batch-mode dynamic light scattering. NIST-NCL Joint Assay Protocol PCC-1. Frederick, MD
(146) Kirby, B. J. and E. F. Hasselbrink. Zeta potential of microfluidic substrates: 1. Theory, experimental techniques, and effects on separations. *ELECTROPHORESIS* **2004**, 25(2): 187-202.
(147) (2012). Zeta potential analysis of nanoparticles. San Diego, Ca, nanoComposix. **1**.
(148) Hassellöv, M., B. Lyvén and R. Beckett. Sedimentation Field-Flow Fractionation Coupled Online to Inductively Coupled Plasma Mass SpectrometryNew Possibilities for Studies of Trace Metal Adsorption onto Natural Colloids. *Environmental Science & Technology* **1999**, 33(24): 4528-4531.
(149) Hall, G. E. M., J. E. Vaive and A. I. MacLaurin. Analytical aspects of the application of sodium pyrophosphate reagent in the specific extraction of the labile organic component of humus and soils. *Journal of Geochemical Exploration* **1996**, 56(1): 23-36.
(150) Lead, J. R. and K. J. Wilkinson (2007). Environmental Colloids and Particles: Current Knowledge and Future Developments. Environmental Colloids and Particles, John Wiley & Sons, Ltd**:** 1-15.
(151) Mori, Y., B. Scarlett and H. G. Merkus. Effects of ionic strength of eluent on size analysis of submicrometre particles by sedimentation field-flow fractionation. *Journal of Chromatography A* **1990**, 515(0): 27-35.
(152) Alasonati, E., V. I. Slaveykova, H. Gallard, J. P. Croue and M. F. Benedetti. Characterization of the colloidal organic matter from the Amazonian basin by asymmetrical flow field-flow fractionation and size exclusion chromatography. *Water Res* **2010**, 44(1): 223-231.
(153) Beckett, R., Z. Jue and J. C. Giddings. Determination of molecular weight distributions of fulvic and humic acids using flow field-flow fractionation. *Environmental Science & Technology* **1987**, 21(3): 289-295.
(154) Marambio-Jones, C. and E. Hoek. A review of the antibacterial effects of silver nanomaterials and potential implications for human health and the environment. *Journal of Nanoparticle Research* **2010**, 12(5): 1531-1551.

(155) Chen, X. and H. J. Schluesener. Nanosilver: A nanoproduct in medical application. *Toxicology Letters* **2008**, 176(1): 1-12.
(156) Lok, C.-N., C.-M. Ho, R. Chen, Q.-Y. He, W.-Y. Yu, H. Sun, P. Tam, J.-F. Chiu and C.-M. Che. Silver nanoparticles: partial oxidation and antibacterial activities. *Journal of Biological Inorganic Chemistry* **2007**, 12(4): 527-534.
(157) USEPA. Biosolids, Frequently Asked Questions. http://water.epa.gov/polwaste/wastewater/treatment/biosolids/genqa.cfm, **2009**.
(158) Bone, A. J., B. P. Colman, A. P. Gondikas, K. M. Newton, K. H. Harrold, R. M. Cory, J. M. Unrine, S. J. Klaine, C. W. Matson and R. T. Di Giulio. Biotic and Abiotic Interactions in Aquatic Microcosms Determine Fate and Toxicity of Ag Nanoparticles: Part 2–Toxicity and Ag Speciation. *Environmental Science & Technology* **2012**, 46(13): 6925-6933.
(159) Zhang, Y., Y. Chen, P. Westerhoff and J. Crittenden. Impact of natural organic matter and divalent cations on the stability of aqueous nanoparticles. *Water Research* **2009**, 43(17): 4249-4257.
(160) Fedotov, P., N. Vanifatova, V. Shkinev and B. Spivakov. Fractionation and characterization of nano- and microparticles in liquid media. *Analytical and Bioanalytical Chemistry* **2011**, 400(6): 1787-1804.
(161) USEPA (1996). Method 3052: Microwave assisted acid digestion of siliceous and organically based matrices. USEPA, Washington, DC.
(162) I. c. p.-m. spectrometry. Method 6020. **1998**.
(163) Kawahigashi, M., H. Sumida and K. Yamamoto. Size and shape of soil humic acids estimated by viscosity and molecular weight. *Journal of Colloid and Interface Science* **2005**, 284(2): 463-469.
(164) VandeVoort, A. R. and Y. Arai. Environmental Chemistry of Silver in Soils: Current and Historic Perspective. *Advances in Agronomy, Vol 114* **2012**, 114: 59-90.
(165) Levard, C., E. M. Hotze, G. V. Lowry and G. E. Brown. Environmental Transformations of Silver Nanoparticles: Impact on Stability and Toxicity. *Environmental Science & Technology* **2012**.
(166) Maurer, F., I. Christl and R. Kretzschmar. Reduction and Reoxidation of Humic Acid: Influence on Spectroscopic Properties and Proton Binding. *Environmental Science & Technology* **2010**, 44(15): 5787-5792.

Vita

Annie Whitley was born on January 26, 1987 in Savannah, Georgia. She received dual Bachelor of Science degrees in Chemistry and Biology from the University of South Carolina at Aiken in 2009. After graduation she worked as a Research Professional at the Savannah River Ecology Laboratory in Aiken, South Carolina. In 2010 she was awarded at Research Fellowship to the College of Agriculture at the University of Kentucky.